October 2017

The Effect of Chemical Composition of Blast-Furnace Slag on Compressive Strength and Durability Properties of Mortar Specimens

William J. Johnson
University of South Florida, emailme@williamjosephjohnson.com

The Effect of Chemical Composition of Blast-Furnace Slag on Compressive Strength and Durability Properties of Mortar Specimens

by

William J. Johnson

A thesis submitted in partial fulfillment
of the requirements for the degree of
Master of Science in Civil Engineering
Department of Civil and Environmental Engineering
College of Engineering
University of South Florida

Major Professor: Abla Zayed, Ph.D.
Rajan Sen, Ph.D.
Gray Mullins, Ph.D.
Michael Stokes, Ph.D.

Date of Approval:
October 20, 2017

Keywords: Sulfate Attack, Alumina Content, X-Ray Diffraction,
Expansion, Decalcification of CSH

DEDICATION

This report is dedicated to my father. The inspiration derived from his constant drive is what helped me throughout this experience.

I would also like to dedicate this to Karilin. Without her unwavering love and support I wouldn't be where I am today.

ACKNOWLEDGMENTS

I would like to thank everyone who has helped me throughout this study. Special thanks to my advisor, Dr. Zayed, for her help and advice throughout the duration of this research experience. I would also like to thank Dr. Mullins, Dr. Sen, and Dr. Stokes for being on my committee and accepting a defense date that was rather short notice. I am grateful for their compassionate understanding to assist a student working tirelessly in an accelerated program.

I would like to specifically state my utmost gratitude for my coworkers who helped me throughout this project: Natallia, Andrew, Yuriy, Ananya, Dhanushika, and Farzaneh. Natallia, you were the most influential person to go to whenever I needed assistance, whether it was asking for clarification on a topic I wasn't fully knowledgeable in or just going to you for advice. Yuriy, you single-handily offered the most contribution of time and work to this project by making daily scans of specimens for months on end and I am forever grateful for that. Thank you Farzaneh for stepping in to maintain some of my experiments while I was away for a brief time, it was greatly appreciated. Dhanushika, your daily smile brightened my day even when I was stressed or feeling overwhelmed. Andrew, our long conversations about life and work really helped me have better perspective in my day-to-day and I'm glad to have you as a friend. Ananya, you always offered help even when you were busy yourself. You are the hardest worker I know and I wish you the best of luck for the remainder of your studies. I would also like to thank Brandon, Mustafa, Jair, Rigo, and Ryan. I wish the best for all of you.

TABLE OF CONTENTS

LIST OF TABLES

LIST OF FIGURES

ABSTRACT

In an effort to make structures more sustainable and durable, supplementary cementitious materials are often used to replace cement. Ground granulated blast furnace slag, for instance, is an industrial by-product of iron refinement and is frequently used in concrete mixture design to not only reduce cost, but also increase later-age strength as well as durability. However, published literature indicates that slags with a high alumina content may have a detrimental effect when concrete is exposed to a sulfate environment. ASTM standard C989 does not suggest any information or guidelines regarding using slags with an alumina content between 11-18%. Therefore, the objective of this study was to fill in the gap of this standard by studying slags of variable alumina content as high as 16 percent.

This study presents data collected for compressive strengths of mortar cubes exposed to lime and 5 percent sodium sulfate solution at ages of 7, 28, 91, and 182 days from the date of mixing as well as expansion data for mortar bar specimens exposed to 5 percent sodium sulfate solution up to 120 days. Slag replacement levels used here were 0, 30, 50, and 70%. Mortar bar specimens showing deterioration were analyzed using x-ray diffraction coupled with Rietveld refinement to assess the mechanism of deterioration. Cubes were stored in lime and sulfate solutions abiding by ASTM C1012 in order to analyze the resistance to sulfate attack. Sulfate resistance was measured in terms of decalcification of the CSH gel as well as expansion.

The results suggest using high alumina slags at a low percentage adversely affects sulfate resistance since the acquired strength at 182 days fell below that of 28 day strength, which is often

used in the industry as the parameter which constitutes whether a mixture is adequate. It was also seen that increasing alumina content of the slag resulted in increased expansion. X-ray diffraction analysis indicates that the mechanism of deterioration, of the control as well as the blended mortar, is due to secondary gypsum and secondary ettringite formation. Therefore, it is recommended that slags having a high alumina content should be further analyzed in laboratory tests to examine their performance especially if concrete will be subjected to a sulfate environment during its service life.

CHAPTER 1: INTRODUCTION

In a societal effort to design building materials in a more efficient and "green" way, supplemental cementitious materials (SCMs) are often used in place of ordinary Portland cement (OPC) in concrete structures. Ground granulated blast-furnace slag (GGBFS) is one of these SCMs and has been used to replace part of the cementitious system throughout time. The first known use of slag in construction was during the Roman Empire when they used it in road base construction nearly 2000 years ago [1]. The use of this material accelerated with the dawn of the Industrial Revolution as iron production dramatically increased. Slag is generated as a by-product of the production of pig iron when added limestone and iron oxide are used to remove the impurities from the metal thus creating two final products in near equal proportions: blast-furnace slag (slag) and clean metal [1]. The resulting slag is made up of the same oxides found in Portland cement; that is, lime, silica, and alumina though in different proportions. In order for slag to be used in cement applications, it must be quenched in the production process so a hydraulically active calcium aluminosilicate glass may form. In 1862, Emil Langen, a director of an ironworks company in Germany, discovered the latent hydraulic property of blast-furnace slag which opened a new door for the cement industry [2]. Since this material was created as a waste product from the metal industry, it is cheaper to use compared to cement. This newfound material was put to use in massive projects in the 19th century including the Paris Underground Metro System and the Empire State building in the beginning of the 20th century [2]. Since then, slag has been used in a

plethora of construction projects to reduce cost and its positive environmental impact while also improving durability and long-term strength of concrete.

This study examines the effects of utilizing slag as a cement replacement on the mechanical properties of cementitious systems; namely, compressive strength development. Additionally, the effect of slag use on performance of concrete and its durability when exposed to a sulfate environment is assessed. The effect of the slag chemical and physical characteristics on durability and strength of plain and blended mortar is therefore the focus of the current study.

This study may play a vital part in how slag is implemented in construction practices in sulfate environments, especially in Florida's marine environment as well as in sulfate-bearing soils. It is important to note that the quality of slag is variable depending on the fluxing material composition and consequently the chemical characteristics of the produced slag. Therefore, the objective of this current study is to provide scientific data to identify the performance of slags of variable chemical and physical characteristics.

The current standard specification for slag cement, ASTM C989, describes the C_3A content of cement and the alumina content of slag as influential factors in concrete's sulfate resistance [3]. It states low alumina slags ($\leq$11%) increases durability whereas high alumina slags (18%) have a negative effect on its chemical resistance to sulfates. The standard, however, does not provide information regarding slags with an alumina content between 11-18%. Therefore, four slags were used which contained alumina contents above, below, and closely near 11%. Additionally, the C_3A content of the cements were analyzed. ASTM standard C150 limits the tricalcium aluminate for Type II cements to 8%, but does not place a limit for Type I cements [4]. This study used two different cements: one which meets the specification for Type II cement and the other which exceeds the 8% limit.

I would like to acknowledge the partial support provided by the Florida Department of Transportation and the US Department of Transportation for conducting this work.

CHAPTER 2: LITERATURE REVIEW

2.1 Introduction

Blast furnace slag (BFS), or ground granulated blast furnace slag (GGBFS), is a common supplementary cementitious material (SCM) and has been used in the cementing industry since the discovery of its latent hydraulic properties in the late 19th century [3]. It is known to improve workability, increase strength at later ages, reduce the overall cost of a project, and decrease permeability which thus enhances durability. However, due to its slow reactivity, the early age strength is less than OPC mixtures and if it is not properly cured higher rates of carbonation, surface scaling, and frost attack may be observed [5].

Several factors that affect the beneficial properties of using slag as a cement replacement include replacement levels, alumina content of the slag, slag fineness, tricalcium aluminate (C_3A) content of the cement, and the imposed curing conditions. These factors play a vital role in the resistance to chemicals, namely, sulfate attack as well as the strength development over time.

Slag cements must abide by ASTM C989 [3] which characterizes slags based on reactivity and limits the sulfide sulfur content to 2.5%. The standard mentions the importance of the alumina content by suggesting low alumina slags (11%) increase sulfate resistance regardless of the C_3A content of the cement, but adversely affects the resistance to sulfates when alumina content is high (18%). The standard, however, does not indicate or provide any advise or guidance on the use of slags with an alumina content between 11% and 18%. Since the content of alumina varies widely throughout the world, and slags are often sourced from out of the United States, it is important to

study the effects of using slags with different alumina contents to recommend a limit, if any, for safe use.

2.2 Characteristics of Slag Cements

Blast-furnace slag may be characterized by its chemical composition, mineralogical composition including its large amorphous content, as well as its reactivity and fineness. First, though, it is essential to understand the process of making the slag to fully grasp how this material may be variable throughout the world.

2.2.1 Slag Origin

BFS decreases the cost of a project since it is created as a by-product in the refinement process of pig iron. ASTM C125 [6] defines blast-furnace slag as "the nonmetallic product, consisting essentially of silicates and aluminosilicates of calcium and other bases, that is developed in a molten condition simultaneously with iron in a blast furnace". As limestone and coke are added to the iron oxide to remove impurities, the silica and alumina components combine with the lime and magnesia to form molten slag which floats on top of the molten iron in the furnace [1, 4]. The general composition of slag can be seen in Table 2-1 [7].

The slag exits the furnace at a temperature of around 1500^0C and its final use is dependent on the subsequent processing. If allowed to cool slowly the final product would be optimal for use as an aggregate; however, if the molten material is quenched, it solidifies into a glass with amorphous content between 90-100% [4, 5]. After it has been finely ground, the amorphous material has hydraulic properties which makes it suitable for use in cement [1]. Similar to cement and other SCMs, increasing the fineness will result in an increased reactivity.

Table 2-1: Typical Slag Composition

Analyte	Content (weight %)
CaO	30 - 50
SiO_2	28 - 38
Al_2O_3	8 - 24
MgO	1 - 18
S	1 - 2.5
Fe_2O_3	1 - 3
MnO	1 - 3
TiO_2	< 4
Na_2O+K_2O	< 2

2.2.2 Slag Reactivity

An important characteristic of slag to assess its effectiveness in concrete is its reactivity. ASTM C989 [3] classifies slag's activity into three grades: Grade 80, Grade 100, and Grade 120, with the higher number reflecting more reactivity. This is evaluated by comparing the compressive strength of OPC mortars to a 50/50 blend of OPC-BFS at 7 and 28 days given that the cement used abides by the limit of a specified total alkali content and has a compressive strength of 5000 psi at 28 days. As previously mentioned, reactivity increases with fineness and since cement is more reactive than slag, reactivity also increases with decreasing replacement levels. Other factors that contribute to reactivity include chemical composition, hydration temperature, characteristics of the activator, water to cementitious ratio (w/cm), and glass content.

Chemical composition, namely CaO, SiO_2, Al_2O_3, MgO, and the overall hydraulic index were found to affect slag reactivity. Thirteen different proposed hydraulic indices, or hydraulic moduli, categorized into three different types are reviewed in [6]. Type I hydraulic indexes only consider SiO_2 as a function of reactivity; Type III indicates Al_2O_3 negatively affects reactivity, and Type II includes effects of minor components. The more commonly used moduli can be seen in

Equation 1. Equation 1 may also be referred to as the basicity factor and generally the higher this factor is the greater slag reactivity [8].

$$\frac{CaO + MgO + Al_2O_3}{SiO_2} \qquad \text{Equation 1}$$

It has been found that increasing CaO and MgO contents in the slag positively affects strength, whereas SiO_2 has a negative impact [9]. The content of Al_2O_3, however, is controversial, as some say an increase results in increased strength due to increased reactivity [6, 7], but others disagree [4, 5].

The reactivity was also found to increase with the hydration temperature, water to cementitious ratio (w/cm), and glass content [10]. The positive effect of increasing w/cm ratio may be explained by the combination of more space being available for hydration products to form and with more cement hydration, the cement-activating environment for the slag increases [10]. Walker and Pavía [11] found a clear correlation between amorphous content and reactivity and concluded that amorphous content is the strongest variable affecting the strength of paste. However, they state chemical composition is not influential in affecting reactivity or strength of paste which goes against previously cited research.

A number of activators may be used to accelerate the hydration of BFS including lime, gypsum, and cement clinker as well as sodium hydroxide, potassium hydroxide, and sodium silicate to name a few [12]. This study, however, will only focus on cement as the activator.

2.2.3 Hydration Reactions

The properties of slag allow it to be used purely in place of cement, but without activation of an alkaline compound, such mixtures would take several months to reach the same 28-day strength of concrete made with Portland cement [8]. Typically, the slag is activated by calcium hydroxide which forms due to the chemical reaction of calcium silicates of OPC with water [13] according to Equation 2:

$$Cement\ (C_3S, C_2S) + H_2O\ \rightarrow CSH\ gel + Ca(OH)_2 \qquad \text{Equation 2}$$

The calcium hydroxide is then consumed in the pozzolanic reaction to form calcium-silicate-hydrate (CSH) gel as can be seen in Equation 3:

$$Ca(OH)_2 + SiO_2 + H_2O \rightarrow CSH\ gel \qquad \text{Equation 3}$$

These equations portray the slow nature of hydration when mineral admixtures are used since the pozzolanic reaction can only occur once the cement reaction takes place. Another reason for the slow hydration may be due to impermeable coatings of amorphous silica and alumina which form around the particles of slag early in the hydration process [8].

The C-S-H gel is an amorphous material which accounts for up to 60% of the paste's volume. It forms a continuous layer that binds together cement particles to create a strong, cohesive structure [14]. It is also the main component of the hydrated cement system that is responsible for properties such as strength and shrinkage [15]. Calcium hydroxide (CH) on the other hand also contributes to strength, but to a lesser degree, by reducing the pore volume as crystals grow inside the voids formed in concrete [8]. However, it has a detrimental effect in terms of durability since

it is more soluble than the C-S-H gel. It may be seen through the previous two equations that adding mineral admixtures such as slag to replace cement further strengthens the mixture by utilizing the weaker CH compound to create more of the stronger C-S-H gel. Removing the CH from the system also benefits its durability, thus improving both strength development and chemical resistance.

Compared to neat cement systems, slag-cement blended systems decrease the Ca/Si ratio and increase the ratio of Al/Si in C-S-H [16], [17]. As the Ca/Si ratio increases, the length of silicate chains within the C-S-H microstructure decreases which reduces the interplanar distance causing an increase in density and strength [18]. Živica [19] concluded the increase in the calcium to silica ratio presents a lower water to silica ratio which combined causes a change within the crystalline structure of particles resulting in increased binding capacity and homogeneity of the pore structure, thus enhancing strength between individual particles. Rowles and O'Connor [20] performed a study analyzing the effects of the Si/Al ratio as well as the Na/Al ratio and determined the optimal ratio for strength is Si:Al:Na = 2.5:1:1.29; their research shows a positive correlation of Si/Al ratio and strength. Both studies [19], [20] tested strength at early ages, 1 day and 7 days, and indicate that a decrease in Ca/Si and an increase in Al/Si results in a lower strength.

2.3 Compressive Strength

It is well-established that the addition of slag in concrete mixtures decreases early age strength but increases the long-term strength. Higher additions of blast-furnace slag (BFS) have the highest strength gain from a week out from mixing to a year [21]. This effect is not linear, however, as studies have shown there seems to be an optimal replacement level of cement with slag for the highest strength at a given age. Oner and Akyuz [21] suggest that the optimal replacement level is approximately 55-59% of the total amount of binding material. Others propose

40% replacement [8], [22], [23]. A more accurate representation for the optimal level may depend on the testing age. Sajedi and Shafigh [24] advocate a replacement level of 40% for testing within 28 days, but their published data show that a 60% replacement is advisable for a later age of 56 days.

2.4 Sulfate Attack

A common form of chemical attack comes from sulfates interacting with concrete both internally and externally. Internally, sulfates within the cement composition may cause damage due to delayed ettringite formation in the form of expansion and cracking [17]. However, this study focuses on the effect of external sulfates (Na_2SO_4, $MgSO_4$, $FeSO_4$, $CaSO_4$, etc.) which may be present in seawater and/or groundwater in areas in the close proximity to industrial waste or where the soil is particularly high in clay, and rainwater from air pollution [8].

The initial reaction of C_3A can be seen in Equation 4. When tricalcium aluminate reacts with gypsum and water, it forms ettringite. If there is not enough sulfate present for the tricalcium aluminate to fully hydrate, then a secondary reaction occurs which produces an unstable product named monosulfoaluminate instead of ettringite (Eq.5). In situations where tricalcium aluminate consumes sulfate ions faster than the formation of gypsum, the monosulfoaluminate may form simultaneously with ettringite.

$$C_3A + 3C\bar{S}H_2(gypsum) + 26H \rightarrow C_6A\bar{S}_3H_{32}\ (ettringite) \qquad \text{Equation 4}$$

$$2C_3A + C_6A\bar{S}_3H_{32}(ettringite) + 4H \rightarrow 3C_4A\bar{S}H_{12}\ (monosulfoaluminate) \qquad \text{Equation 5}$$

This phase transformation is the basis for sulfate attack. As the monosulfoaluminate comes in contact with an external source of sulfate ions, it is able to form more ettringite according to (Eq.6).

$$C_4A\bar{S}H_{12} + 2C\bar{S}H_2 + 16H \rightarrow C_6A\bar{S}_3H_{32} \quad \text{Equation 6}$$

This transformation degrades the concrete specimen since the transformation is accompanied by an increase in solid volume by 55% [8] which causes cracking, spalling, and softening of the cement paste. The expansion in volume is also caused by the increased water absorption due to the ettringite crystal growth. This expansion in sodium sulfate solutions was categorized into two stages in [25] where during the first stage, the paste undergoes low expansion followed by the second stage of rapid expansion until cracking. This expansion is different in magnesium sulfate solutions which generates rapid expansion continuously. Sulfate attack may cause more than just expansion as it also decalcifies the C-S-H gel which greatly affects the compressive strength of the mix.

Gollop and Taylor [26] studied slag blends subjected to water, sodium sulfate solution, and magnesium sulfate solution through scanning electron microscopy. They concluded similar trends in the decalcification of the C-S-H in both solutions, with the $MgSO_4$ being more pronounced. The increased attack in the magnesium sulfate solution is due to other forces beyond the ingress of sulfate ions which was explained in [27]. The attack by magnesium ions forms a brucite layer at the exposed surface which consumes a large amount of CH. As the CH is depleted, the pH of the pore solution decreases, prompting the C-S-H to release CH in order to maintain stability. Eventually the calcium ion is completely replaced by the magnesium ions leading to the formation of M-S-H.

Santhanam, Cohen, and Olek [25] proposed a mechanism for sodium sulfate attack in six steps which will be briefly reviewed in the following paragraphs. The mortar is initially subjected to external sulfates in a solution with a pH of 6-8. The pH increases within minutes after the mortar specimens are introduced to a range of 11-12 and remains constant as long as the water is stagnant. They report this is different in field conditions since usually sulfated groundwater flows continuously, which keep the pH at the low levels of 6-8. One report [28] studied the effects of keeping pH at a constant level compared to laboratory conditions and found expansion and compression tests were affected, especially in slag blends. From their results, expansion is lowest when the pH was kept at a constant level of 7 and increased at lower and higher levels of 3 and 12, respectively. This was more evident in slag mixes compared to other blends of mineral admixtures, such as silica fume and fly ash. Strength reduction is also greater as the pH is lowered due to more prominent decalcification of the CSH [28].

In the second step of the proposed mechanism for attack, gypsum and ettringite form near the surface and were described as “skin trying to expand” but is being resisted by the unaffected mortar beneath the surface layer [25]. This imposed compressive force in the surface region and tensile force throughout the rest of the system causes cracks in the interior of the mortar which accounts for steps 3 and 4. These cracks create an opening for sodium sulfate solution to ingress where it is then able to react with the hydration products seen in Equation 6. The fifth step is characterized as the phase in which deposition zones are filled with gypsum. As the newly formed gypsum expands and creates tensile stresses within the interior of the mortar, new cracks appear. Three zones are now present: the disintegrated surface, areas of deposition of attacked products and the cracked interior which is chemically unaltered. The final step in the process leaves the

surface vulnerable to thaumasite formation since the solution is capable of accessing the decalcified CSH gel and ettringite.

Thaumasite formation is different than that of ettringite or monosulfoaluminate formations in that it occurs when external sulfates attack the CSH, not the aluminate phases. Crammond described the attack from studies performed in the UK [29] as having significant effects on the cement paste matrix by replacing CSH with thaumasite turning the matrix into a "white, mushy incohesive mass". Since thaumasite does not have binding ability, the aggregate particles are being held together loosely, which can greatly affect strength. However, Alapour and Hooton [30] concluded after 38 years in 50g/L sodium sulfate solution, thaumasite was not observed in slag mixes regardless of the cement type used. Similar findings were established in [31] where OPC mixes produced much thaumasite but OPC-slag mixes produced only trace amounts and slag systems had no thaumasite formation at all.

There are three ASTM tests that can measure the sulfate resistance of a given cement or cement blend. ASTM C452 [32] is a test which involves using a high amount of gypsum in cement to measure length change in mortar bars. The drawback of using this test is it is only applicable to Portland cement and is not suitable to evaluate cement blended with pozzolans or slags. ASTM C1012 [33] is suitable for neat and blended cementitious systems and measures sulfate resistance by supplying an external sulfate solution of 5% Na_2SO_4 to mortar bars and measuring their expansion over time. ASTM C109 [34] is a standard test that may be employed to measure the compressive strength of mortar cubes over time. The strength loss of specimens may imply decalcification of CSH if they were stored in sulfate solutions similar to ASTM C1012.

Several factors that affect sulfate durability include permeability, w/cm ratio, use of mineral admixtures, and the chemical composition of the cement and admixtures. The most

influential of these factors is permeability, as the more permeable the microstructure is, the more sulfate ions are able to enter the system and cause degradation. In fact, according to Mehta, controlling permeability of concrete is more important than controlling the chemistry of cement [35]. This can be considered the first line of defense against sulfate attack and may be deemed the physical resistance of concrete whereas the chemical resistance depends on the binder used. Regardless of the curing conditions or age, using slag greatly reduces permeability [36]. It was shown in a study at King Fahd University of Petroleum and Minerals that a 70% replacement with slag reduced the coefficient of permeability tenfold [37]. Al-Gahtani et. al concluded that a 50% replacement offered the best corrosion protection and using 70% replacement results in better sulfate resistance than plain Type V sulfate-resistant cement [37].

The w/cm ratio plays an important role in durability and strength as well. Kim et. al [38] performed a study to determine the effect of the w/cm ratio on durability and porosity using a constant amount of cement and found that an increase in w/cm ratio from 0.45 to 0.60 results in an increased porosity by 150% and decreased compressive strength by 75.6% at 91 days. The same trend was observed in [39] where the w/c ratio increased from 0.23 to 0.27 caused a decrease in compressive strength by 2.06% after 28 days. These trends can be explained by realizing there is an optimal w/cm ratio and excessive water can result in segregation of the aggregates from the cement paste as well as bleeding from the pores. Any extra water that does not react with the cement may leave the system through evaporation or bleeding, resulting in shrinkage, internal cracks and strength loss.

The type of cement and its composition can also affect durability. ASTM C150 imposes limitations on certain chemicals found within the composition of cements including the aluminum, ferric, and magnesium oxides as well as sulfur trioxide and tricalcium silicate. As previously

mentioned, the standard does not have a limit on the C_3A content of Type I cement but limits that for all other cements, including a maximum of 8% for Type II and 5% for Type V which is deemed as the most resistant to sulfate attack. A long-term study performed by the Portland Cement Association showed increasing durability with progressively lesser C_3A contents based on visual appearance [40]. Osborne [41] also reported degradation in visual appearance based on C_3A content as well as a loss in strength evolution over a 5 year period. Controlling the C_3A content of cement restricts the amount of AFm phases available after hydration which are vulnerable to sulfate attack, such as monosulfoaluminate as seen in Equation 5. C_4AF is another source responsible for AFm phases, which is a reason why ASTM C150 limits $2C_3A + C_4AF$ contents to 25%.

The standard, however, does not limit C_2S or C_3S except for Type IV which is used when a low heat of hydration is desired. Cements with similar C_3A contents and variable C_3S contents were studied in [42] and showed that C_3S has a clear effect on sulfate resistance. Data from this report showed cements with high C_3S contents expanded 1% at 330 days where low C_3S cements only expanded 0.18% in the same time. It can be concluded that the resistance to sulfates is not solely dependent on one single variable. Durability is a function of various parameters and large studies with incremental changes in each variable are needed to determine how combinations of each factor affects chemical resistance. There is a need to not only reduce the C_3A content of cement but also to lower C_3S as well. This was confirmed by Cao et al. [28] in which cement with low C_3S and low C_3A offered the best resistance to sulfate attack in terms of expansion and strength development.

CHAPTER 3: MATERIALS AND METHODS

This chapter presents the materials used in this study as well as the methods and tests performed during the course of this research.

3.1 Materials

Two cements and four slags were used in this study to determine the effects of chemical and physical characteristics of the as-received materials on durability and strength in lime and sulfate solutions. The cements were chosen to have similar fineness and Na_2O_{eq} contents but with different C_3A content. C_3A was chosen as a variable in this study based on the information provided in [3] in that C_3A can impact sulfate durability. ASTM C150 [4] imposes a limit for C_3A content for Type II/IIA cements to 8% but does not recommended a limit for Type I/IA cements. Cement A was chosen to meet this limit of 8% whereas Cement B has C_3A content in excess of the limit. These cements have C_3A contents that are mid to high range for cements available on the market.

Slags were selected based on the alumina contents. There is no limit of Al_2O_3 content in slags but ASTM C989 [3] suggests low-alumina slags (Al_2O_3 <11%) increases sulfate resistance regardless of the C_3A content of cement and high alumina (Al_2O_3 >18%) adversely affects sulfate resistance when blended in low percentages (50% or less). The standard does not provide guidance or information regarding slags of alumina content in the range of 11 - 18%; therefore, slags were chosen to have Al_2O_3 below, at, and above 11%. Two of the slags used were in between the range in question with S3 having 14.25% alumina content and S4 containing 16.29%.

As mentioned in the literature review, CaO, SiO_2, MgO as well as Al_2O_3 affect slag's reactivity. Therefore, to limit the variables being studied, CaO and SiO_2 were similar for all slags. The slags were named based on increasing Al_2O_3 contents; however, the MgO contents should be evaluated as well since they are different for each cement with Slag 1 having the highest content and Slag 3 having the lowest.

For mineralogical analyses, quantitative x-ray diffraction was conducted on all as-received materials. Prior to these measurements, the cements were wet-ground with ethanol in a McCrone micronizing mill to a particle size between 1 and 10μm. This procedure was used in order to minimize temperature increases during grinding and avoid dehydration of gypsum to hemihydrate or anhydrite. Following this grinding, the samples were dried in an oven at 40^0C.

The C_3S and C_3A crystal structures as well as other minor phases present in the cements were identified through the use of selective dissolutions (extractions) such as the Salicylic acid/methanol (SAM) extraction method and the potassium hydroxide/ sucrose extraction procedure (KOSH). SAM extraction was used to dissolve alite, belite, and free lime in order to isolate a concentrated residue of aluminates, ferrites, and minor phases such as periclase and alkali sulfates [45]. Potassium hydroxide/ sucrose extraction was the second procedure performed to further dissolve aluminates and ferrites to obtain a residue of C_3S, C_2S, alkali sulfates, and MgO.

XRD scans were collected using the Phillips X'Pert PW3040 Pro diffractometer equipped with the X'Celerator Scientific detector and a Cu-Kα x-ray source. Tension and current were set to 45 kV and 40 mA respectively and 5 mm divergence and anti-scatter slits were used in the automatic mode. Scans were collected for the 7-70˚ 2θ angular range. The back-loading technique was used to load samples into the sample holder in order to minimize preferred orientation. The sample holder was rotated at 30 rpm during data collection to improve counting statistics [46].

Three samples were prepared for each cement, and the average values were used and tabulated along with their standard deviations (σ).

The potential cement phase compositions for both cements are formulated in Table 3-4 and were calculated based on the bogue equations published in ASTM C150 [4]. These values do not necessarily match results from quantitative x-ray diffraction which is known to be the direct phase analyses tool for phase quantification. This discrepancy has been described in literature [45], [47], [48]. In either case, cement B is shown to have the highest C_3A content and is therefore expected to have a higher rate of heat generation at early ages, but lower sulfate durability.

Table 3-1: Bogue Calculated Potential Compound for As-Received Cement

Phase	Cement A	Cement B
C_3S	52	59
C_2S	22	13
C_3A	7.5	11.5
C_4AF	11	6
C_4AF+2C_3A	26	29
$C_3S+4.75C_3A$	88	113

Phase quantification was performed using the Rietveld refinement functionality of the Panalytical HighScore Plus 4.5 software. An external standard method was used to calculate the amorphous content of the as-received cements and slags [49]–[52]. Corundum (Standard Reference Material 676a) obtained from the National Institute of Standards and Technology (NIST) was used as an external standard in this study. The mass absorption coefficient (MAC) of corundum, calculated using the MAC calculator functionality in the Panalytical HighScore Plus 4.5 software, was equal to 30.91 cm^2/g. MAC values for cements and slags were calculated based on their respective chemical oxide compositions. Loss on ignition content was attributed to carbonate decomposition and release of CO_2.

Another key component which may have an effect on strength evolution is the fineness of the cements and more importantly, of the slags. Particle characterization was determined using the Blaine method as well as laser particle size analysis. Density and particle size distribution were also determined.

Density measurements for all cementitious materials were performed three times according to the procedures outlined in ASTM C188 [53] and their standard deviations were within the recommended limits.

The Blaine fineness method followed the procedure described in ASTM C204 [54]. This is considered an indirect method since fineness is determined by the flow of air through a compacted bed of material. There are several drawbacks to this method. A reference material with a known Blaine fineness, SRM114q, is needed for calibration, but Arvaniti et. al. [55] states that "the reference material must have similar shape, particle size distribution, and surface properties to the material of interest or it cannot be a valid comparison." Another drawback is this test is designed for cement, so according to another study published by Arvaniti et. al. [56] it is particularly difficult to quantify fineness of SCMs since it is hard to "form a good compacted bed of specific porosity, especially in finer SCMs." ASTM C204 [54] states a b-value must be determined for calculations. Typically, the b-value of cement is taken as 0.9 and for materials other than cement, it needs to be adjusted. However, a recent discussion at the ASTM C04 December 2016 slag subcommittee meeting suggests that altered b-values from 0.9 are unreliable and 0.9 should be used for slags as well.

Laser particle size analysis was also performed to verify the findings using Blaine fineness. This method has been shown to have a better correlation with heat of hydration of cements [57] but may be problematic since clusters of material may be present leading to inaccurate results.

Particle size distribution was determined using the LA-950 laser scattering particle size analyzer manufactured by HORIBA Instruments using the wet method. The materials were combined with reagent-grade ethanol.

3.2 Methodology of Mortar Preparation and Testing

The proportion of materials used the procedures in [34] with one part cementitious to 2.75 parts of graded sand conforming to ASTM C778 [58] and using a constant water to cementitious (w/cm) ratio of 0.485 for both control mixes and slag mixes. DI water was used. Slag was replaced with cement at levels of 30%, 50%, and 70% and neat cement systems were made for comparison. All slags were used for the compressive strength testing, but slag 3 was excluded for expansion bar measurements due to the significant difference in MgO content.

Sulfate solutions were made abiding by [33] with 5% Na_2SO_4. Lime solutions were made using 3g of calcium hydroxide per liter of DI water.

3.2.1 Compressive Strength Testing

Mortar cubes were prepared following the procedure in ASTM C109 [34] and were mechanically mixed in accordance with ASTM C305 [59]. Specimens were placed in a mold and compacted by hand tamping as described in [34]. Following compaction, a smooth trowel was used to ensure an even top surface and the molds were placed in moisture cabinet conforming to ASTM C511 [60] for 24 hours. Upon demolding, the cubes were evenly divided into two curing regimes being lime and sulfate solutions. Testing was performed 7, 28, 91, and 182 days from mixing. Lime solutions were not changed throughout the duration of the testing. Sulfate solutions were changed following the protocol outlined in [33].

3.2.2 Mortar Bar Expansion Testing

Mortar bars were prepared following [33] and tested accordingly. Bars were initially placed on a riser in a container with preheated water and cured in an environmental chamber at 35 ± 3^{0}C for 23 ½ hours. Plastic sheeting was used to cover the wet mix when placing the molds in the container as to prevent evaporation from the system. Comparison cubes were made in order to test when the bars met a strength of 2850 psi. Cubes prepared according to this method followed the same curing protocol as the mortar bars. Bars and cubes were placed in a lime solution until the companion cubes met the desired strength. Measurements of length change were performed at 1, 2, 3, 4, 8, 13, and 15 weeks and then 4 months from the day the bars met strength. At each testing age the used sulfate solution was discarded and replaced. The initial reading was taken before immersing sulfate solution.

3.2.3 X-Ray Diffraction and Phase Identification

Small samples taken from cubes that had undergone compressive strength testing were used for XRD analysis. Samples were ground to a fine powder using a mortar and pestle until at least 0.800 grams were obtained passing No. 325 sieve. Samples were then mixed with corundum at 10 weight percent for phase quantification. Rietveld analysis was performed according to ASTM C1365 [44] to quantify the hydration products and anhydrous phases.

CHAPTER 4: RESULTS AND DISCUSSION

4.1 Material Characterization

4.1.1 Elemental Oxide Composition of Slags and Cements

Table 4-1: Elemental Oxide Composition of As-Received Cement

Analyte	Cement A (wt%)	Cement B (wt%)
SiO_2	21.20	20.10
Al_2O_3	5.15	5.60
Fe_2O_3	3.61	2.00
CaO	63.91	64.40
MgO	0.70	0.90
SO_3	2.59	3.60
Na_2O	0.14	0.08
K_2O	0.31	0.47
TiO_2	0.29	0.18
P_2O_5	0.15	0.33
Mn_2O_3	0.03	0.03
SrO	0.06	0.07
Cr_2O_3	0.02	0.01
ZnO	0.06	0.03
L.O.I. (950^0C)	1.66	1.80
Total	99.89	99.56
Na_2O_{eq}	0.35	0.39
SO_3/Al_2O_3	0.50	0.64

The elemental oxide compositions for each cement and slag were determined using x-ray fluorescence spectroscopy (XRF) according to ASTM C114 [43] and can be seen in Table 4-1 and

Table 4-2, respectively. The results indicate that Cement A has a lower alumina, alkali and sulfur trioxide content compared to Cement B which therefore might indicate that Cement A will have better performance in a sulfate environment. However, mineralogical analysis will be more revealing and a better indicator to assess sulfate performance of the selected cements.

Table 4-2: Oxide Chemical Analysis for As-Received Slags

Analyte	Slag 1	Slag 2	Slag 3	Slag 4
SiO_2	38.59	35.67	35.44	32.86
Al_2O_3	8.09	10.82	14.25	16.29
Fe_2O_3	0.51	0.54	0.45	0.36
CaO	38.11	41.93	41.06	37.98
MgO	10.83	7.9	5.25	8.88
Total SO_3	2.21	1.91	1.99	2.61
S	0.89	0.68	0.67	0.952
Corrected SO_3	-0.02	0.22	0.31	0.23
Na_2O	0.3	0.2	0.2	0.37
K_2O	0.38	0.37	0.3	0.44
TiO_2	0.37	0.59	0.5	1.21
P_2O_5	<0.01	<0.01	0.01	<0.01
Mn_2O_3	0.59	0.25	0.22	0.25
SrO	0.05	0.08	0.05	0.1
Cr_2O_3	<0.01	<0.01	<0.01	<0.01
ZnO	<0.01	<0.01	<0.01	<0.01
BaO	0.03	0.08	1.06	0.08
L.O.I (950˚C)	1.15	-0.48	0.05	-1.03
Corrected L.O.I (950˚C)	-0.17	0.53	1.06	0.4
Total	99.89	99.85	99.84	100.41
Na_2O_{eq}	0.55	0.44	0.40	0.66

An analysis into the SO_3 content was conducted on slags to determine if slags were formerly interground with gypsum as is allowed in ASTM C989 [3]. The corrected SO_3 content is therefore the value to consider for sulfate content in slags as it excludes sulfides. Sulfides were

determined according to ASTM C114 [43]. The corrected values show that the sulfur present in each slag is mainly in the form of sulfide which would indicate that the slags used in this study were not interground with gypsum. The results also indicate that the CaO and SiO_2 content of the slags are similar while the Al_2O_3 and MgO content vary considerably.

4.1.2 Mineralogical Composition of Slags and Cements

Table 4-3: Cement Phase Content Using XRD

Phase	Cement A (wt %)	σ	Cement B (wt %)	σ
C_3S	48.1	0.1	54.0	0.5
C_2S	23.1	0.2	17.3	0.4
C_3A	5.5	0.2	8.4	0.1
Ferrite	9.9	0.1	5.6	0.0
Gypsum	2.6	0.2	4.3	0.1
Hemihydrate	1.5	0.1	1.4	0.1
Anhydrite	-	-	0.1	0.0
Calcite	1.2	0.2	0.3	0.1
Portlandite	-	-	0.2	0.0
Syngenite	0.7	0.1	0.4	0.0
Quartz	0.1	0.0	0.1	0.0
Aphthitalite	-	-	0.2	0.0
Amorphous/ unidentified	7.2	0.4	7.8	0.4

In order to assess the performance of ordinary Portland cements and slags, mineralogical analysis was conducted on all as-received materials. The mineralogical analysis reveal the crystalline phases present as well as the amorphous content. Table 4-3 and 4-4 present the mineralogical composition of the as-received cements and slags as determined by x-ray diffraction

(XRD) measurements according to ASTM C1365 [44]. The findings indicate that Cement B has higher C_3S and C_3A content but lower ferrite. It is well established in the literature that higher tricalium silicate and aluminate content promote sulfate attack. It is therefore expected that Cement A will have a better performance when exposed to an external sulfate source.

The XRD results for slags shown in Table 4-4 indicate the slags are predominantly amorphous in nature, with only a few weight percent of crystalline phases. As stated in the literature review, amorphous content is the most significant factor affecting the overall reactivity of the slag, which further leads to strength development [11].

Table 4-4: Slag Phase Content Using XRD

Phase	Slag S1 (wt %)	σ	Slag S2 (wt %)	σ	Slag S3 (wt %)	σ	Slag S4 (wt %)	σ
Calcite	0.7	0.1	0.3	0.0	0.6	0.1	0.3	0.0
Melilite	0.5	0.1	0.2	0.0	0.5	0.0	0.7	0.0
Merwinite	-	-	0.7	0.0	-	-	-	-
Quartz	-	-	-	-	1.5	0.0	-	-
Gypsum	-	-	-	-	0.4	0.0	-	-
Amorphous/ unidentified	98.9	0.2	98.8	0.1	97.0	0.1	99.0	0.0

4.1.3 Fineness and Density

Table 4-5 depicts the Blaine fineness results where it can be seen that the fineness of both cements are nearly similar, with Cement A having a slightly higher fineness. As seen from the data in Table 4-6 for slags, using a variable b-value leads to different results than when using a constant b-value of 0.9. Nevertheless, the finest slag is S2 and the coarsest is S4, regardless of the b-value used for the analysis. The difference lies with the remaining slags S1 and S3, with S1 being finer

than S3 using a constant b-value, but being coarser when a variable b-value is employed. The spread of these fineness values is also greater when a constant b-value is used. The results obtained through laser particle size analysis (Figures 4.1 through 4.4) mimic the trend observed when a constant b-value is used in the Blaine fineness calculations.

Table 4-5: Cement Particle Size Analysis, Blaine Fineness and Density

Physical Properties	**Cement A**	**Cement B**
D_{10} (µm)	2.046	2.326
D_{50} (µm)	12.183	13.232
D_{90} (µm)	35.372	38.168
Mean size (MPS) (µm)	15.915	17.415
ASTM C204-Blaine Fineness (m^2/kg)	485	474
Density (g/cm^3)	3.15	3.15

Table 4-6: Slag Particle Size Analysis, Blaine Fineness and Density

Physical Properties	**Slag S1**	**Slag S2**	**Slag S3**	**Slag S4**
D_{10} (µm)	1.00	0.77	1.49	1.57
D_{50} (µm)	7.80	7.34	9.88	10.04
D_{90} (µm)	18.81	16.94	22.29	23.68
Median particle size (µm)	7.80	7.34	9.88	10.04
Mean size (MPS) (µm)	9.16	8.36	11.15	11.8
Blaine Fineness (m^2/kg), b-value = 0.9	642	680	574	466
Blaine Fineness (m^2/kg), variable b	567 (0.936)*	607 (0.923)	584 (0.904)	515 (0.878)
Density (g/cm^3)	2.87	2.86	2.89	2.90

* The value in parenthesis represents the b-value determined for each slag

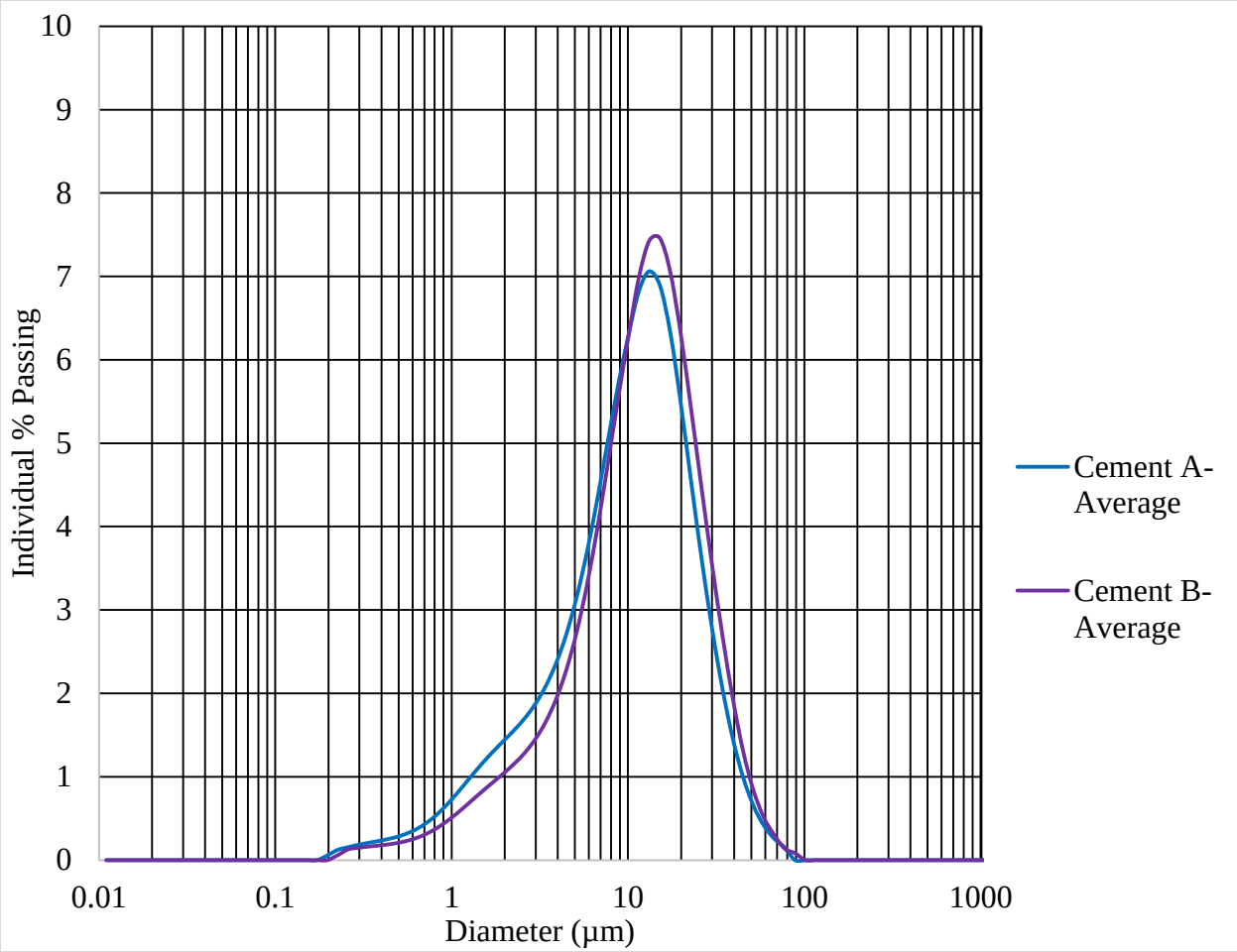

Figure 4.1: Differential Particle Size Distribution for Cements

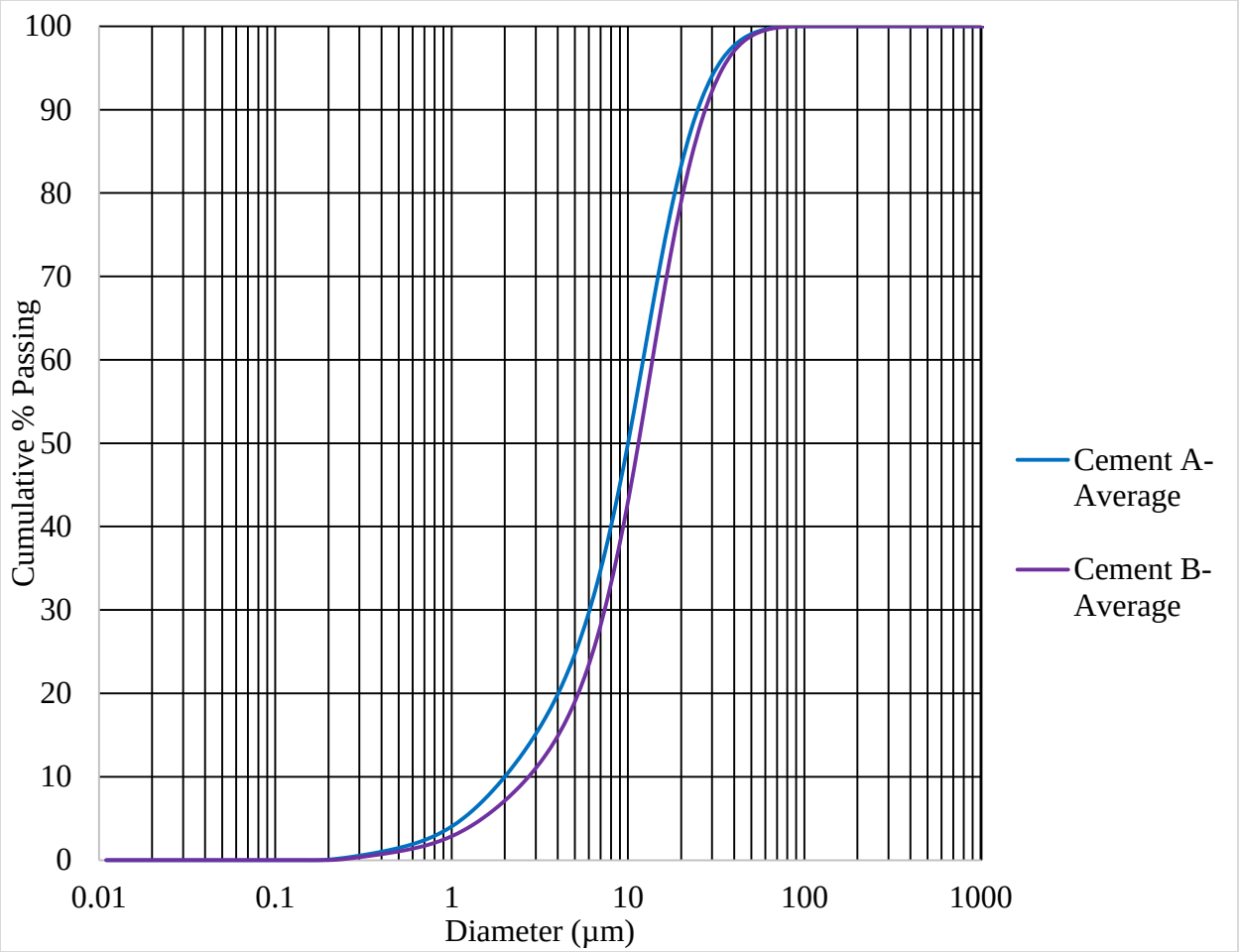

Figure 4.2: Cumulative Particle Size Distribution for Cements

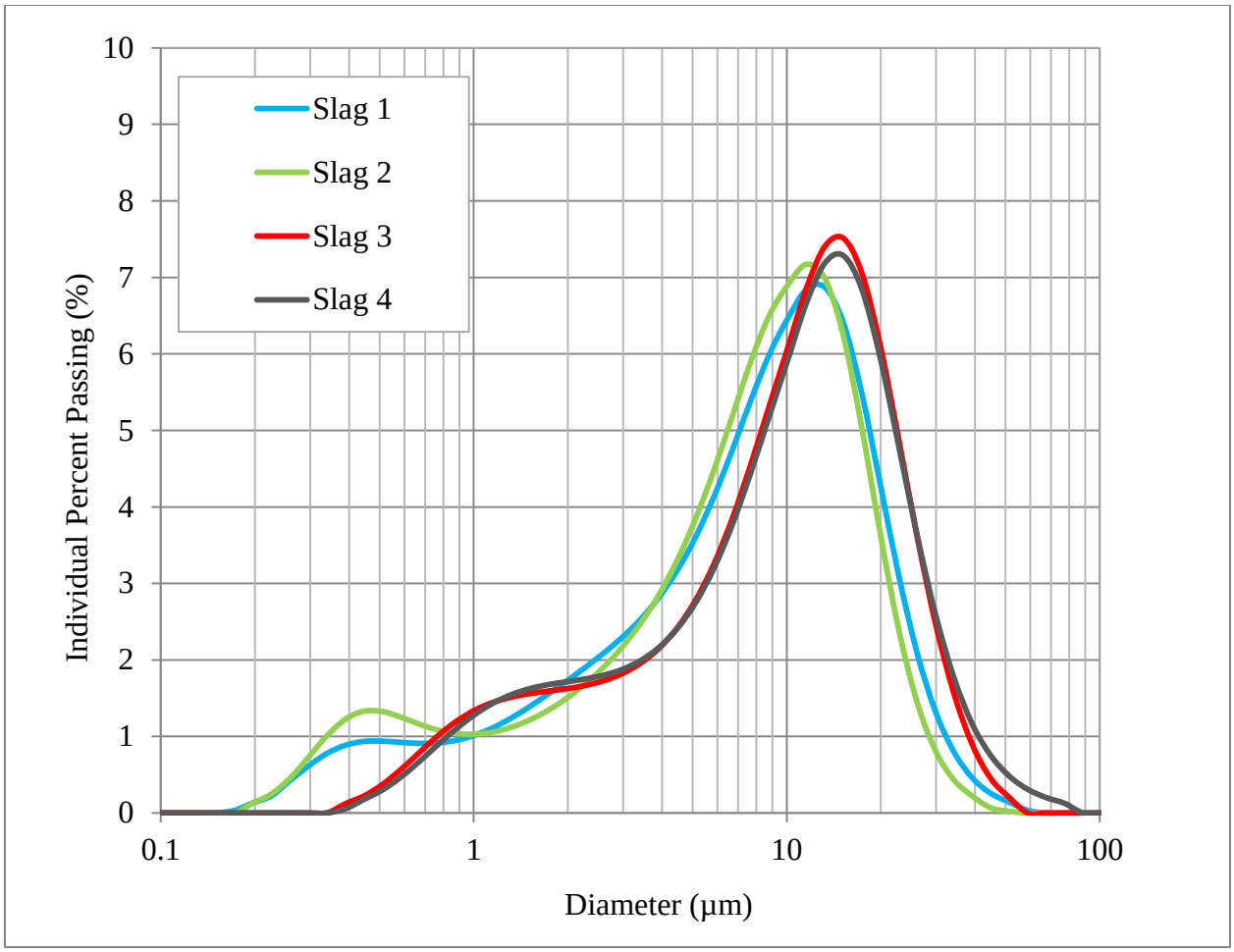

Figure 4.3: Differential Particle Size Distribution for Slags

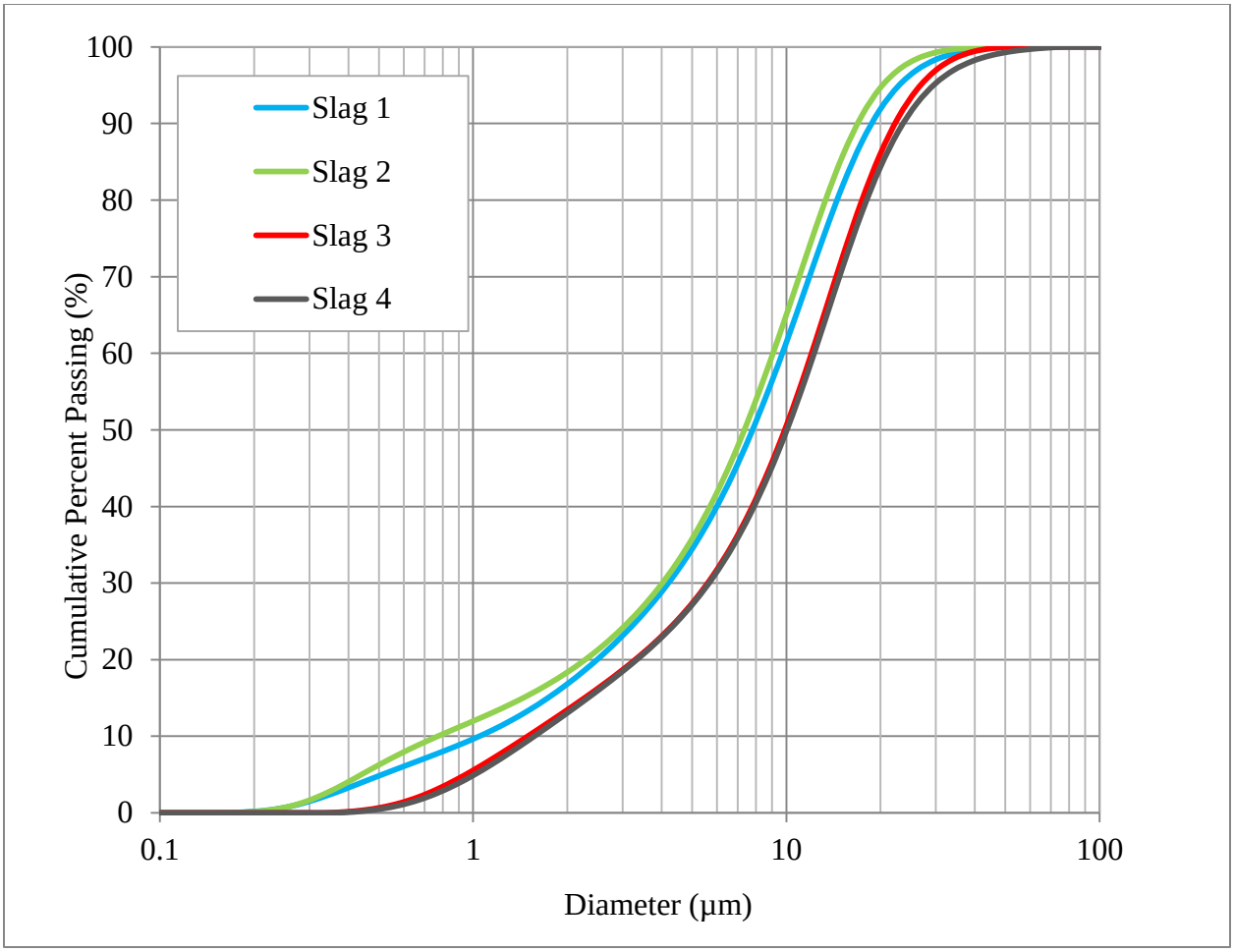

Figure 4.4: Cumulative Particle Size Distribution for Slags

The preceding results indicate that alumina content of the slags is not the only variable that may affect reactivity, and therefore strength gain and sulfate durability. Fineness, too, may have a significant effect on the results. Although S4 had the highest alumina content, it also has the lowest fineness. Based on Equation 1, slag reactivity increases with alumina content, but it is also understood that reactivity increases with fineness. Therefore, fineness and alumina content may exhibit a competing effect on early-age reactivity and temperature rise. S4 is expected to have the worst performance in terms of sulfate durability due to its coarseness and high alumina content,

followed by S3. S1 and S2 are expected to improve sulfate durability since their fineness is relatively high and the alumina content is low.

4.2 Compressive Strength

The collected data from this study was placed into multiple comparison graphs in order to better understand and visualize the effect of the chemical, mineralogical and physical characteristics of cementitious systems on their performance. The first set of graphs will evaluate the role of an external sulfate solution when compared to specimens stored in lime solution. This depiction will establish which mixes are most sulfate resistant. Next, the overall strength gain in both curing conditions are compared for slags of different characteristics in order to indicate which slag is most beneficial for strength development. The section will end with graphs portraying the effect of cement replacement levels and how they perform in a sulfate environment.

4.2.1 Lime Versus Sulfate Exposure

Figures (4.5 through 4.8) and (4.13 through 4.15) offer a visual comparison between the strengths reached in lime and sulfate solutions for cement A. Figures (4.9 through 4.12) and Figures (4.16 through 4.18) show the same graphs for cement B. From these figures, it can be observed that the strength in sulfate relative to lime is higher at 7 days for all mixtures, then rapidly declines to 28 days. Figures (4.13 through 4.18) show a peak in which mortars incorporating slag have a higher percentage of strength in sulfate over lime compared to that found in the control mixtures. However, the values are approximately the same at 28 days. After this point, the sulfate solution affects the pure OPC mortars faster than the blended slag mortars.

A noticeable difference between cement A and cement B is observed at 91 days with low replacement levels of slag; that is, at a replacement level of 30%. For cement A, mortar cubes remained stronger in sulfate environments compared to lime; however, in cement B, the lime-

exposed cubes were stronger. The notable difference lies in the C_3A contents of the cements. Cement B has a higher C_3A content which accelerates the attack in sulfate solutions. Osborne [41] suggests that that "C_3A content of cement is the predominant chemical factor governing sulfate resistance". However, some research shows a lower C_3S content may also play a role in offering increased sulfate resistance [28], [61]. Since cement A has lower values for both for these parameters, the difference in the trend observed at 91 days for low replacement levels may be explained by a combination of both low C_3A as well as low C_3S.

The difference in developed strength between lime and sulfate curing regimes was even more pronounced at 182 days. At this age, all of the mixtures in lime solution outperformed their counterparts in sulfate solution, excluding 70S2-A. This shows a clear sign of sulfate attack and can be better observed in the relative strength graphs plotted in Figures (4.13 through 4.18).

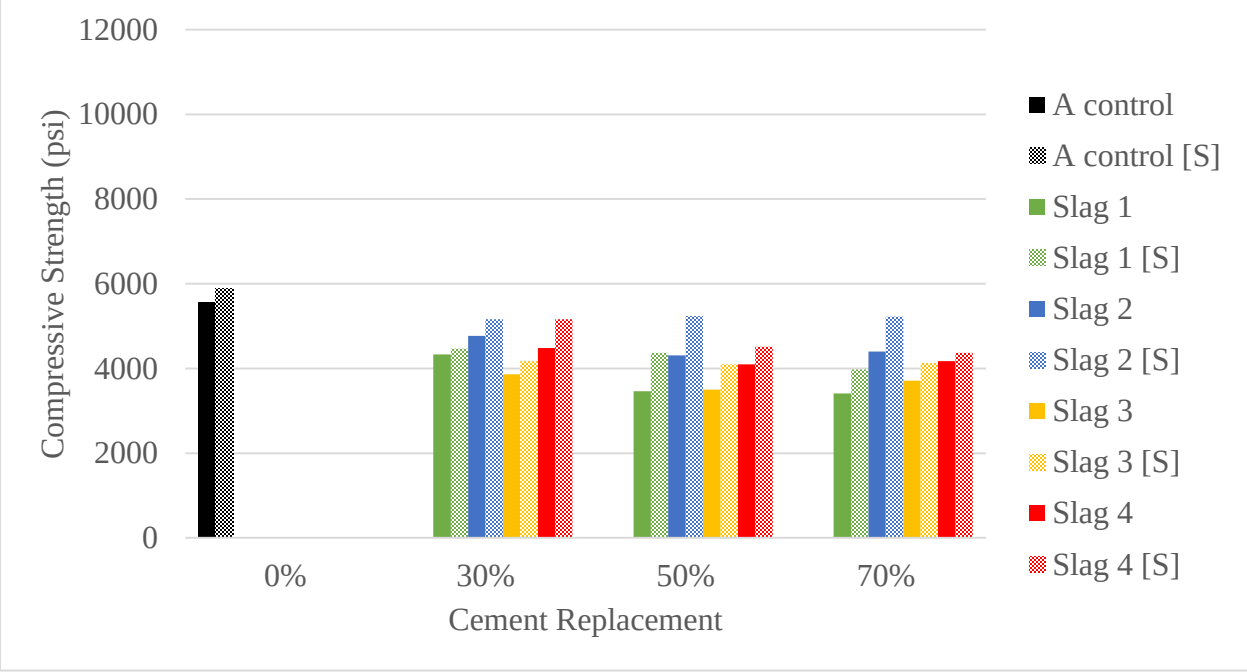

Figure 4.5: Compressive Strength Data at 7 Days for Cement A

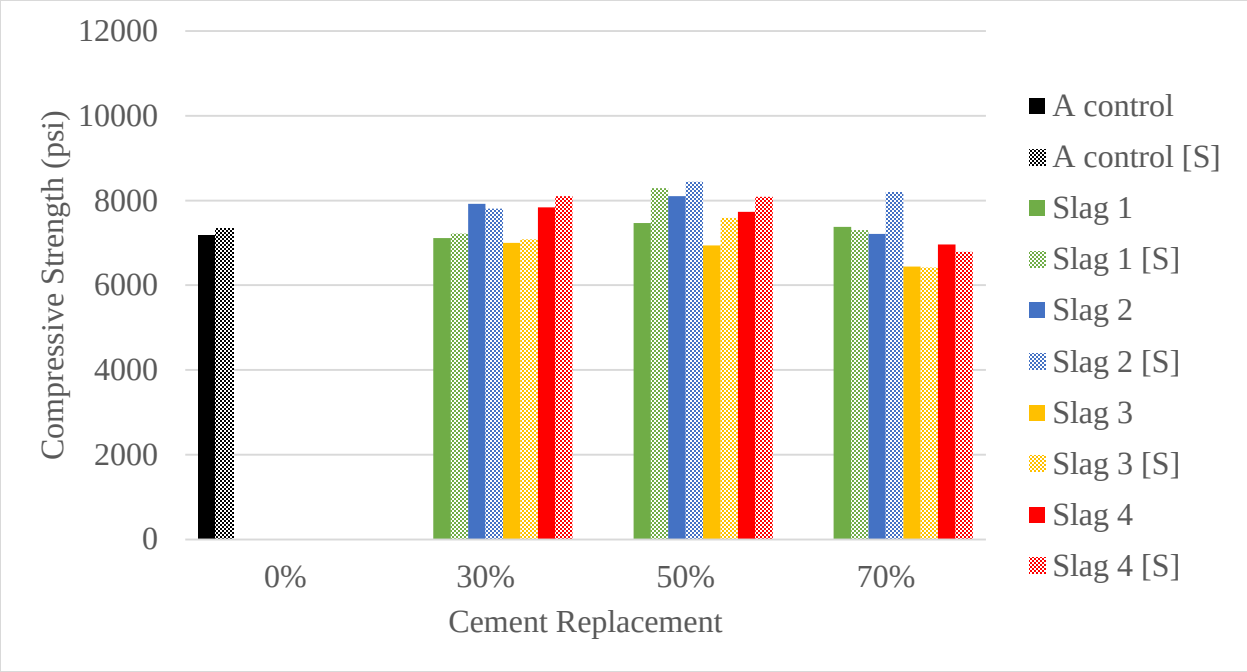

Figure 4.6: Compressive Strength Data at 28 Days for Cement A

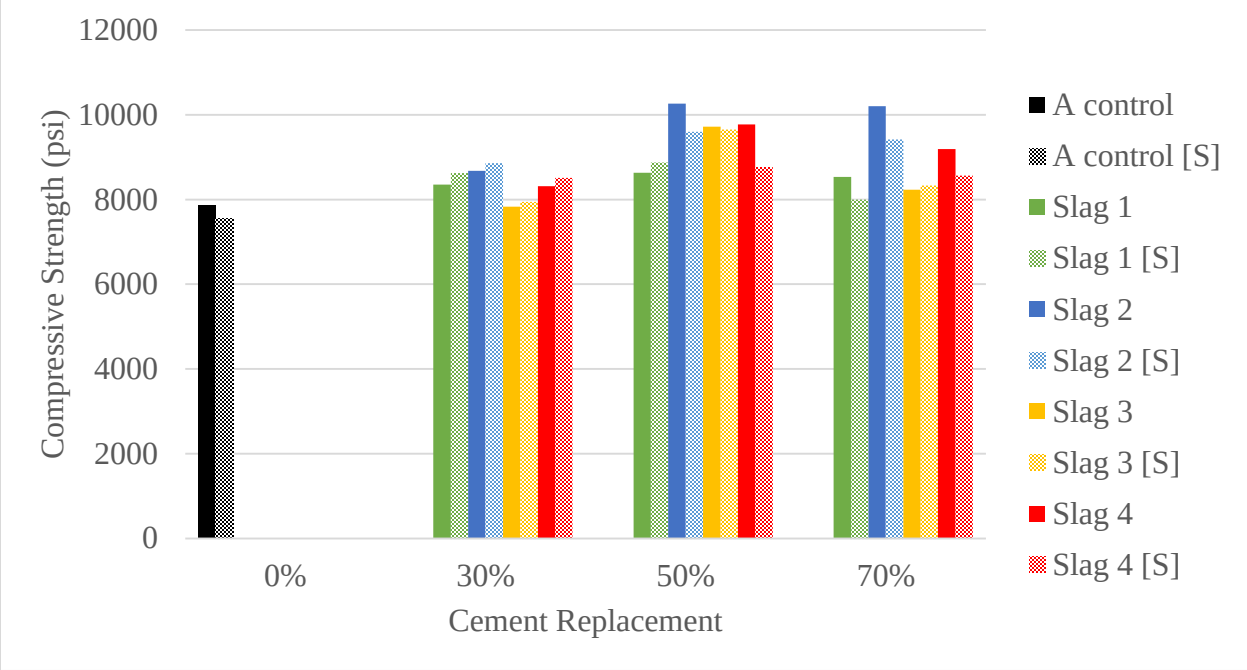

Figure 4.7: Compressive Strength Data at 91 Days for Cement A

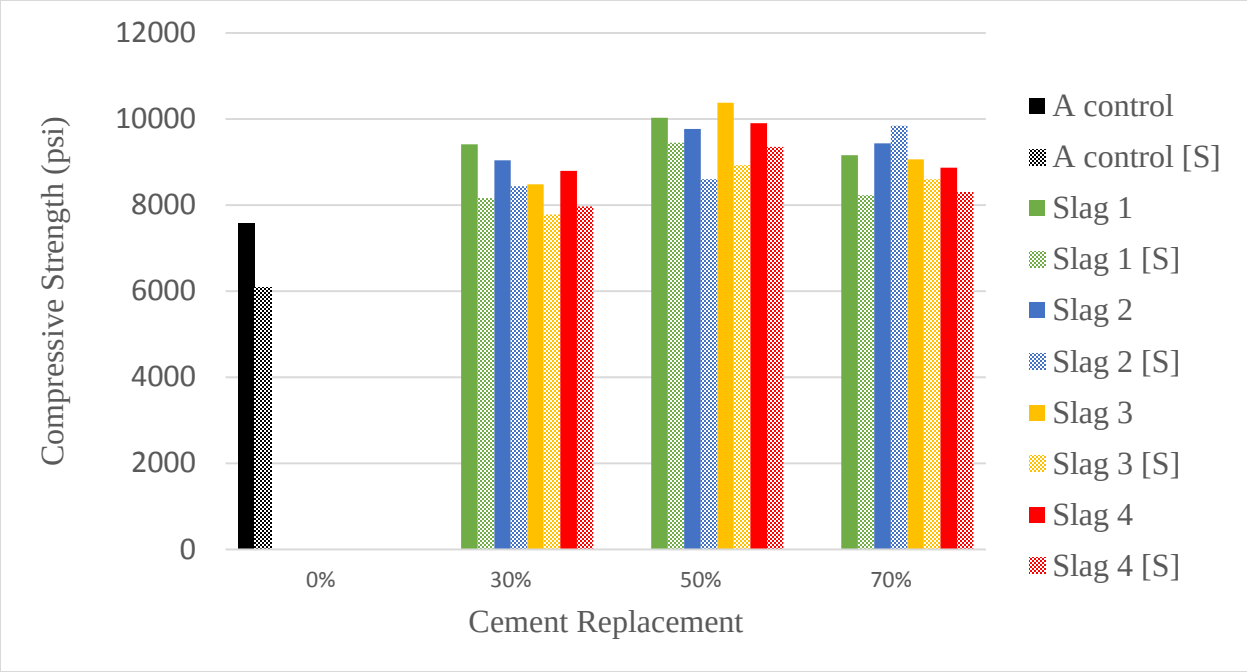

Figure 4.8: Compressive Strength Data at 182 Days for Cement A

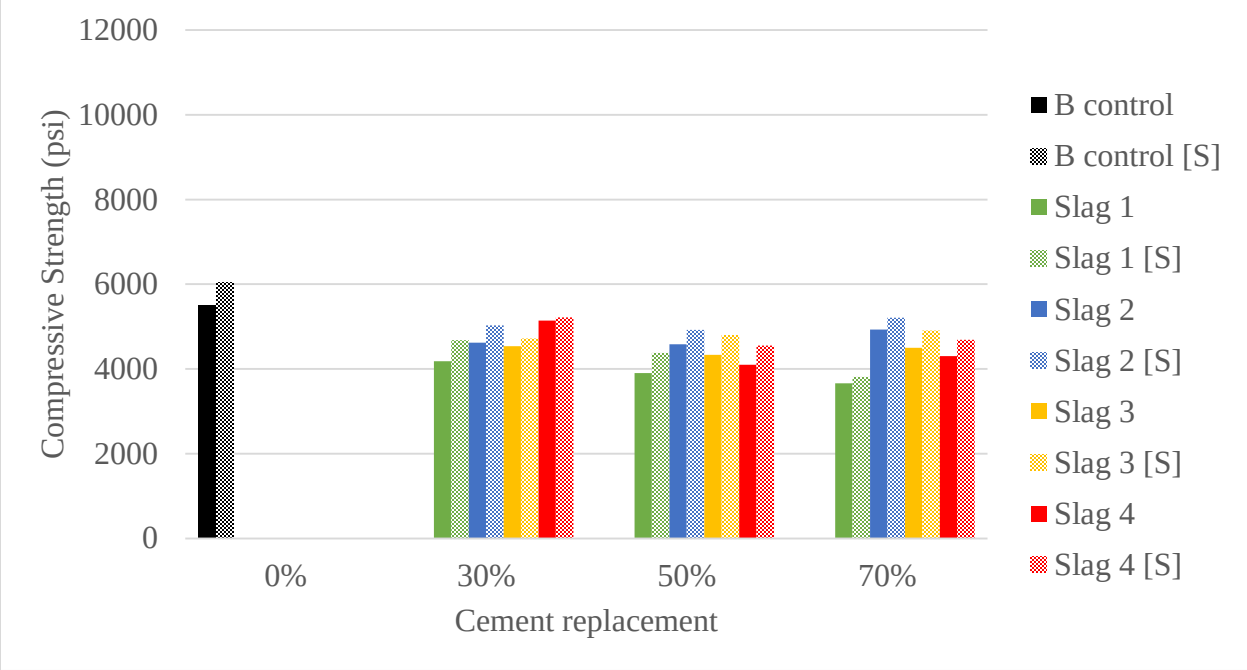

Figure 4.9: Compressive Strength Data at 7 Days for Cement B

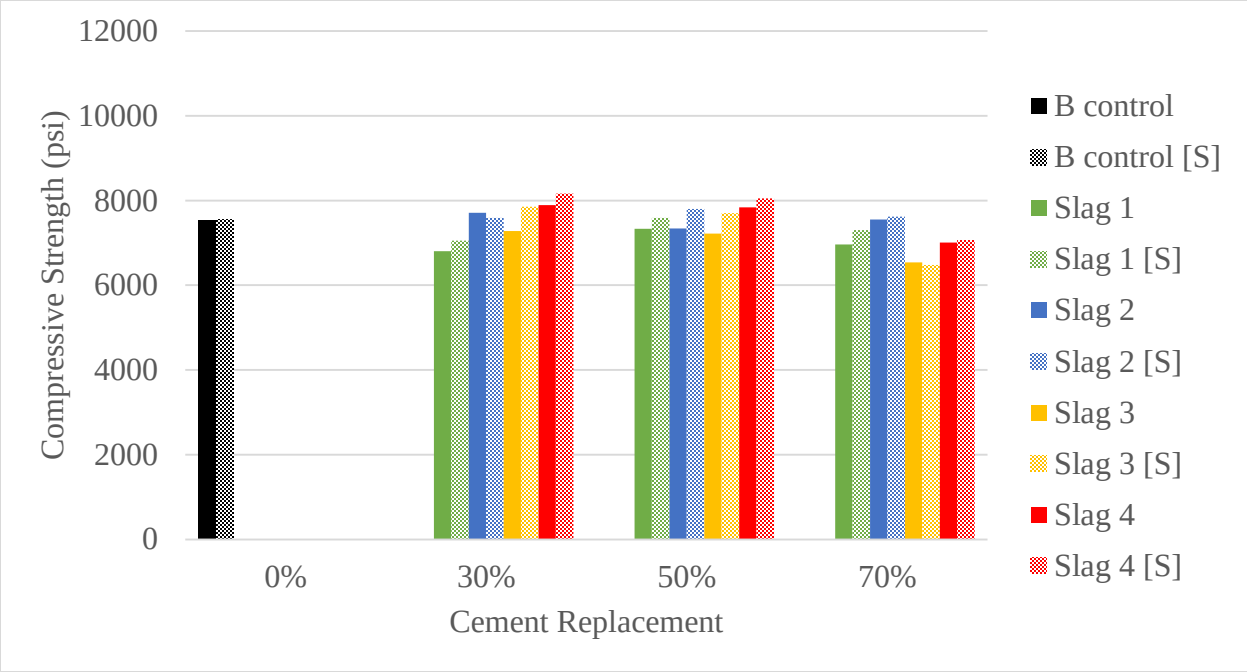

Figure 4.10: Compressive Strength Data at 28 Days for Cement B

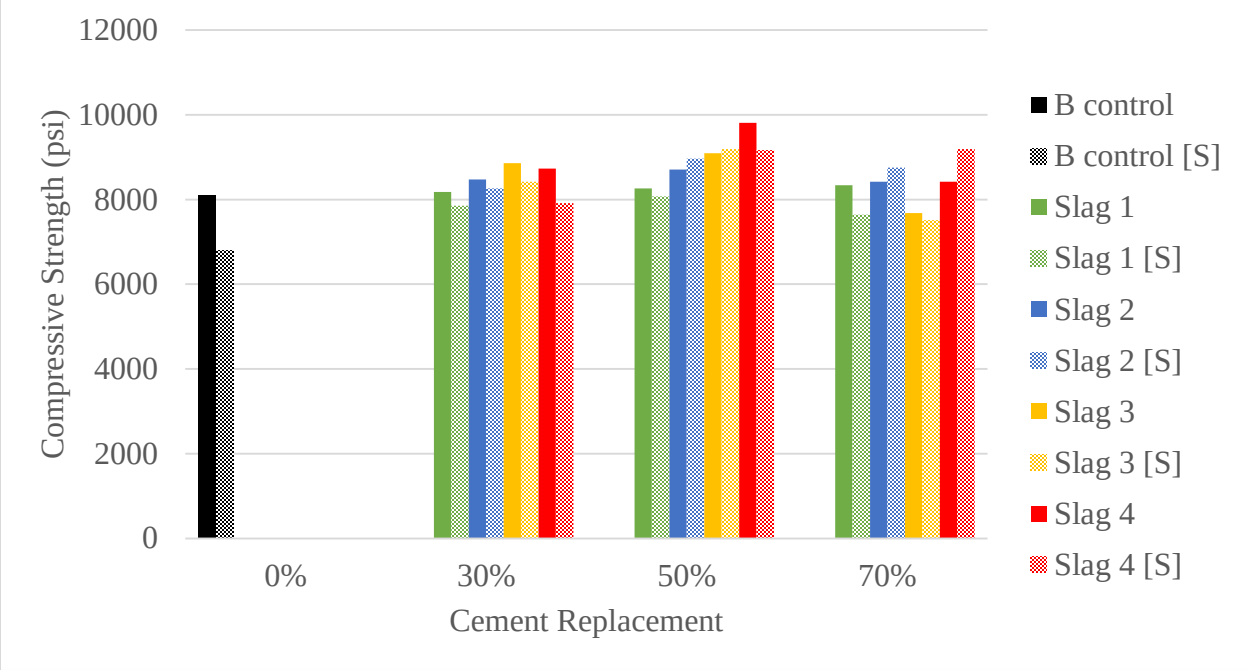

Figure 4.11: Compressive Strength Data at 91 Days for Cement B

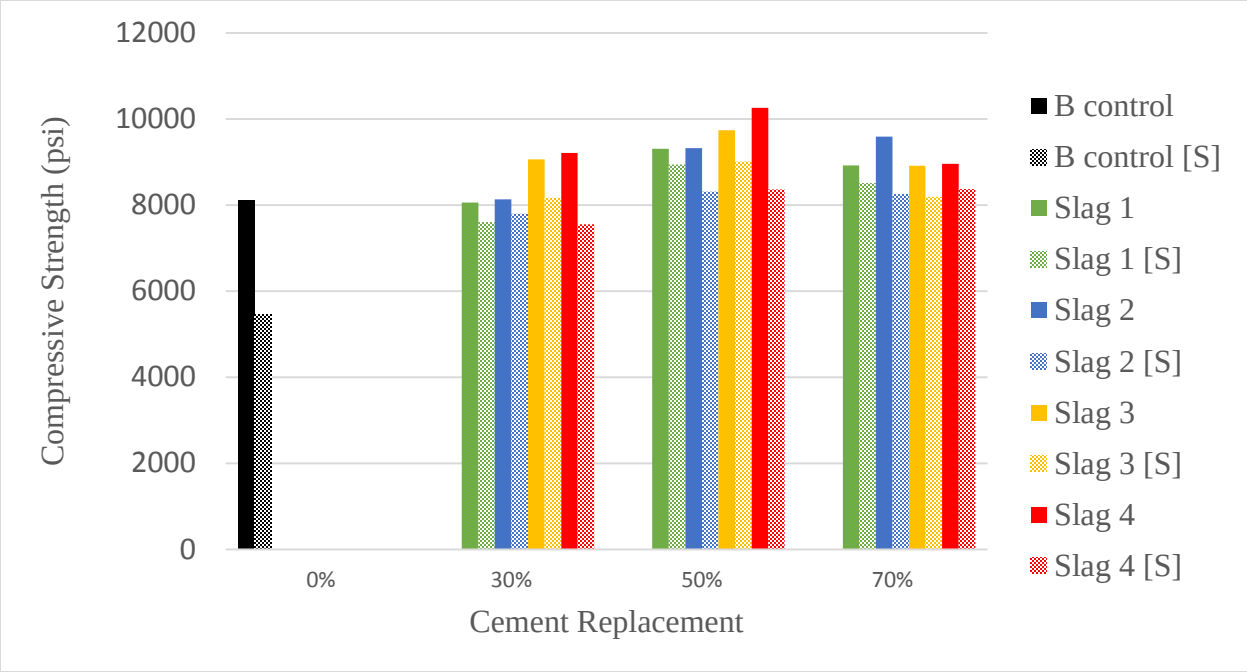

Figure 4.12: Compressive Strength Data at 182 Days for Cement B

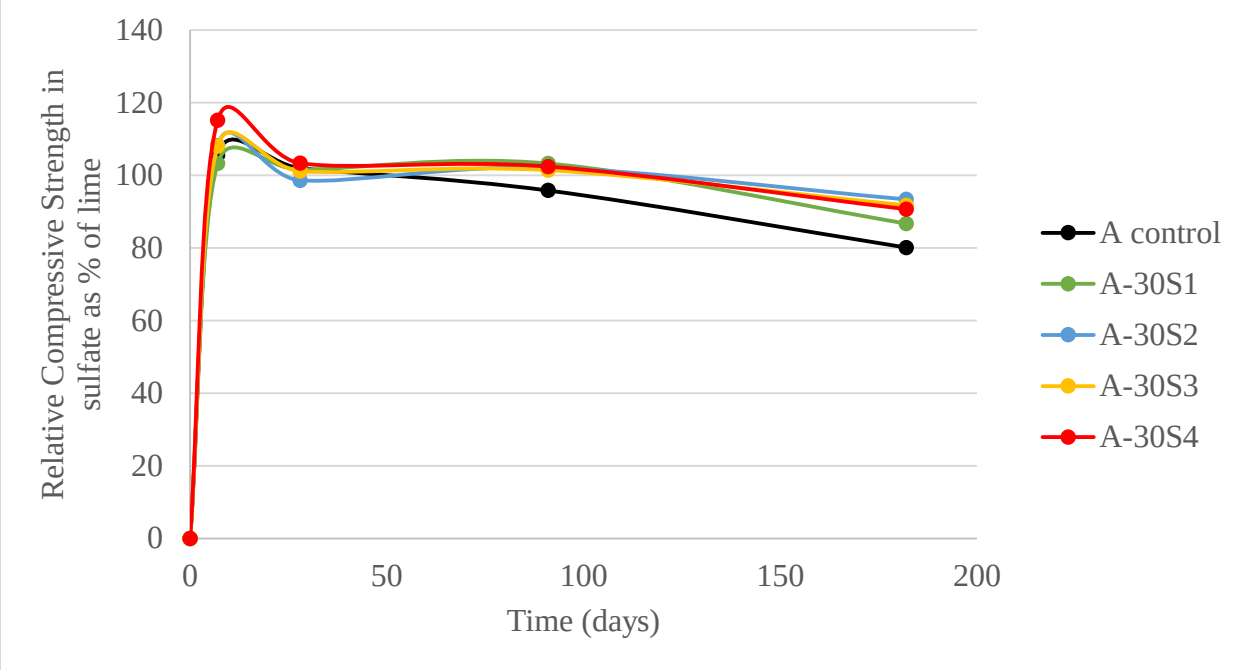

Figure 4.13: Relative Compressive Strength in Sulfate Solution as Percent of Lime Using 30% Replacement of Cement A

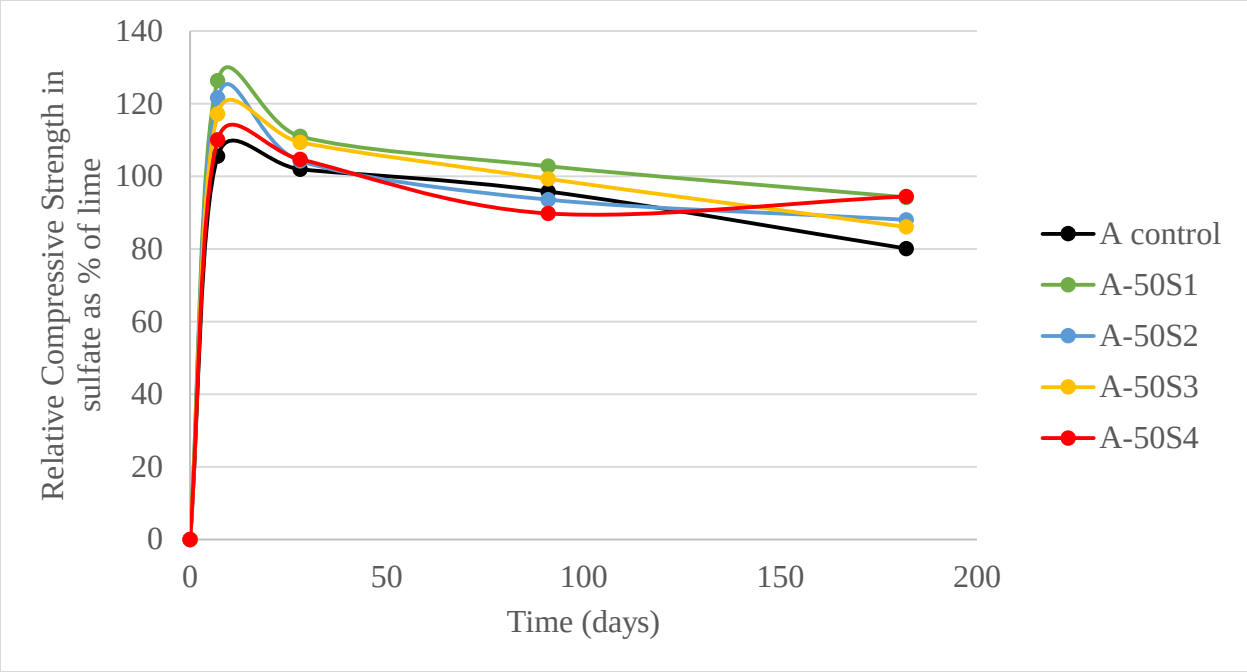

Figure 4.14: Relative Compressive Strength in Sulfate Solution as Percent of Lime Using 50% Replacement of Cement A

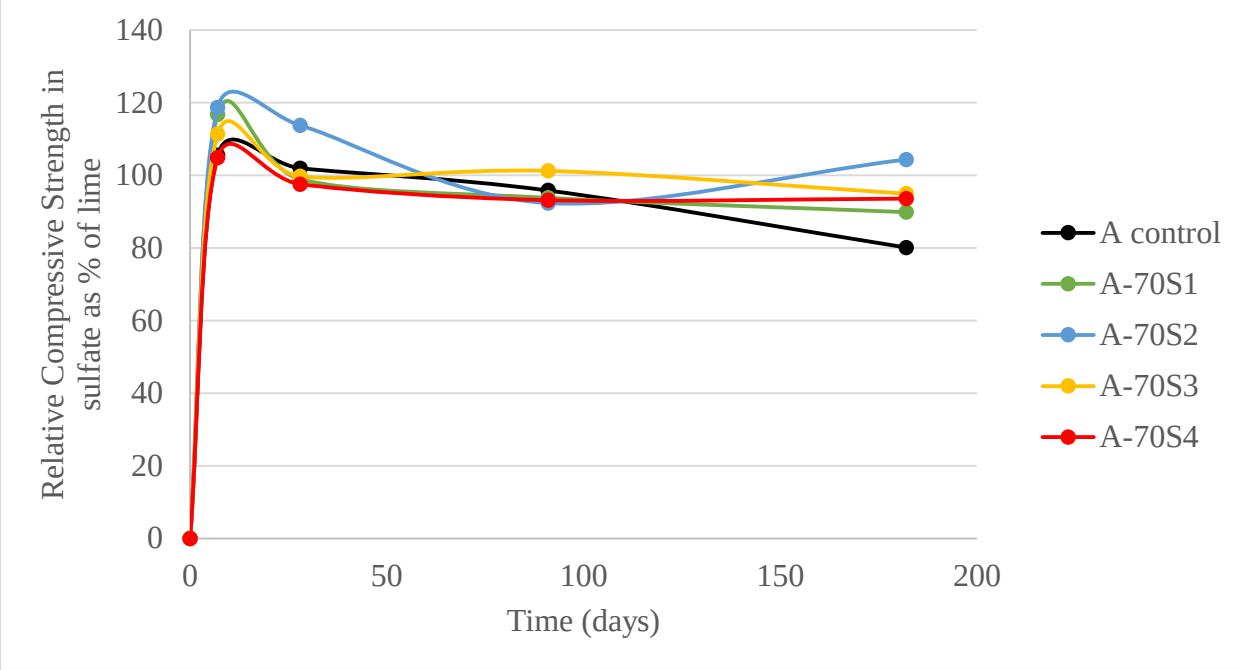

Figure 4.15: Relative Compressive Strength in Sulfate Solution as Percent of Lime Using 70% Replacement of Cement A

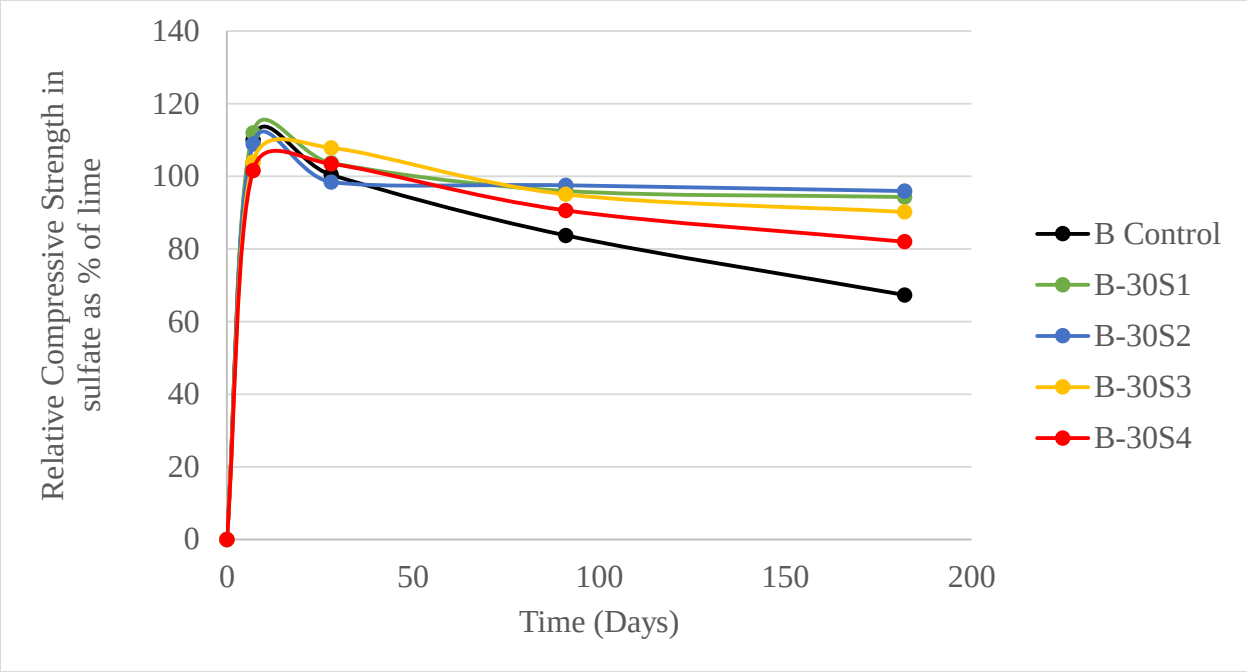

Figure 4.16: Relative Compressive Strength in Sulfate Solution as Percent of Lime Using 30% Replacement of Cement B

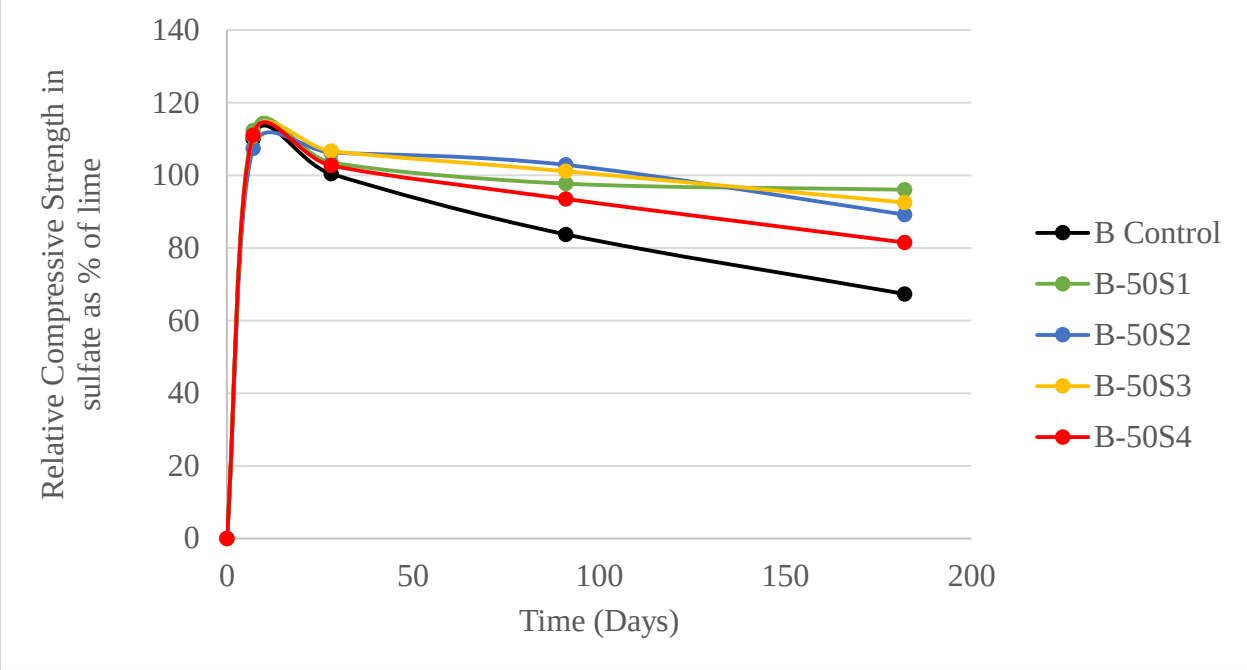

Figure 4.17: Relative Compressive Strength in Sulfate Solution as Percent of Lime Using 50% Replacement of Cement B

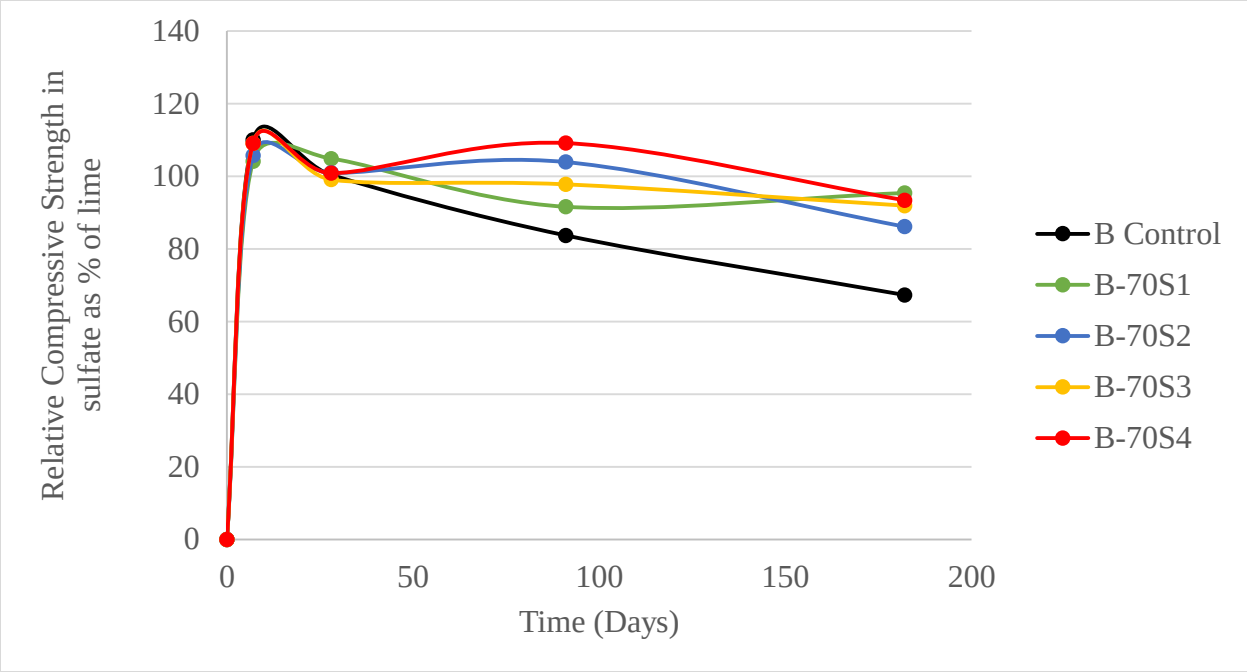

Figure 4.18: Relative Compressive Strength in Sulfate Solution as Percent of Lime Using 70% Replacement of Cement B

4.2.2 Strength Development for Slags of Variable Chemical Composition

As expected, the control mixture developed highest strength at 7 days compared to all slag mixtures in both lime and sulfate solutions. This has been widely observed in the literature [8], [23], [24] and is most likely due to the lower rate of slag hydration compared to OPC. Also, all slag mixtures developed higher strengths compared to the control at later ages of 91 and 182 days in both curing regimes, though the difference in strength is more pronounced in cement A when observing lime cured cubes, but cement B when sulfate exposure is compared.

An important note to discuss though is the strengths reached at 28 days. This is the age at which most cement producers analyze the quality of a mixture. The type of slag used as well as the replacement percentage seems to affect the strength compared to the referenced control mixture. For high early strength concrete, high percentages of slag should not be used since there

is not sufficient time for the slag to fully react as can be seen in Figures 4.23 and 4.29 for cements A and B, respectively. Lower replacement content may be employed but caution is needed and analysis should be done before placement. For cement A, low replacement levels lead to comparable results to that of the control mixture. However, for cements with high C_3A content, as with Cement B, slags with high fineness or high alumina content is needed to surpass the strength of the control mixture at 28 days when 30% is used. At 50% replacement with cement B, the results are analogous. It is to be remembered that strength alone is not enough of an indicator for concrete performance and durability is critical for consideration of any particular mixture proportioning and design.

The observations from these graphs cannot be made to firmly state whether one slag is superior to another. Specimens with a high content of slag undergoing lime exposure were shown to have similar strengths at 182 days except for S2 which was shown to be higher. The greater strength of S2 at this age and replacement level may be attributed to the higher particle fineness of the materials compared to the other slags. However, when cement A was replaced with a low percentage, a clear trend was observed in the following order of increasing strength: S3 < S4 < S2 < S1. This trend aligns precisely with the order of slags with decreasing Al_2O_3/MgO contents. Cement B mixtures showed different results, indicating the importance of the cement composition and its interaction with slags. At a high replacement level with Cement B, nearly all the slags had the same strength at 182 days except for S2 which was only slightly higher. However, at 30% and 50%, slags with higher alumina contents developed higher strength at 182 days.

Strengths obtained from cubes placed in a sulfate solution follow a similar trend. At 28 days, S1 and S3 had lower strengths than the reference cements, further implying the importance of fineness and alumina content for early age strength development. At 70%, most mixtures had

lower strength than plain cement systems, aligning with the results seen in the lime cubes. The only replacement percentage that is beneficial at this early age is 50%. At later ages, however, all slags drastically improve performance against sulfate attack when compared to the reference cements, most noticeably in cement B. S2 outperforms the remaining slags when Cement A is analyzed, which is most likely due to its high fineness and its effect on the degree of reaction and therefore its ability of blocking more sulfate intrusion. With cement B, a slight advantage is given to S3 in terms of late age strength in a sulfate environment. However, it must be stated that longer exposure times are critical in developing a better understanding to the effect of slag chemistry and physical characteristics on performance of blended mortar when exposed to sulfate solution. At 180 days of exposure, strength drop for blended mortars in sulfate solution is not providing enough time for conclusive observation.

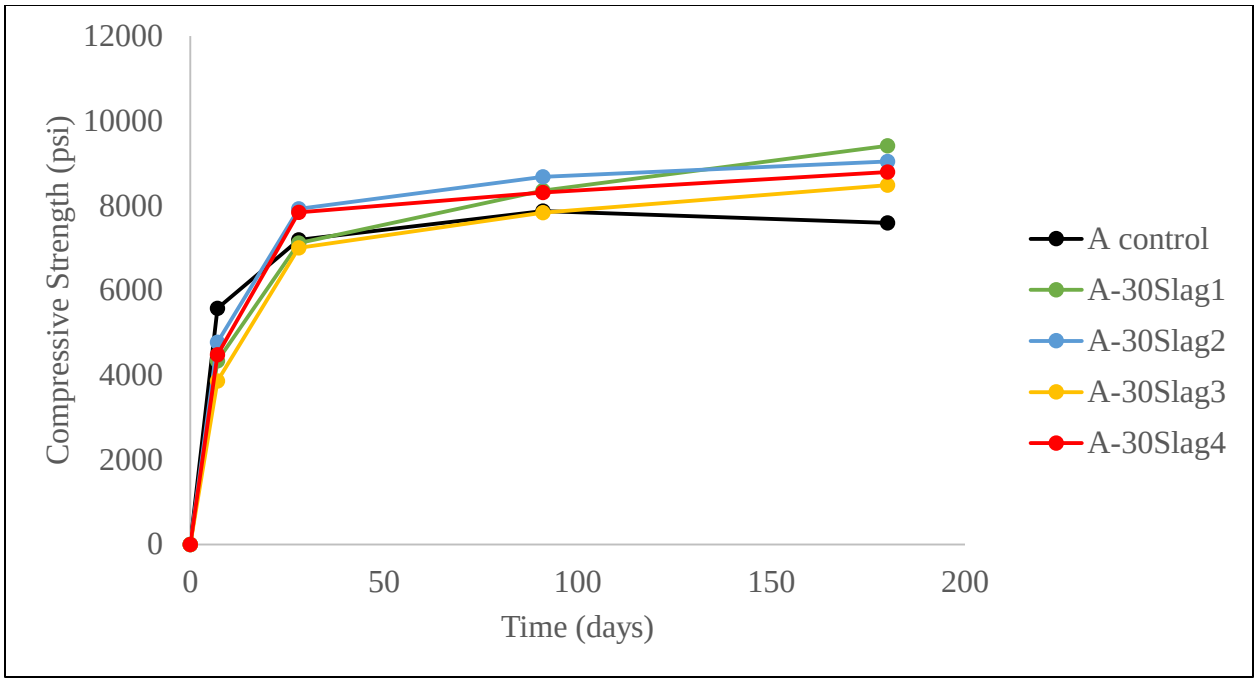

Figure 4.19: Strength Development for 30% Replacement of Cement A in Lime Solution

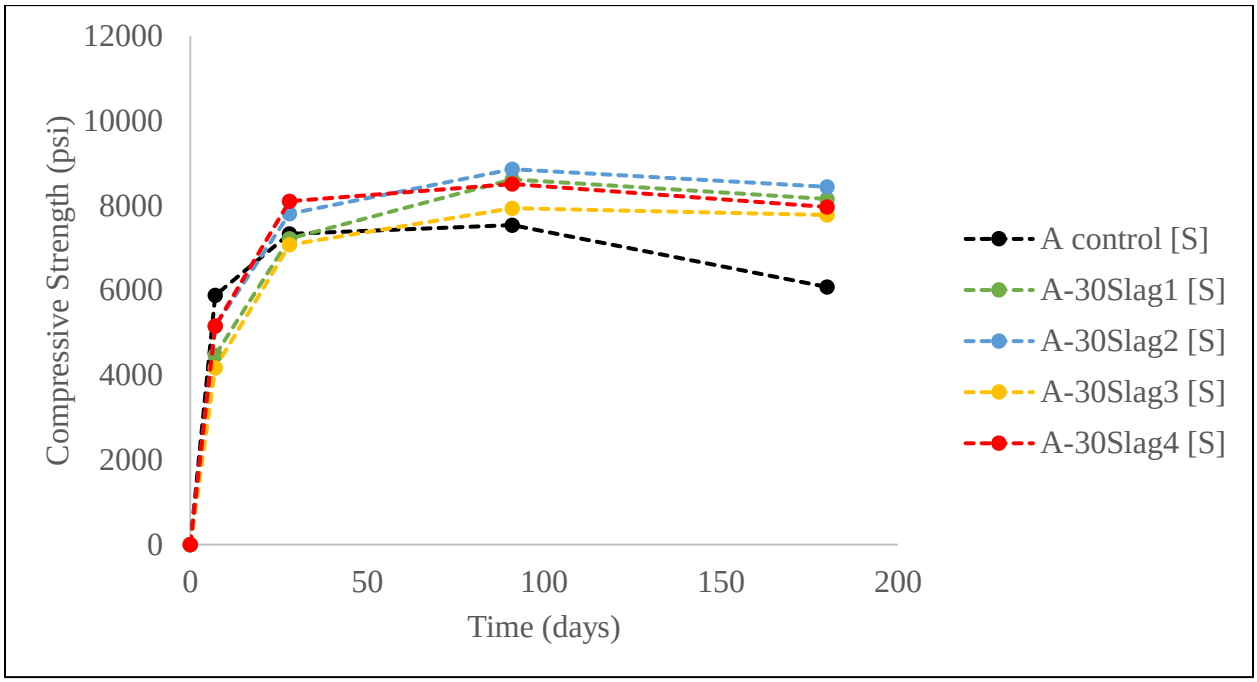

Figure 4.20: Strength Development for 30% Replacement of Cement A in Sulfate Solution

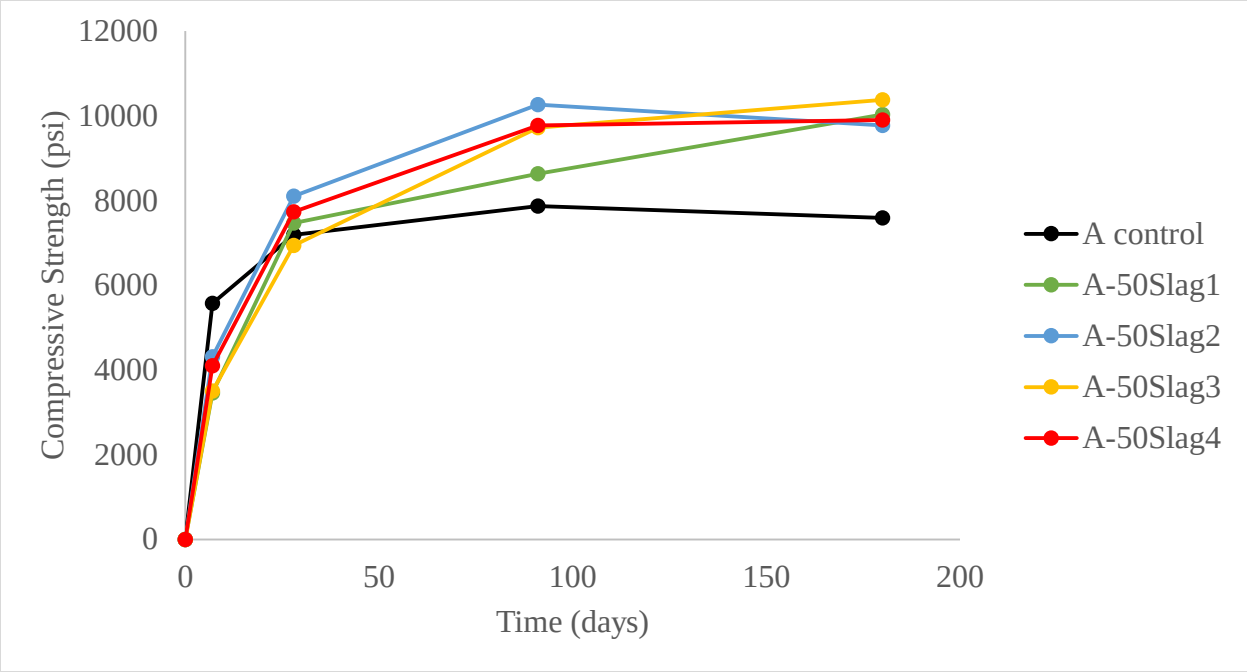

Figure 4.21: Strength Development for 50% Replacement of Cement A in Lime Solution

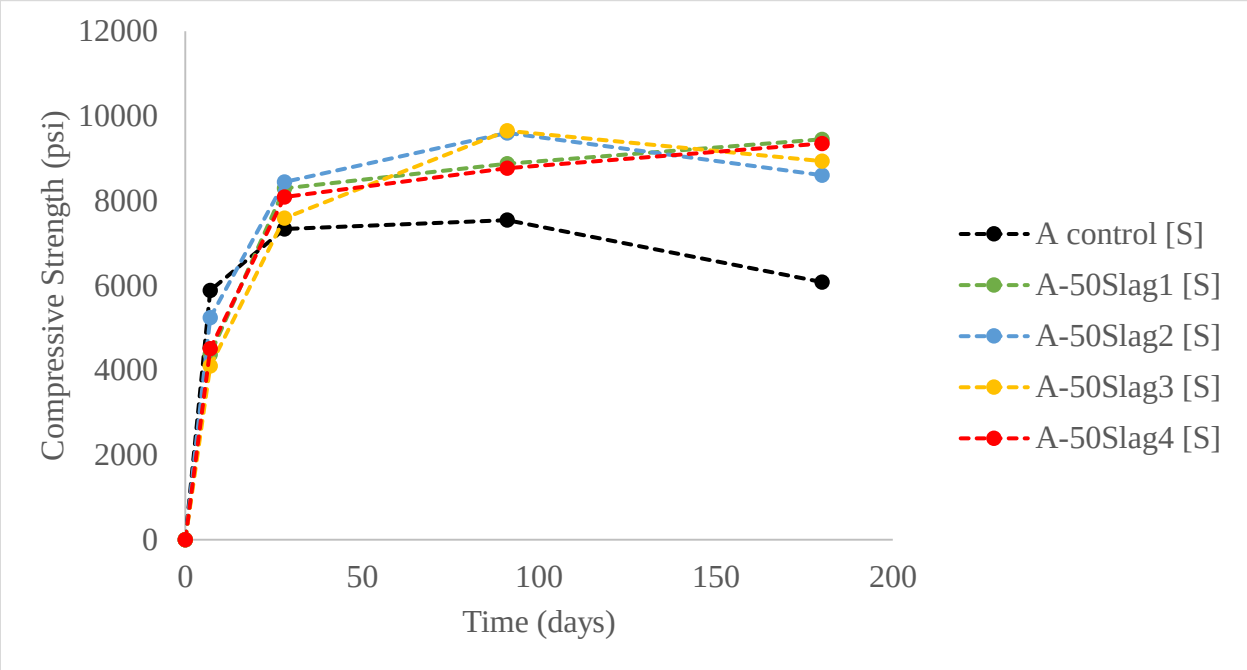

Figure 4.22: Strength Development for 50% Replacement of Cement A in Sulfate Solution

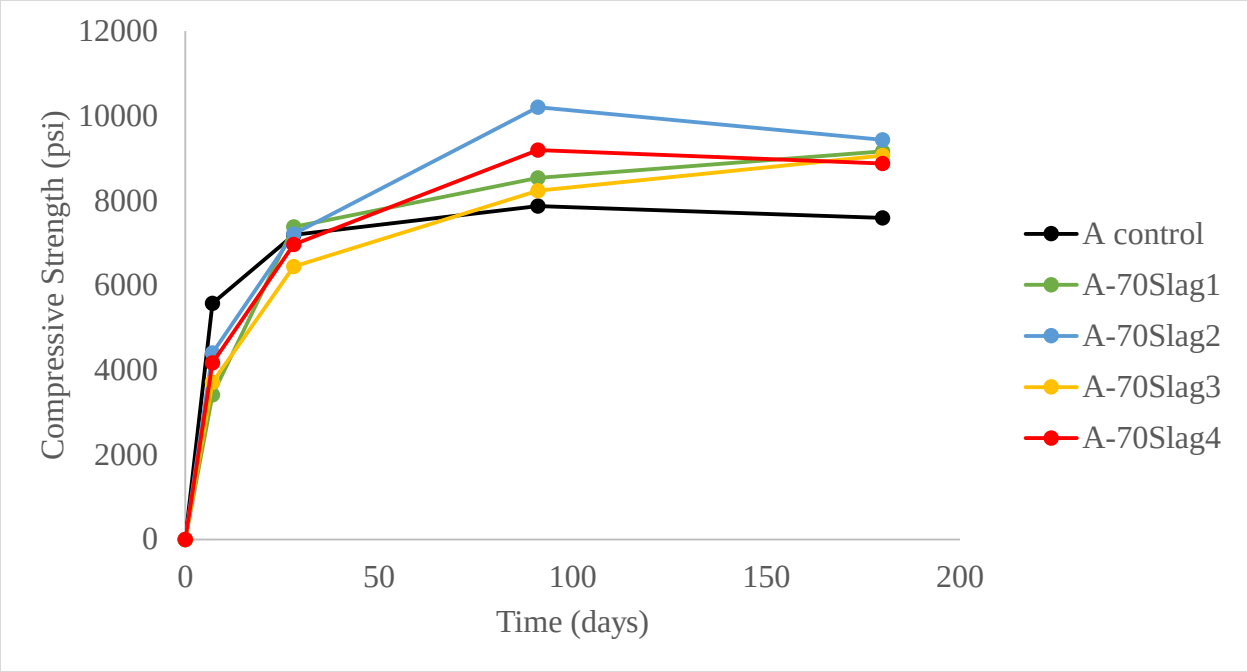

Figure 4.23: Strength Development for 70% Replacement of Cement A in Lime Solution

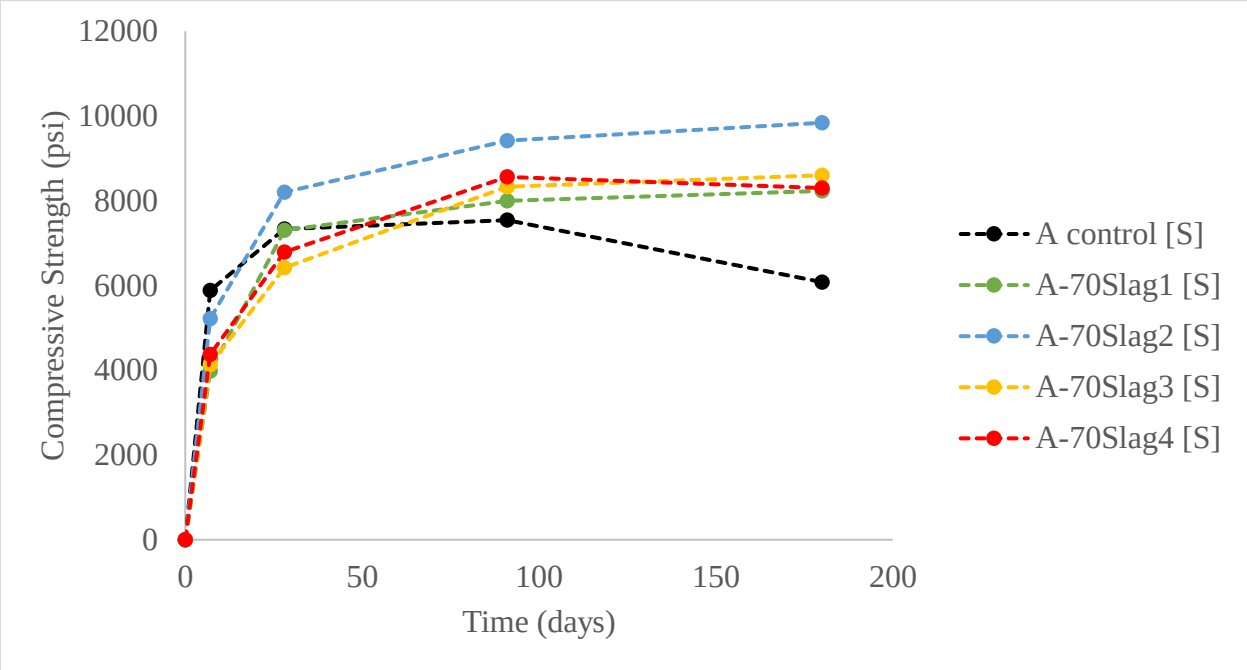

Figure 4.24: Strength Development for 70% Replacement of Cement A in Sulfate Solution

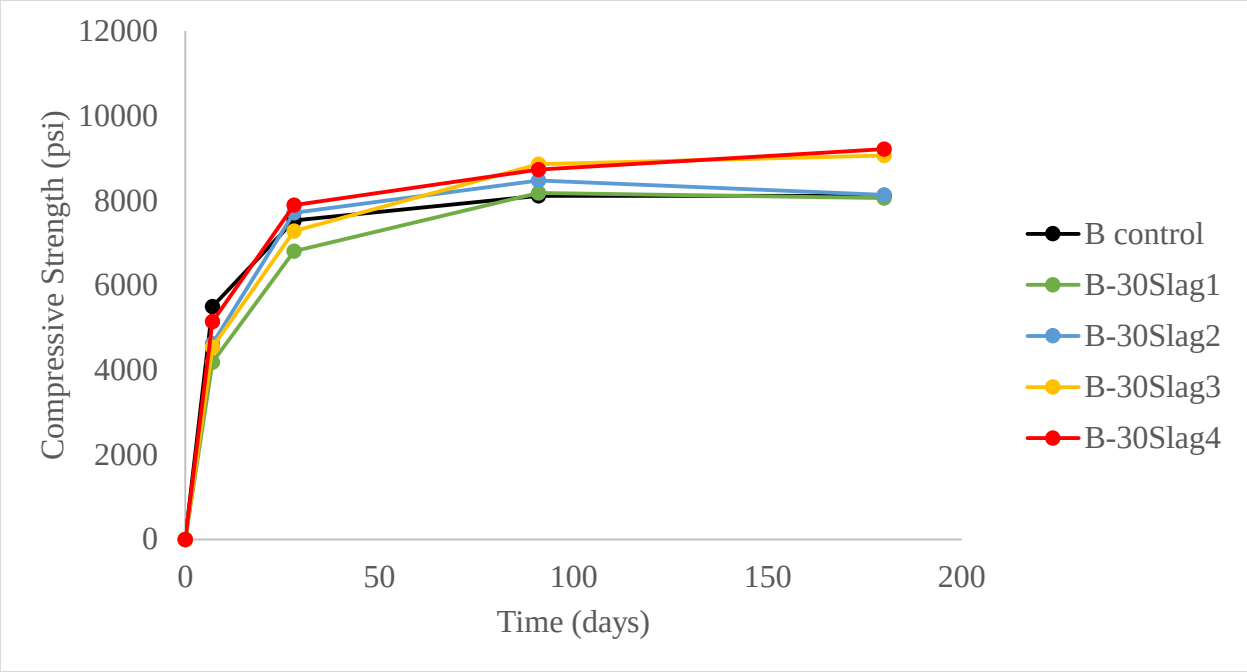

Figure 4.25: Strength Development for 30% Replacement of Cement B in Lime Solution

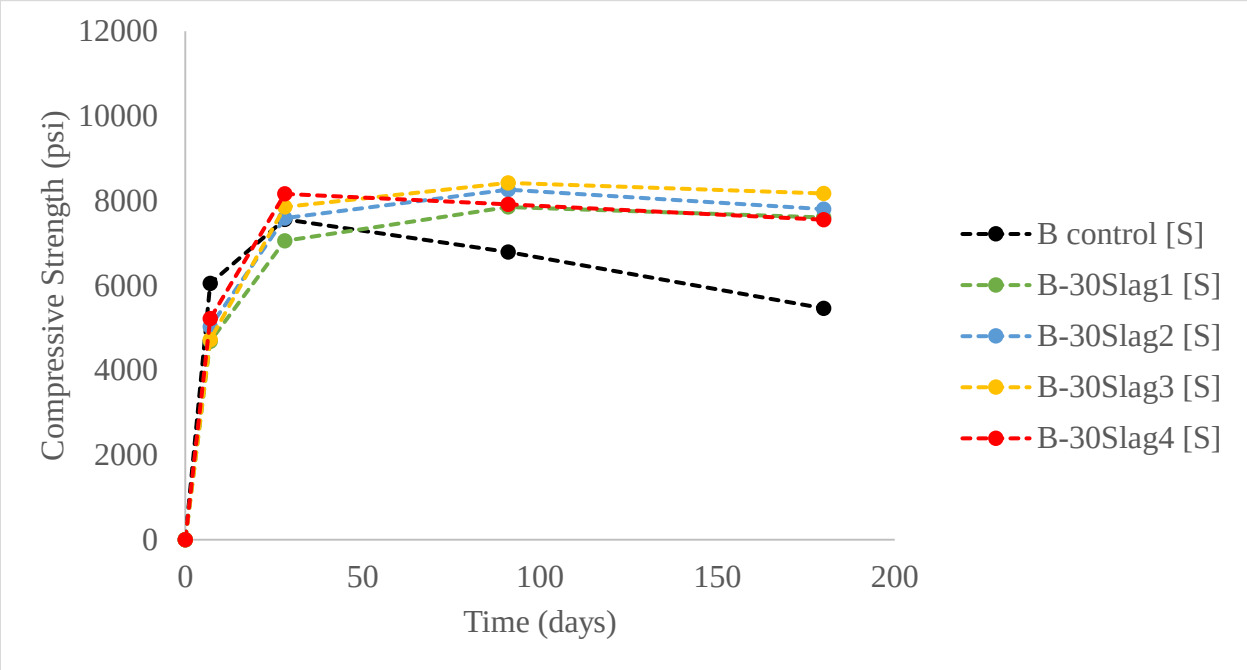

Figure 4.26: Strength Development for 30% Replacement of Cement B in Sulfate Solution

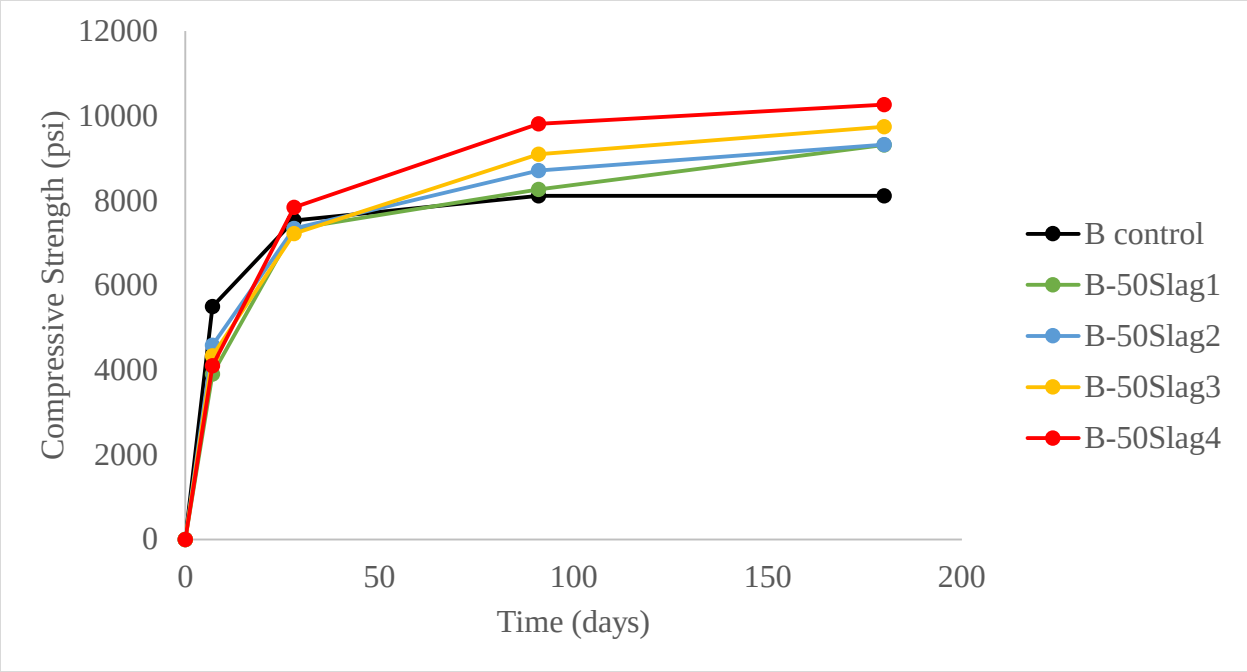

Figure 4.27: Strength Development for 50% Replacement of Cement B in Lime Solution

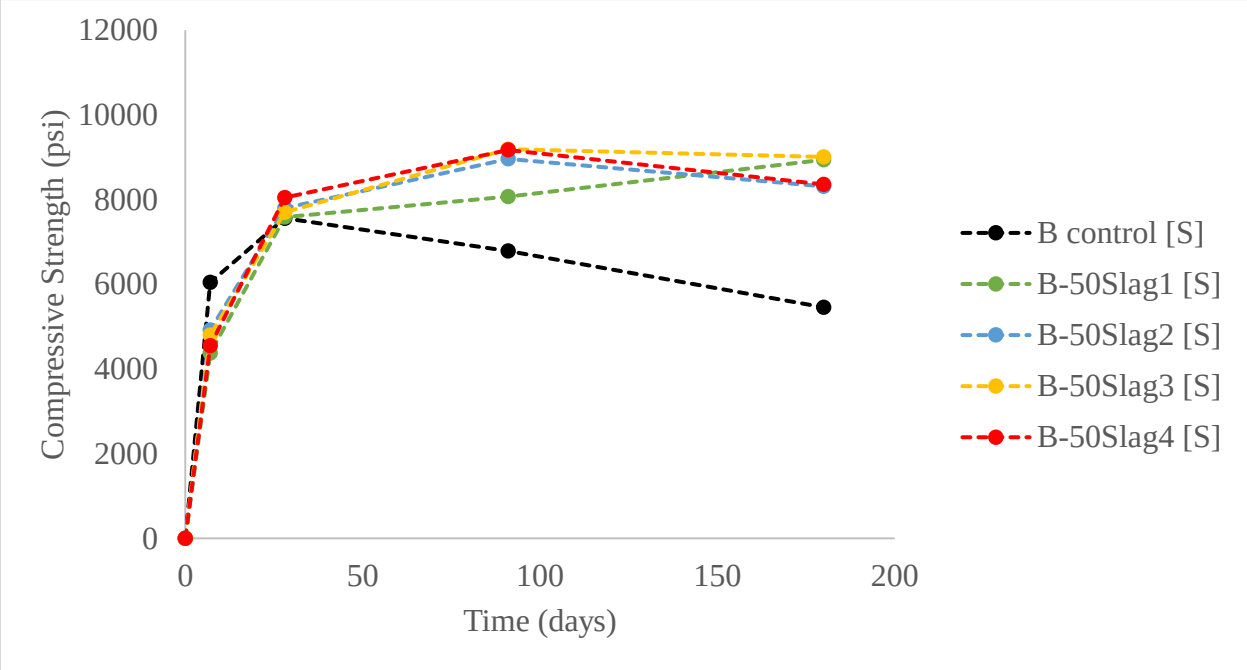

Figure 4.28: Strength Development for 50% Replacement of Cement B in Sulfate Solution

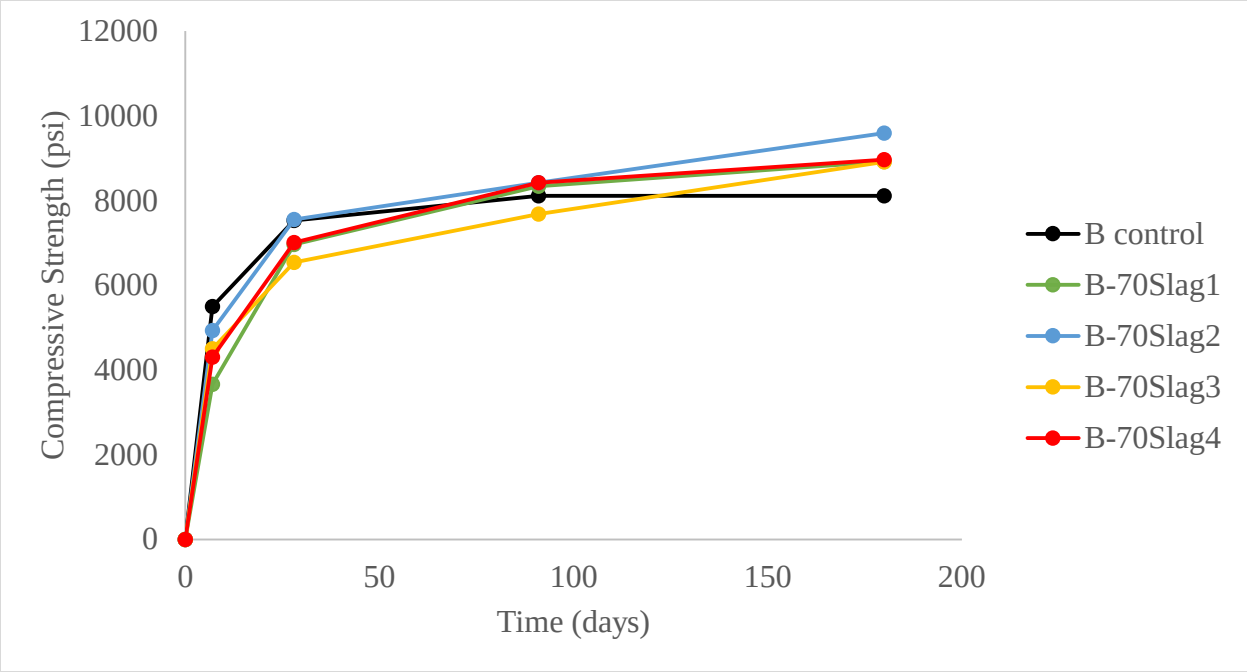

Figure 4.29: Strength Development for 70% Replacement of Cement B in Lime Solution

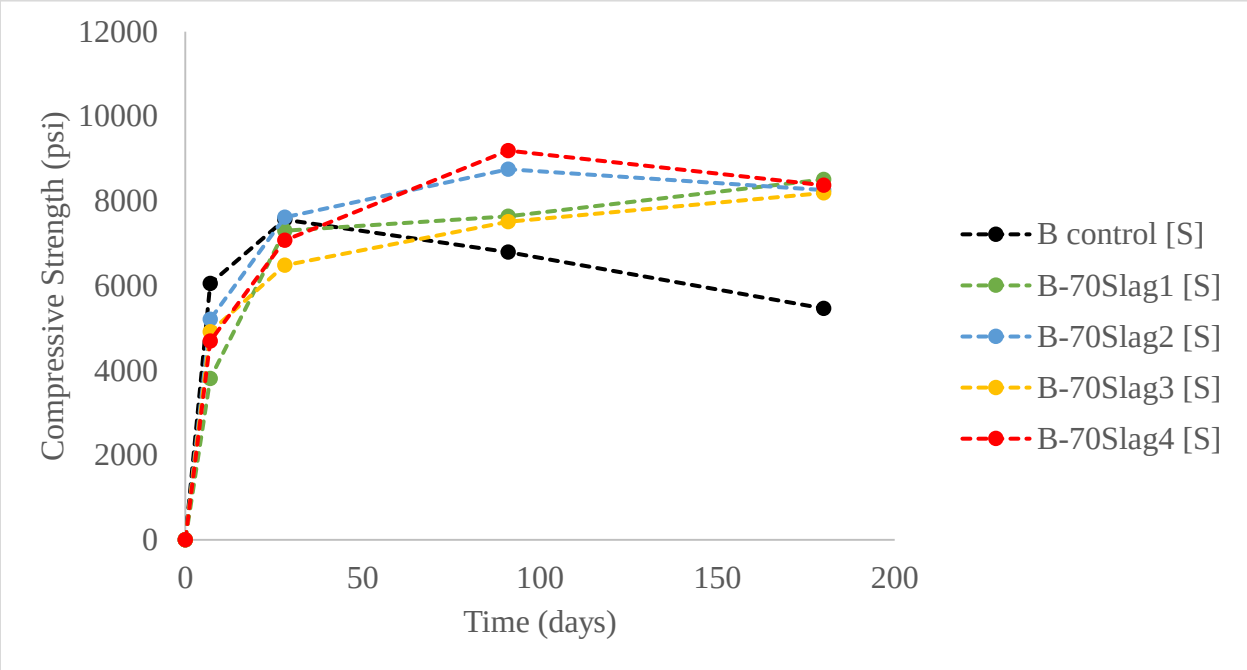

Figure 4.30: Strength Development for 70% Replacement of Cement B in Sulfate Solution

4.2.3 Strength Versus Percent Replacement

Figures 4.31 through 4.38 (Cement A) and Figures 4.39 through 4.46 (Cement B) depict differences in strength development between replacement percentages for the same slag. These graphs portray the optimum replacement percentage for maximum strength. The trends seen align with the published findings, in that there is an optimum point to which slag should be used before increasing the content leads to decreased strength. Oner and Akyuz [21] suggest unreacted slag begins to act as a fine aggregate instead of a supplementary cementitious material (SCM) after the replacement levels exceeds 55-59%. In all conditions except S2-A in sulfate solution, 50% replacement leads to better overall strength in both curing regimes.

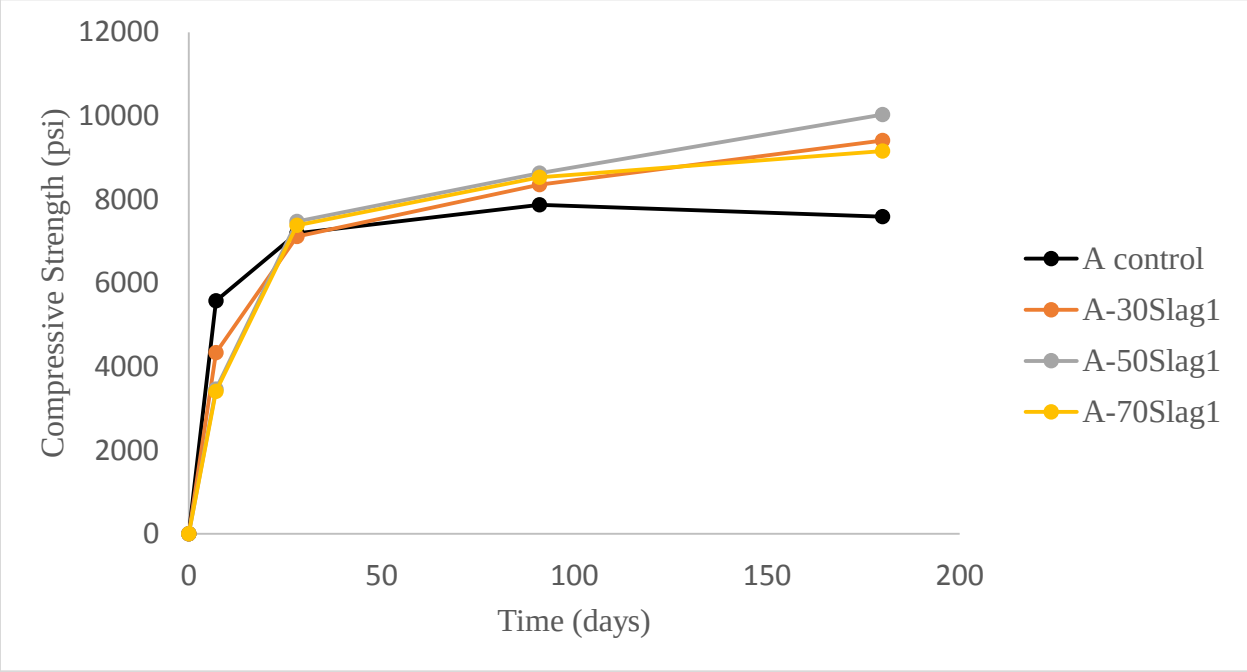

Figure 4.31: Strength Development Using Various Percentages of Slag1 with Cement A in Lime Solution

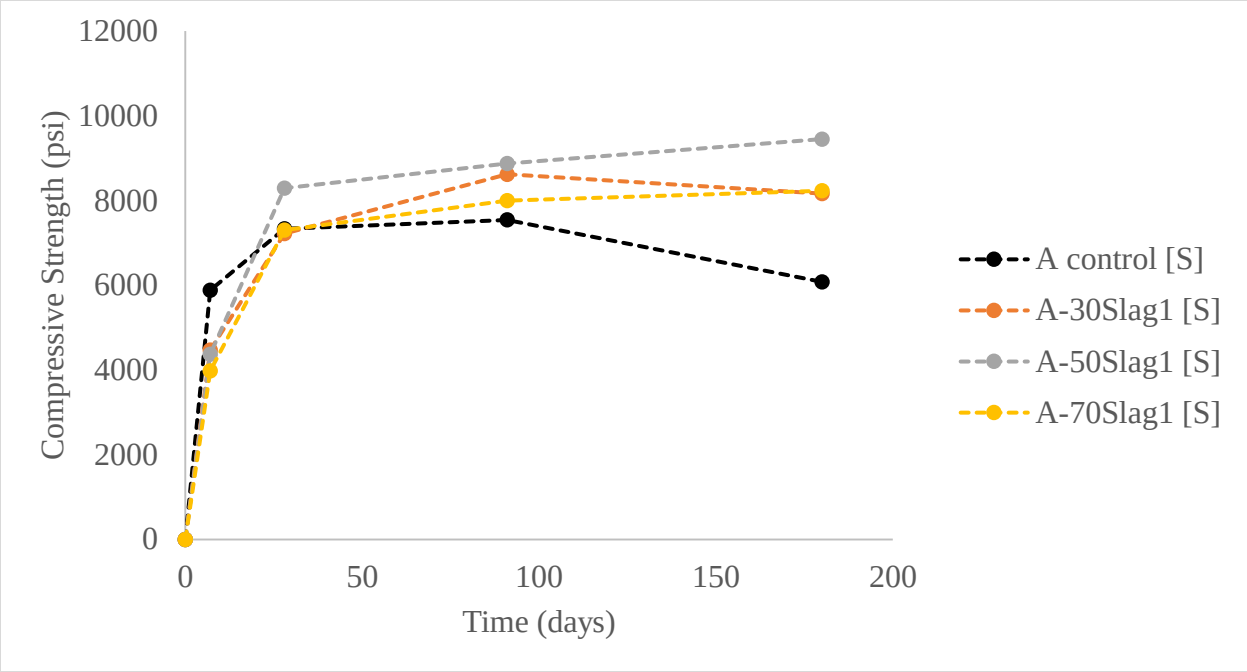

Figure 4.32: Strength Development Using Various Percentages of Slag1 with Cement A in Sulfate Solution

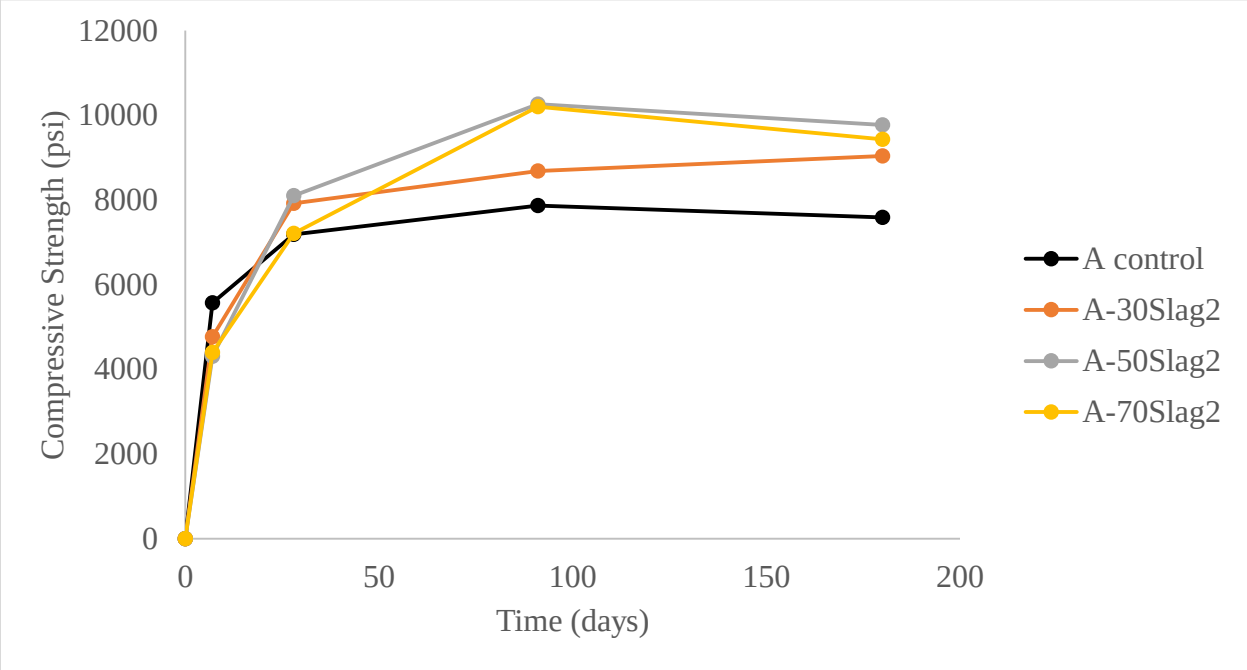

Figure 4.33: Strength Development Using Various Percentages of Slag2 with Cement A in Lime Solution

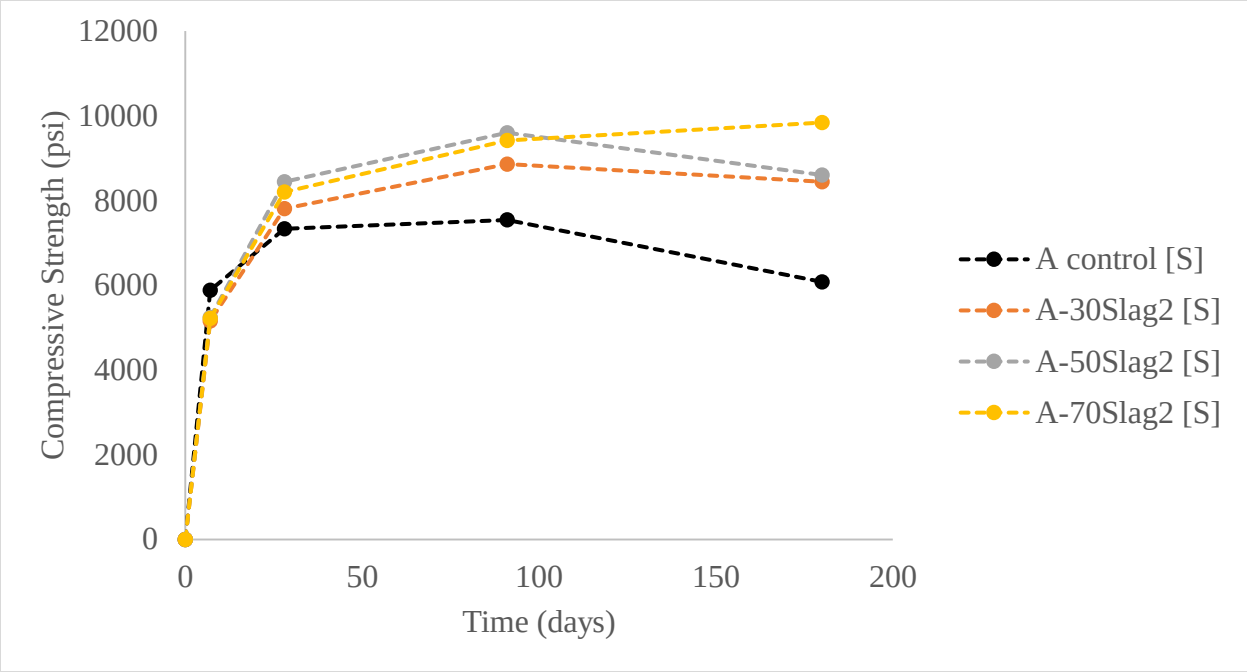

Figure 4.34: Strength Development Using Various Percentages of Slag2 with Cement A in Sulfate Solution

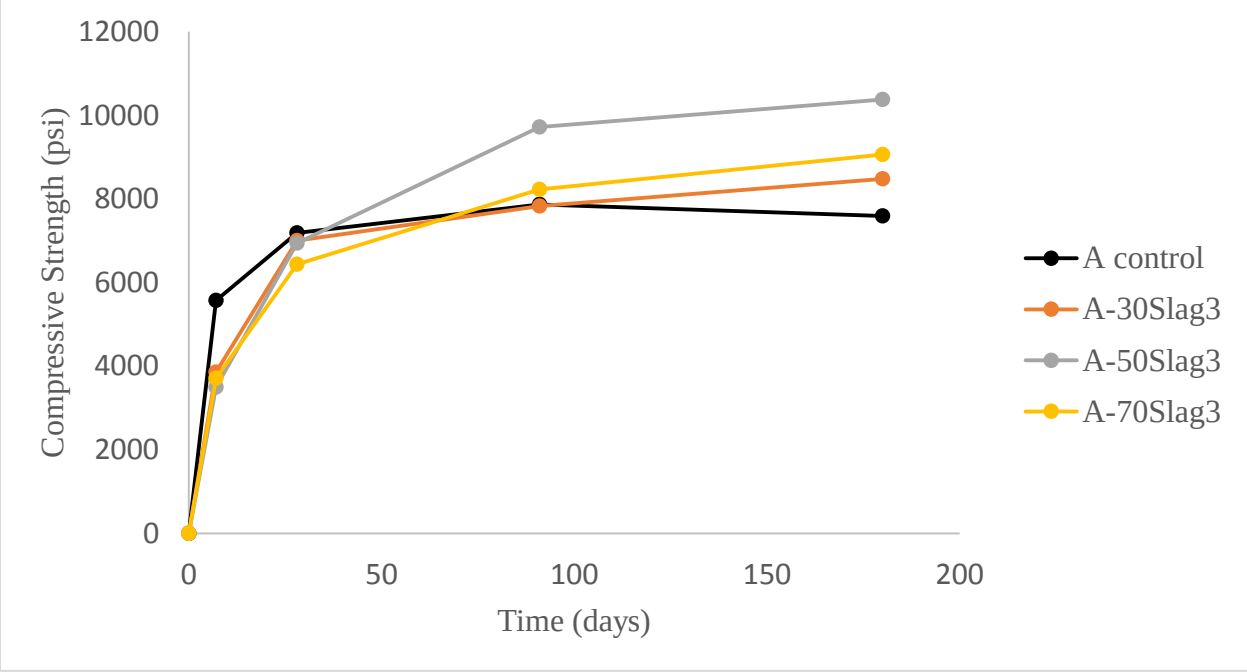

Figure 4.35: Strength Development Using Various Percentages of Slag3 with Cement A in Lime Solution

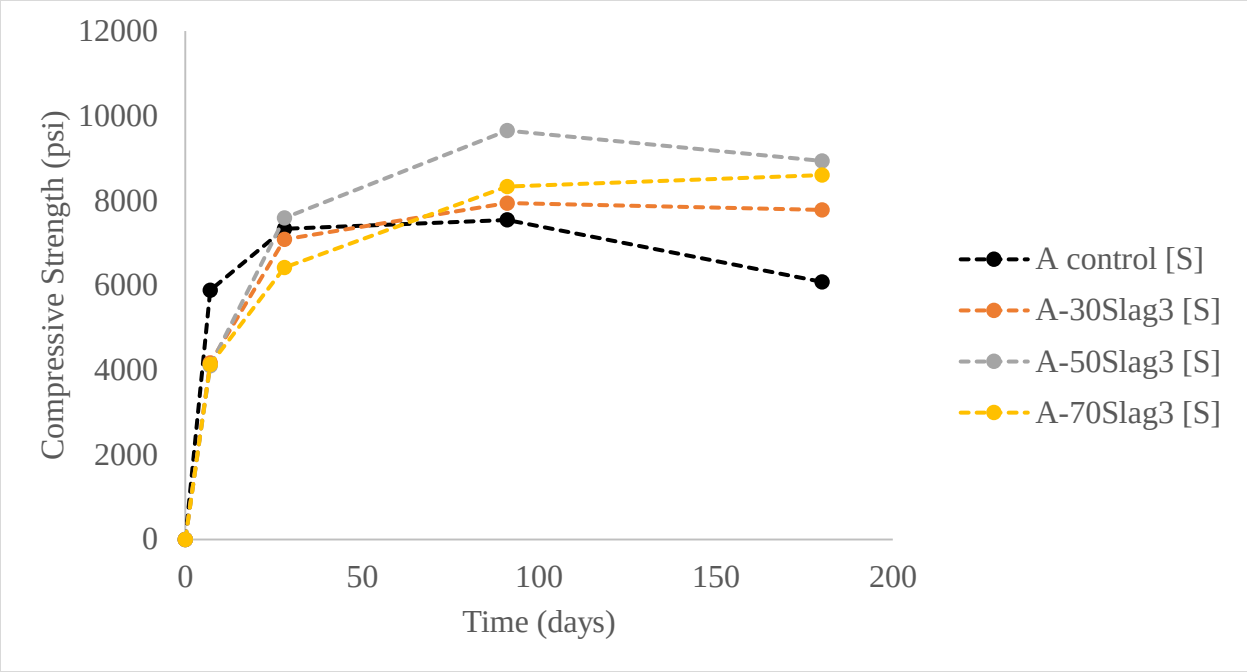

Figure 4.36: Strength Development Using Various Percentages of Slag3 with Cement A in Sulfate Solution

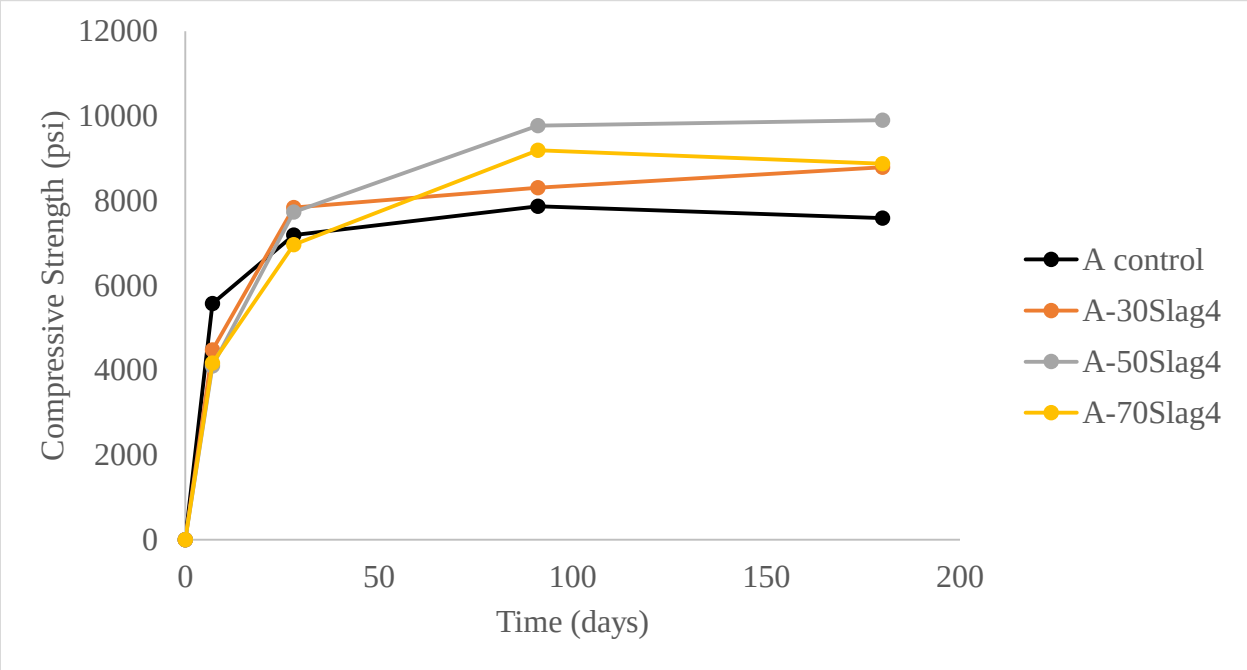

Figure 4.37: Strength Development Using Various Percentages of Slag4 with Cement A in Lime Solution

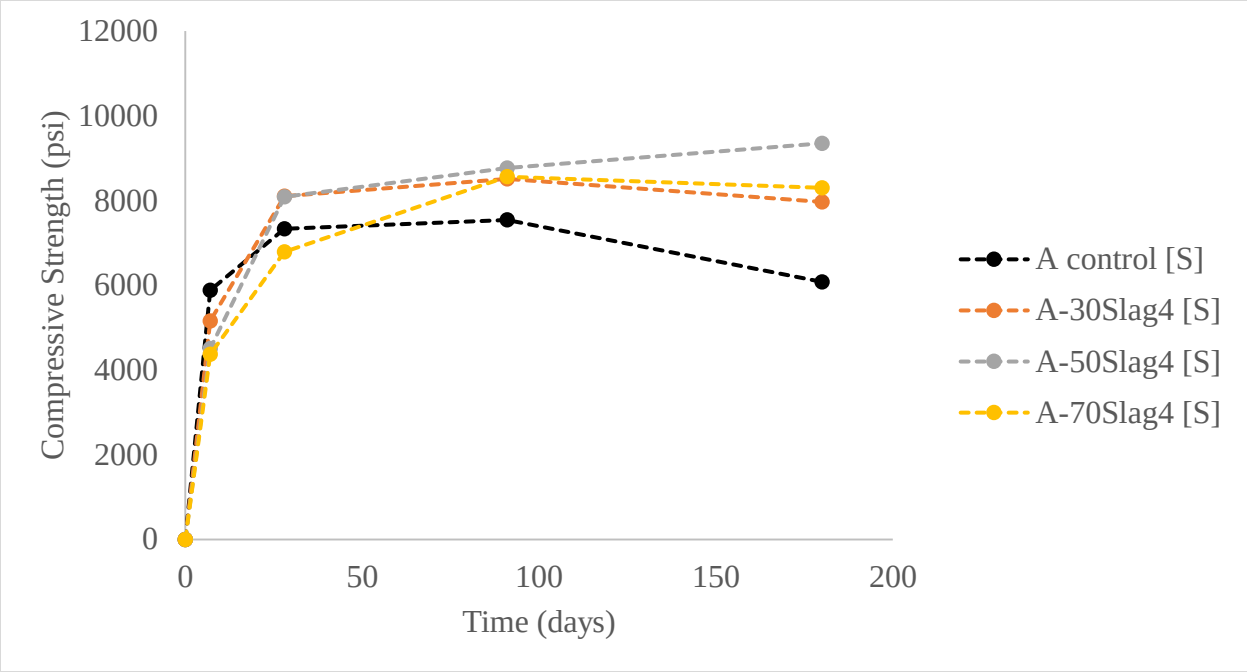

Figure 4.38: Strength Development Using Various Percentages of Slag4 with Cement A in Sulfate Solution

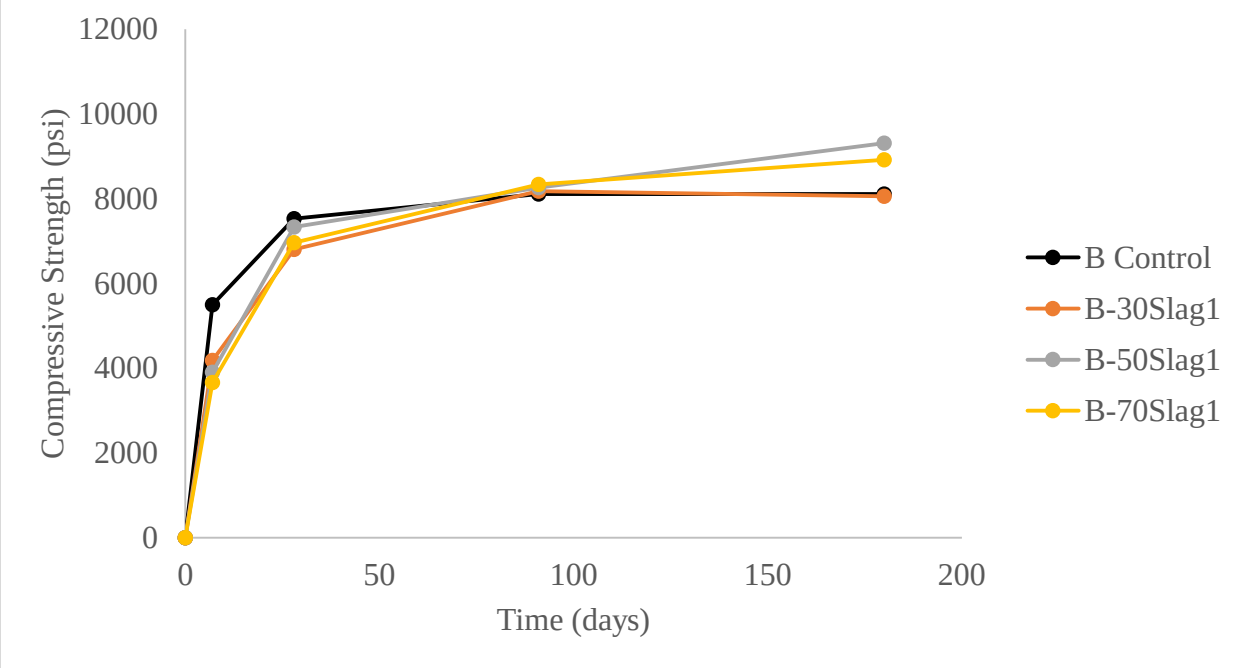

Figure 4.39: Strength Development Using Various Percentages of Slag1 with Cement B in Lime Solution

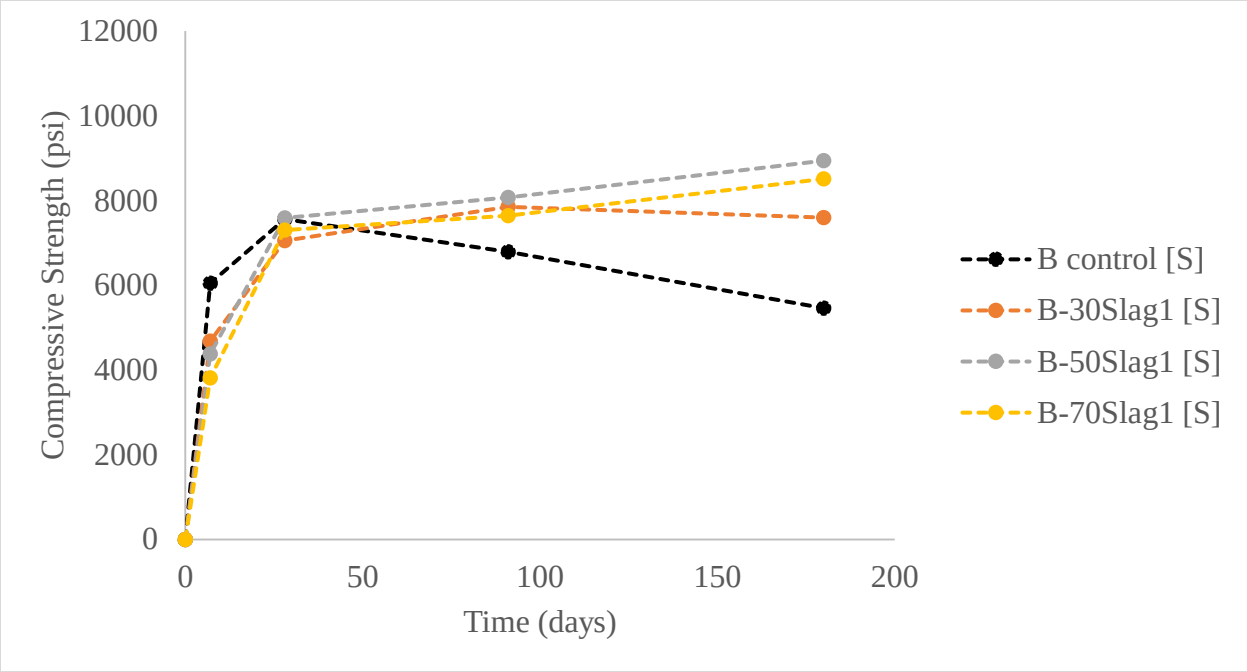

Figure 4.40: Strength Development Using Various Percentages of Slag1 with Cement B in Sulfate Solution

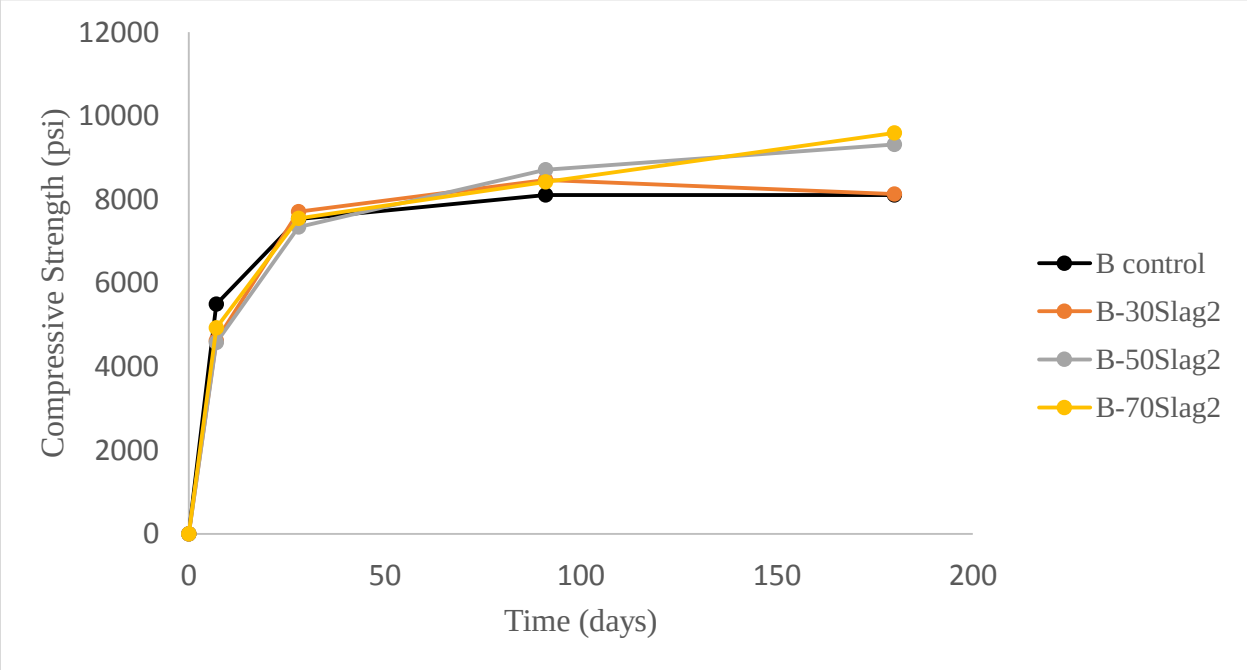

Figure 4.41: Strength Development Using Various Percentages of Slag2 with Cement B in Lime Solution

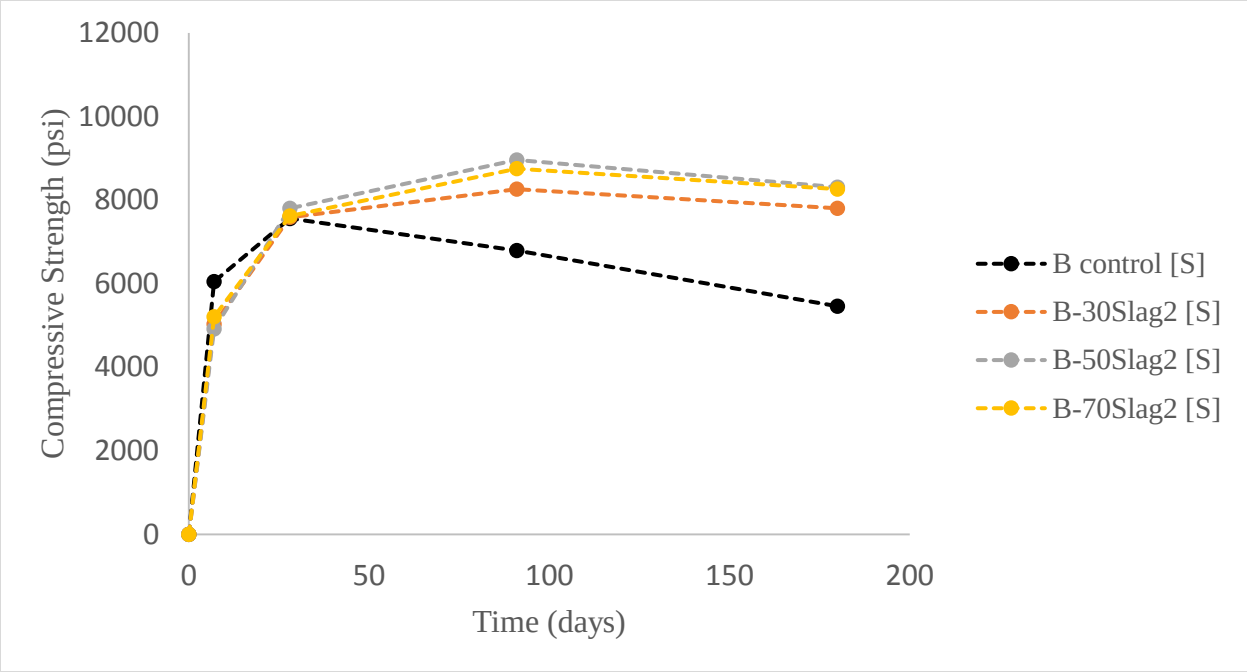

Figure 4.42: Strength Development Using Various Percentages of Slag2 with Cement B in Sulfate Solution

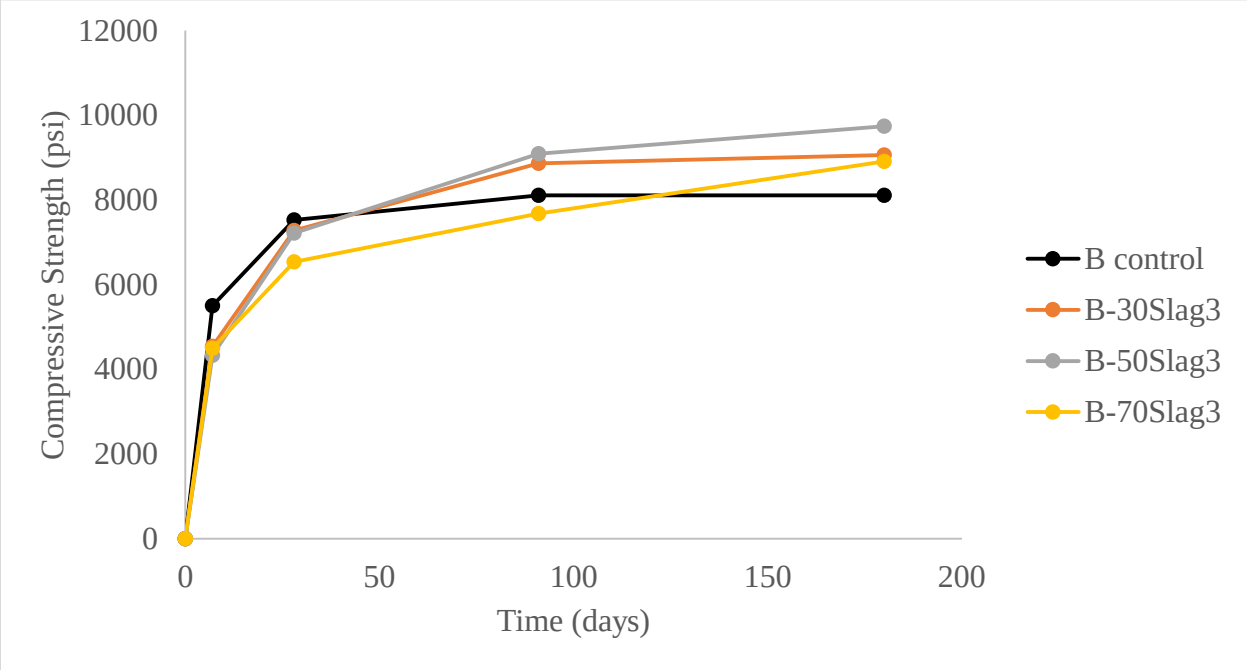

Figure 4.43: Strength Development Using Various Percentages of Slag3 with Cement B in Lime Solution

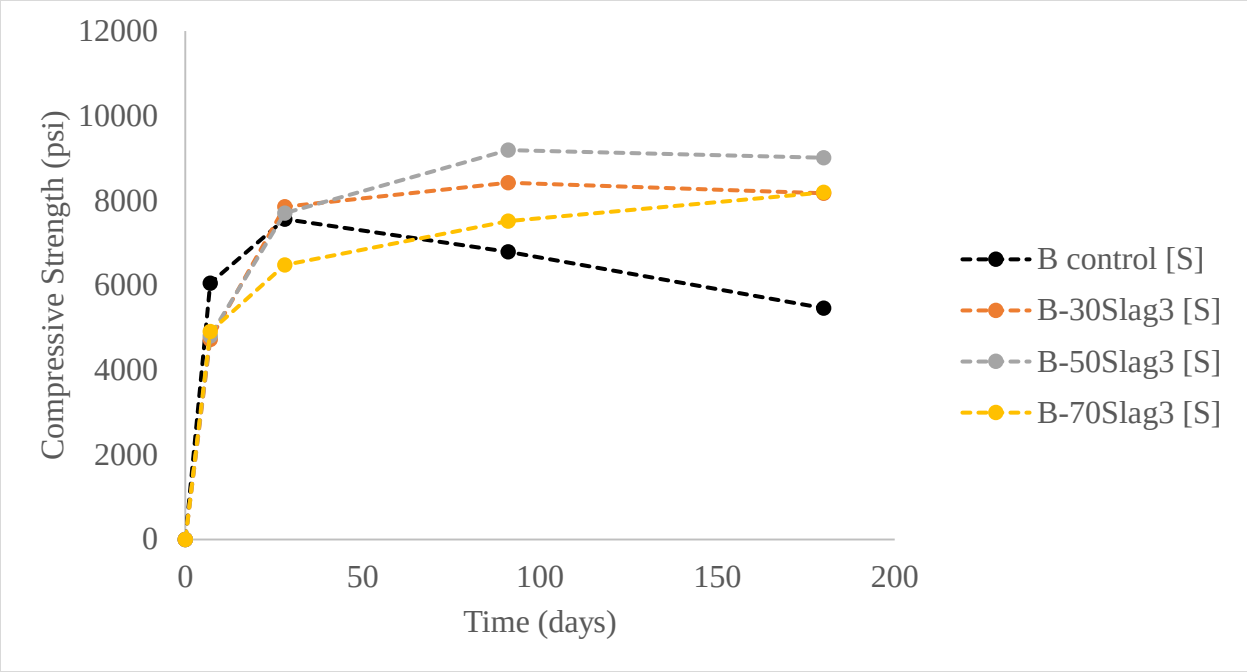

Figure 4.44: Strength Development Using Various Percentages of Slag3 with Cement B in Sulfate Solution

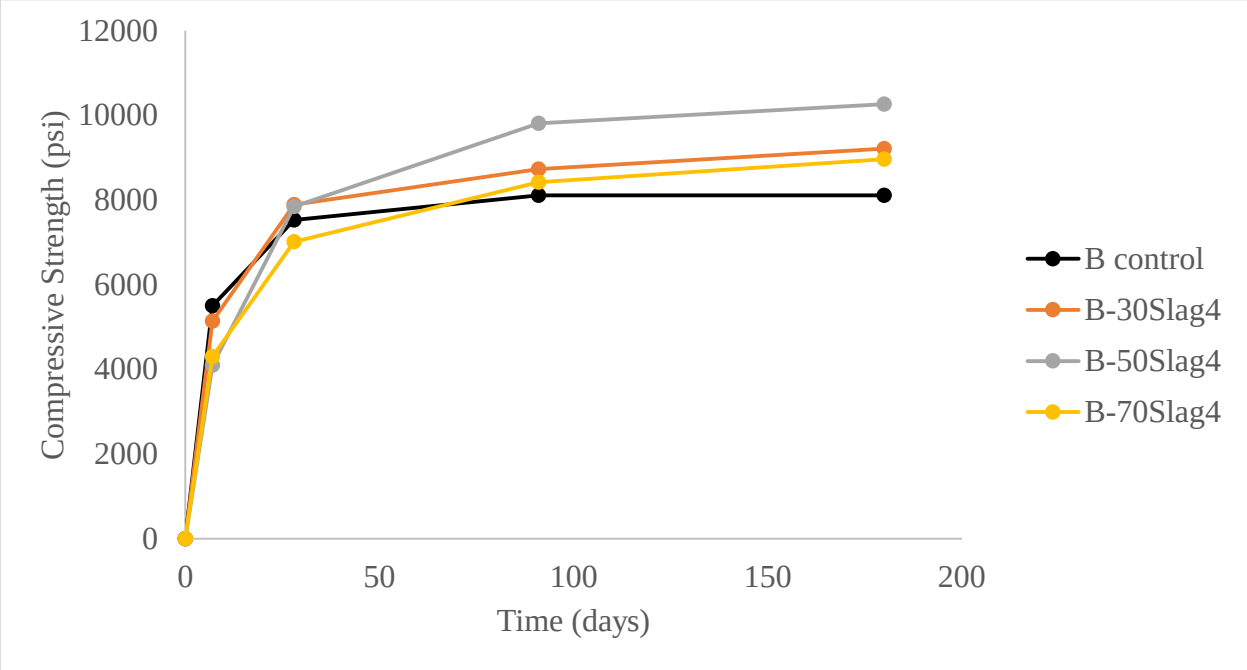

Figure 4.45: Strength Development Using Various Percentages of Slag4 with Cement B in Lime Solution

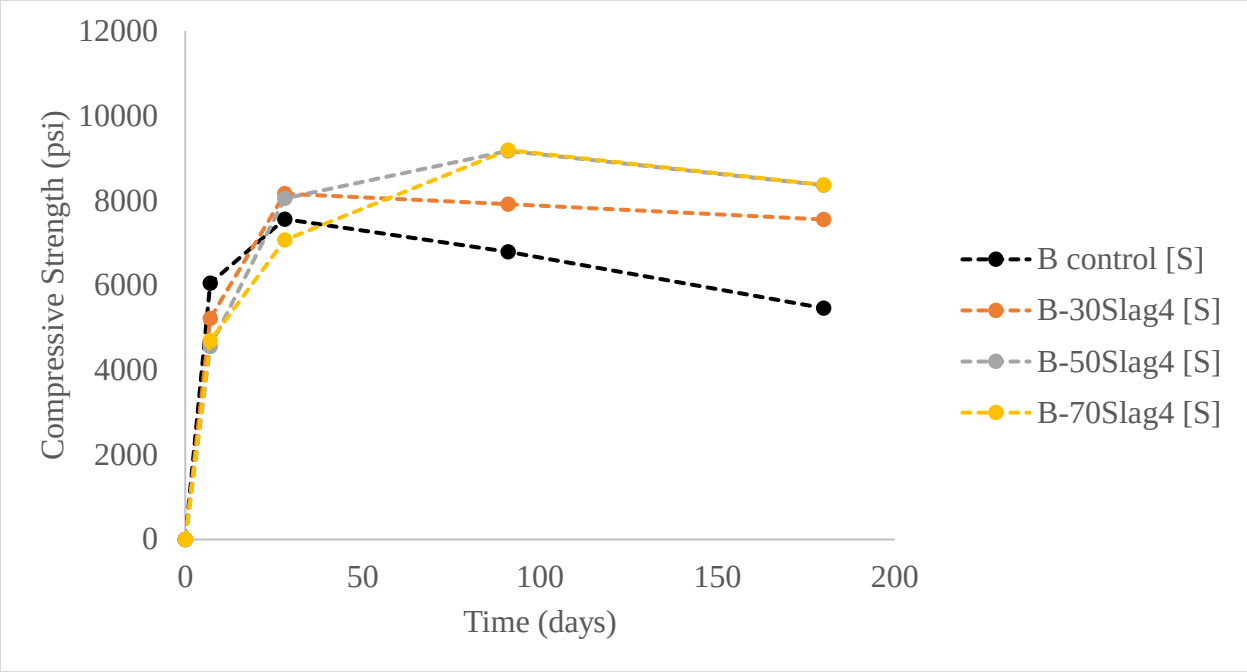

Figure 4.46: Strength Development Using Various Percentages of Slag4 with Cement B in Sulfate Solution

As seen from the results, increasing the slag content to 70% would generally offer better strengths compared to lowering the slag content to 30%, especially in sulfate conditions. This is seen in both tested cements, but to a greater degree in Cement B possibly due to the dilution effect on lowering the C_3A content. Ultimately, the amount of BFS that should be used depends on its use or application. If strength is desired within the first two weeks of mixing, low replacement percentages should be used; that is, 30-50%. Raado and Hain [62] found a decreasing linear trend of compressive strength when slag content increased at 28 days. Past the initial early stage, though, 50% is highly recommended. 70% should be used in situations where strength is needed at later ages and for situations that involve durability since higher contents of slag generally lead to more sulfate resistance.

4.3 Expansion

The following figures represent how much the mortar bars expanded over time when exposed to 5 percent sodium sulfate solution. Expansion was seen to increase with increasing the alumina content of slag. In some cases, at 120 days of exposure, the incorporation of slag was beneficial for cement B but detrimental for cement A. This dissimilarity stems from the difference in C_3A content of the cements. Control B failed after 105 days when the range of expansion between the 6 bars exceeded the maximum permissible range stated in ASTM C1012 [33]. Addition of any slags, regardless of the alumina content, prevented high expansion at this age. However, it may be seen in Figure 4.52 that the rate of expansion for mortar bars including S4 with cement B is rather large and is expected to fail within a year from mixing. This cannot be said regarding the other slags as the expansion rate using S1 and S2 is much smaller.

Incorporating Slag 1 with cement A did not affect the expansion of the mortar bars with respect to the control mix up to 120 days of exposure, as seen in Figure 4.47. Conversely, including S2 (Figure 4.48) and S4 (Figure 4.49) resulted in more expansion compared to the control mixture. This may be explained by the inclusion of more alumina content within the system as these slags have more than double the content present in cement itself.

It was shown in the literature that increasing slag content in mortar mixtures results in decreased expansion [63]–[66]. This is due to the consumption of more CH as slag content increases, resulting in less expansive ettringite formation. Although the data presented in this report suggest otherwise, the spread of expansion percentages using slags are too miniscule to report the effect that slag replacement had on expansion at this time of publication. It should be noted, though, that standards suggests having data up to at least 6 months before conclusions can be made regarding their performance. For example, ACI 201.2R [67] provides maximum

expansion values at 6 months, but includes maximum limits for expansion at 12 and 18 months as well. Therefore, the continuation of these measurements are required to fully understand the effect of slag chemical and physical characteristics on blended systems performance in a sulfate environment.

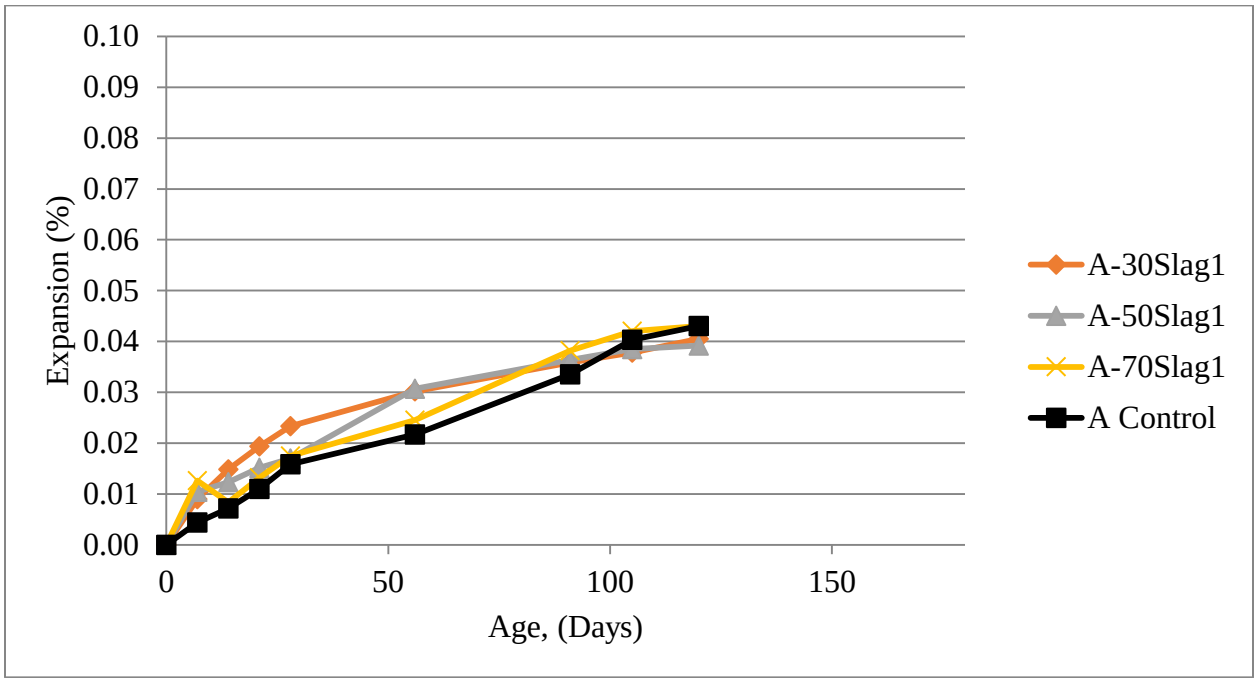

Figure 4.47: Bar Expansion Percent as a Function of Time for Various Percentages of Slag1 with Cement A

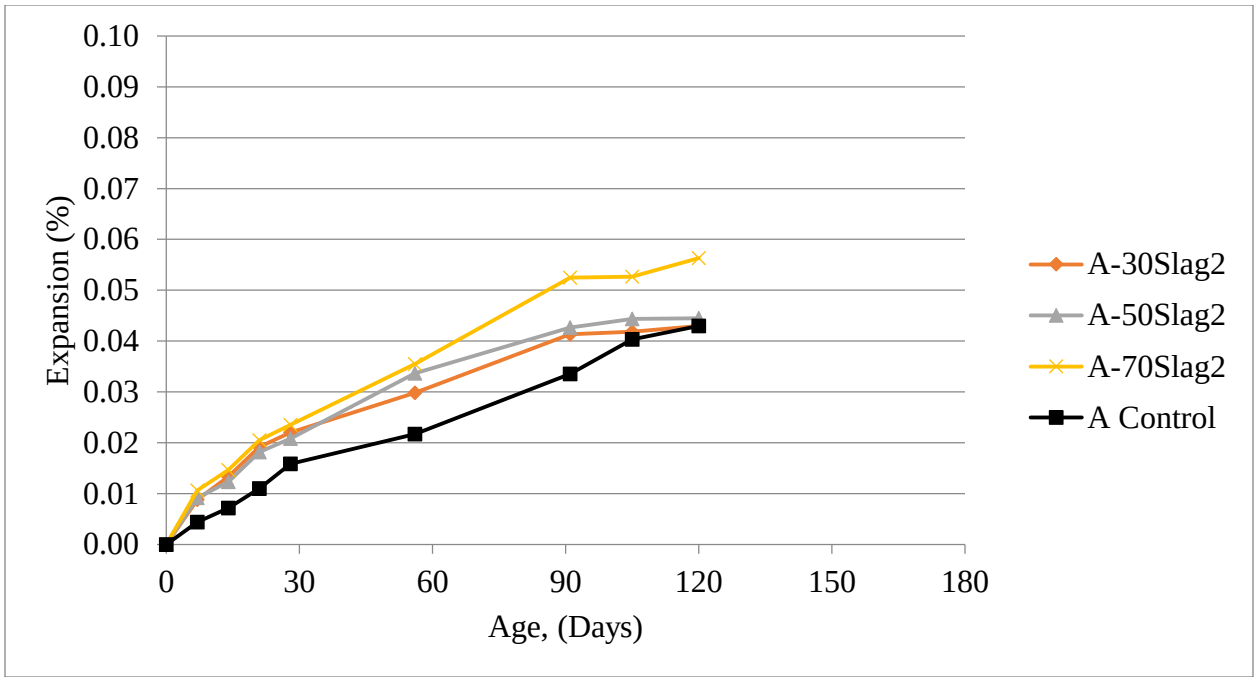

Figure 4.48: Bar Expansion Percent as a Function of Time for Various Percentages of Slag2 with Cement A

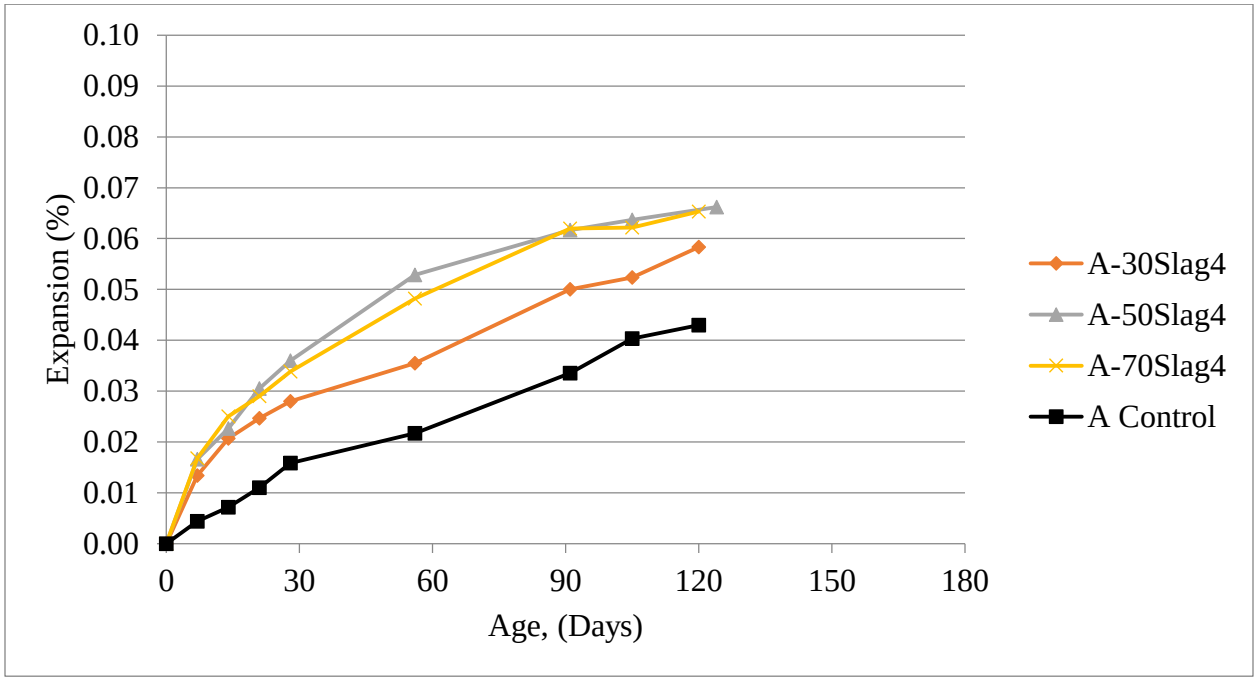

Figure 4.49: Bar Expansion Percent as a Function of Time for Various Percentages of Slag4 with Cement A

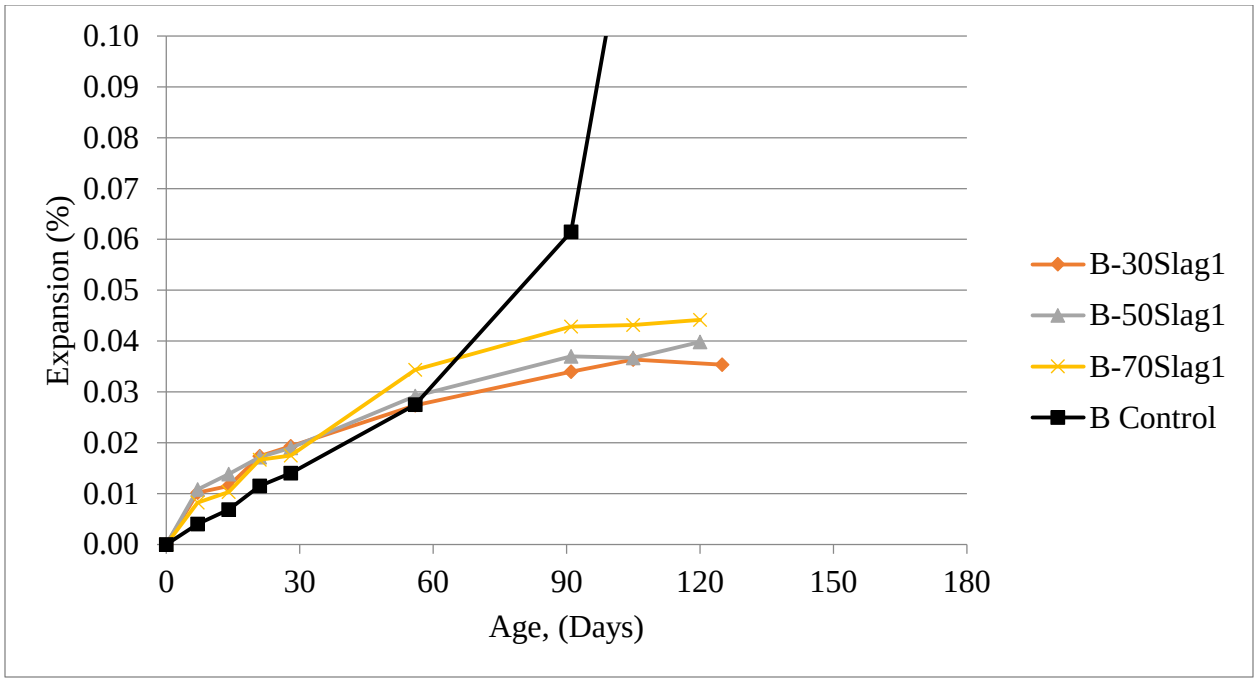

Figure 4.50: Bar Expansion Percent as a Function of Time for Various Percentages of Slag1 with Cement B

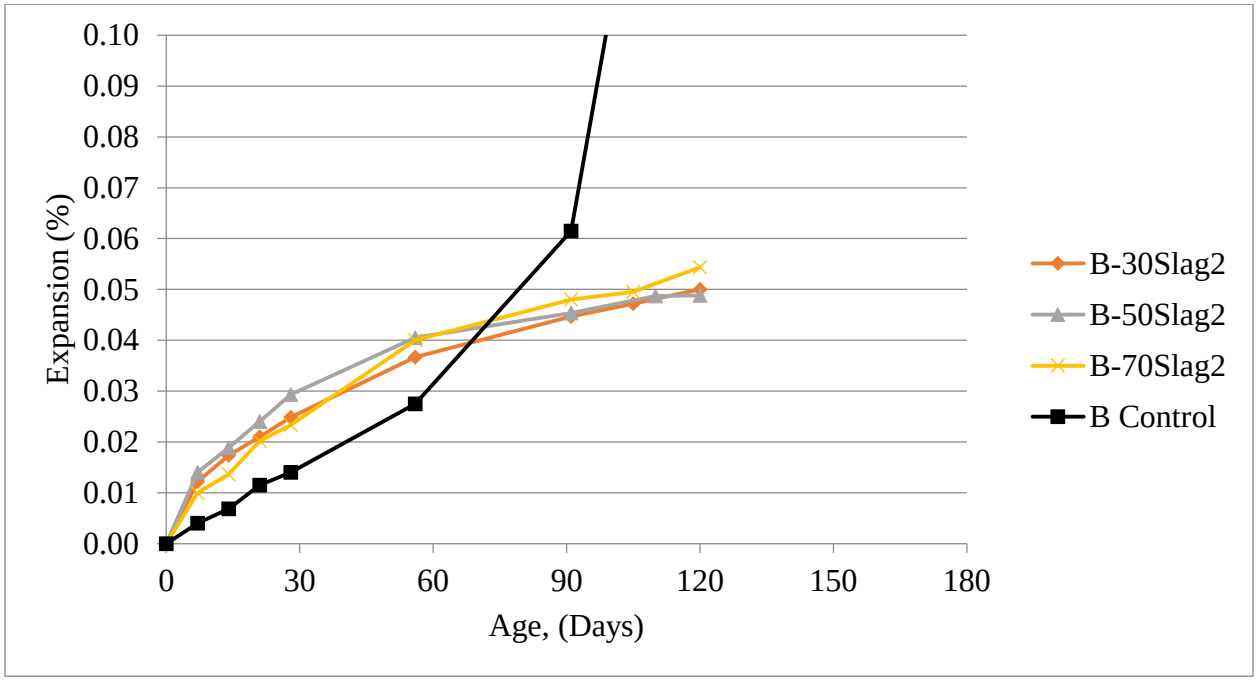

Figure 4.51: Bar Expansion Percent as a Function of Time for Various Percentages of Slag2 with Cement B

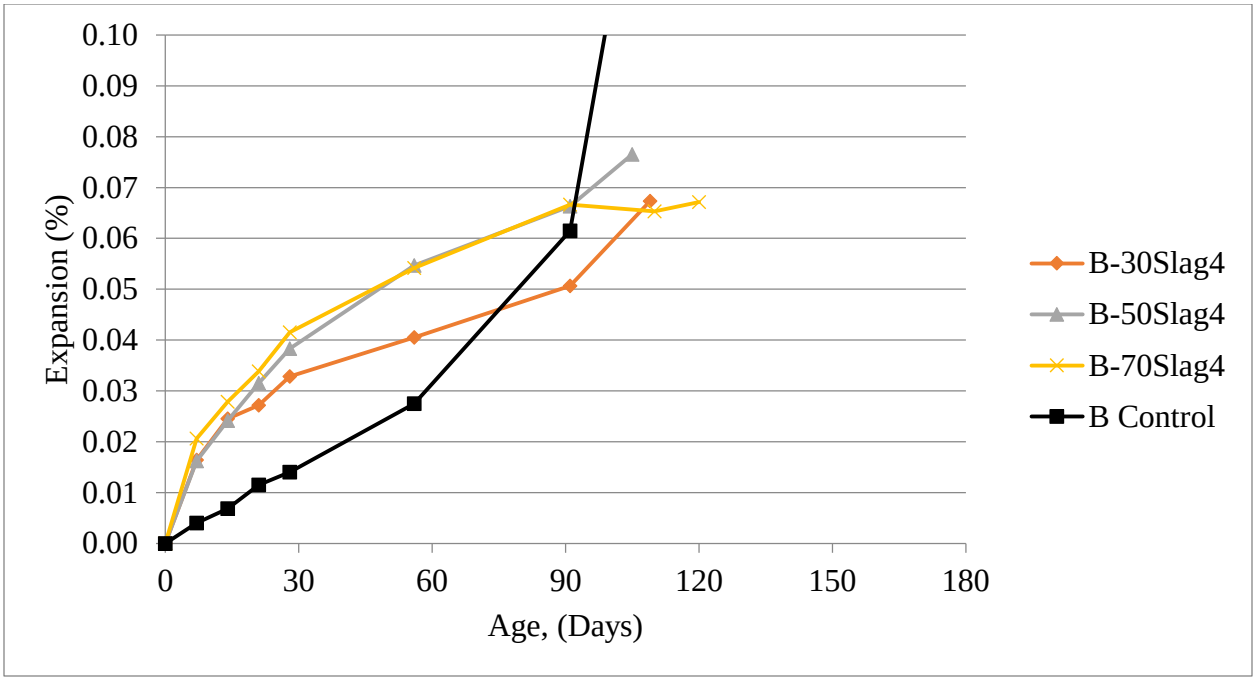

Figure 4.52: Bar Expansion Percent as a Function of Time for Various Percentages of Slag4 with Cement B

4.4 Hydration Products for Failed Mortar Cubes Using XRD Analysis

Table 4-7: Crystalline Weight Fractions of Present Phases for Cement A Mortar

	A control (L)		A control (S)		30S4-A (L)		30S4-A (S)	
Phase	7 days	182 days	7 days	182 days	7 days	182 days	7 days	182 days
Alite	0.9	0	0.7	0	-	-	-	-
Belite	9.4	2.1	10.4	1.6	8	2.1	7.4	1.8
Calcite	-	-	-	-	-	-	0	0.5
Ferrite	0.4	0	0.4	0	-	-	-	-
Portlandite	14.8	17.4	13	12.8	7.3	9.2	7.5	7.2
Gypsum	-	-	0	2.2	-	-	0	1.4
Ettringite	4.1	3.4	2.5	5.8	0.1	0	0.6	2.1
Monosulfo-aluminate	0	0.3	0	0.6	1.5	4.6	1.8	3.5
Hemicarbo-aluminate	-	-	-	-	0	0.2	-	-
Hydrotalcite	-	-	-	-	0.2	1.6	0.3	1.3
Amorphous content	70.3	76.7	74.3	76.9	82.8	82.2	82.4	82.2

In assessing the mechanism of failure for mixtures that showed deterioration in sulfate solution, specimens were examined using x-ray diffraction coupled with Rietveld refinement for phases quantification. For the Control A mixture, sulfate exposure results in increasing secondary ettringite content in addition to secondary gypsum formation. Similarly, the control mortar for Cement B shows similar trends but more substantial formation of ettringite. This is expected as the mineralogical analysis of the as-received Cement B shows higher tricalcium aluminate content. Similar trends are observed for the blended mortar using either cements with S4 at 30% replacement.

Table 4-8: Crystalline Weight Fractions of Present Phases for Cement B Mortar

	B control (L)		**B control (S)**		**30S4-B (L)**		**30S4-B (S)**	
Phase	7 days	182 days	7 days	182 days	7 days	182 days	7 days	182 days
Alite	0.6	0	1.7	0	-	-	-	-
Belite	10.6	1.3	9.2	1.3	7.7	1.5	7.4	1.5
Calcite	-	-	0	0.6	-	-	0	0.7
Ferrite	-	-	-	-	-	-	-	-
Portlandite	16.5	16.2	15.1	12.8	8.7	9.2	7.9	8
Gypsum	-	-	0	2.4	-	-	0	0.8
Ettringite	3.7	3.7	3.3	9.4	0.3	0.1	1.1	1.4
Monosulfo-aluminate	0.8	1.3	0.5	1.8	3.3	6.3	3.9	4.8
Hemicarbo-aluminate	-	-	-	-	0.3	0.2	-	-
Hydrotalcite	-	-	-	-	0.2	1.6	0.3	1.4
Amorphous content	67.7	77.4	70.2	71.6	79.5	81.2	79.5	81.5

It is to be remembered that the strength data showed that those mixtures showed a drop in strength at 180 days of exposure to sodium sulfate solution. The XRD data indicates that the mechanism of failure is due to secondary ettringite formation and secondary gypsum similar to the control mixtures. The findings of this study indicates that the high alumina slag might not offer

significant improvement in sulfate resistance when performance is compared to the control mixture.

CHAPTER 5: CONCLUSIONS AND FURTHER ANALYSIS

From the data obtained in this study it can be concluded that:

1. 50% replacement of slag is recommended for optimal strength, regardless of the chemical composition of the Portland cement. However, in terms of sulfate resistance, higher contents of slag (70%) are more advantageous.
2. The following statements can be made when only analyzing specimens exposed to a lime solution. For cements with moderate C_3A content (≤8%), incorporating slag with low alumina contents is more beneficial in terms of strength compared to high alumina content slags. However, with cements that have high C_3A (~12%), using high alumina slag leads to increased strength at 182 days. Caution should be made when these high alumina slags are used with sulfate exposure, as this can lead to lower sulfate resistance.
3. Sulfate attack begins to be observed after 28 days of exposure to a sodium sulfate solution. This is true for both OPC mortars as well as blended mortars, although OPC mortars showed a more rapid attack compared to slag blended-cement mixtures.
4. Expansion percent is highly dependent on the alumina content of the slag. Slags with a high alumina content mixed with moderate C_3A cements expand more than the plain system, at 120 days of exposure. There might be a delay in expansion when cements are high in C_3A, but this delay is most likely attributed to pore refinement and the slow nature of slag hydration. C_3A content, therefore, is influential in expansion behavior as well as the alumina content of slag.
5. Using low replacement levels of slags with high alumina content were shown to have less strength at 182 days of exposure to a sulfate environment when compared to the 28-day compressive strength. This indicates that a further analysis is needed when slags with high alumina content are used in a mixture design for construction projects where sulfate exposure is of concern.

6. X-ray diffraction indicates the mechanism of deterioration for high alumina slag is due to secondary ettringite formation as well as secondary gypsum formation.

Future research is needed to

1. Evaluate the effects of slag at varying alumina contents using a constant fineness.
2. Determine the different effects of MgO contents and Al_2O_3 in terms of compressive strength evolution in sulfate solutions.

REFERENCES

[1] D. Keys, "How rome polluted the world," *Geographical*, pp. 45–48, Dec-2003.

[2] M. Thomas, *Supplementary Cementing Materials in Concrete*. CRC Press, 2013.

[3] ASTM C989/ C989M-13, "Standard Specification for Slag Cement for Use in Concrete and Mortars 1," West Conshohocken, PA: ASTM International, 2013.

[4] ASTM C150/ C150M-16, "Standard Specification for Portland Cement," West Conshohocken, PA: ASTM International, 2016.

[5] G. J. Osborne, "Durability of Portland blast-furnace slag cement concrete," *Cem. Concr. Compos.*, vol. 21, no. 1, pp. 11–21, 1999.

[6] ASTM C125-13b, "Standard Terminology Relating to Concrete and Concrete Aggregates," West Conshohocken, PA: ASTM International, 2013.

[7] R. Snellings, G. Mertens, and J. Elsen, "Supplementary Cementitious Materials," *Rev. Mineral. Geochemistry*, vol. 74, pp. 211–278, 2012.

[8] M. M. Islam, D. M. S. Islam, M. A. Rahman, and A. Das, "Strength Behavior of Mortar Using Slag as Partial Replacement of Cement," no. 1, 1978.

[9] V. Kocaba, "Development and Evaluation of Methods to Follow Microstructural Development of Cementitious Systems Including Slags," ÉCOLE POLYTECHNIQUE FÉDÉRALE DE LAUSANNE, 2009.

[10] J. I. Escalante, L. Y. Gómez, K. K. Johal, G. Mendoza, H. Mancha, and J. Méndez, "Reactivity of blast-furnace slag in Portland cement blends hydrated under different conditions," *Cem. Concr. Res.*, vol. 31, pp. 1403–1409, 2001.

[11] R. Walker and S. Pavía, "Physical properties and reactivity of pozzolans , and their influence on the properties of lime – pozzolan pastes," *Mater. Struct.*, vol. 44, pp. 1139–1150, 2011.

[12] F. Sajedi and H. A. Razak, "The effect of chemical activators on early strength of ordinary Portland cement-slag mortars cement-slag mortars," *Constr. Build. Mater.*, vol. 24, no. 10, pp. 1944–1951, 2010.

[13] S. Mindess, J. F. Young, and D. Darwin, *Concrete*, Second Edi. Upper Saddle River: Pearson Education, 2003.

[14] J. Thomas and H. Jennings, "Calcium-Silicate-Hydrate (C-S-H) gel." [Online]. Available: http://iti.northwestern.edu/cement/monograph/Monograph5_4_2.html.

[15] L. Raki, J. Beaudoin, R. Alizadeh, J. Makar, and T. Sato, "Cement and Concrete Nanoscience and Nanotechnology," pp. 918–942, 2010.

[16] B. Lothenbach, K. L. Scrivener, D. Hooton, B. Lothenbach, K. Scrivener, and R. D. Hooton, "Supplementary Cementitious Materials Supplementary cementitious materials," *Cem. Concr. Res.*, vol. 41, no. 12, pp. 1244–1256, 2011.

[17] M. J. Whittaker, "The Impact of Slag Composition on the Microstructure of Composite Slag Cements Exposed to Sulfate Attack," The University of Leeds, 2014.

[18] F. Pelisser, P. Jean, P. Gleize, and A. Mikowski, “Effect of the Ca/Si Molar Ratio on the Micro/nanomechanical Properties of Synthetic C‐S‐H Measured by Nanoindentation,” *J. Phys. Chem.*, vol. 116, pp. 17219–17227, 2012.
[19] V. Živica, “Effects of the very low water / cement ratio,” *Constr. Build. Mater.*, vol. 23, pp. 3579–3582, 2009.
[20] M. Rowles and B. O. Connor, “Chemical optimisation of the compressive strength of aluminosilicate geopolymers synthesised by sodium silicate activation of metakaolinite,” 2003.
[21] A. Oner and S. Akyuz, “An experimental study on optimum usage of GGBS for the compressive strength of concrete,” *Cem. Concr. Compos.*, vol. 29, no. 6, pp. 505–514, 2007.
[22] C. Poon, S. Azhar, M. Anson, and Y. Wong, “Comparison of the strength and durability performance of normal- and high-strength pozzolanic concretes at elevated temperatures,” vol. 31, pp. 1291–1300, 2001.
[23] H. Lee, X. Wang, L. Zhang, and K. Koh, “Analysis of the Optimum Usage of Slag for the Compressive Strength of Concrete,” pp. 1213–1229, 2015.
[24] F. Sajedi and P. Shafigh, “Optimum Level of Replacement Slag in OPC – Slag Mortars Optimum Level of Replacement Slag in OPC-Slag Mortars,” *J. Civ. Eng. Archit.*, vol. 4, no. June 2017, pp. 11–19, 2010.
[25] M. Santhanam, M. D. Cohen, and J. Olek, “Mechanism of sulfate attack : a fresh look Part 2 . Proposed mechanisms,” *Cem. Concr. Res.*, vol. 33, pp. 341–346, 2003.
[26] R. . Gollop and H. F. . Taylor, “Microstructural and Microanalytical studies of sulfate attack v. comparison of different slag blends,” *J. Chem. Inf. Model.*, vol. 53, no. 9, pp. 1689–1699, 2013.
[27] M. Santhanam, M. D. Cohen, and J. Olek, “Sulfate attack research - whither now ?,” vol. 31, pp. 845–851, 2001.
[28] H. T. Cao, L. Bucea, a. Ray, and S. Yozghatlian, “The effect of cement composition and pH of environment on sulfate resistance of Portland cements and blended cements,” *Cem. Concr. Compos.*, vol. 19, no. 2, pp. 161–171, 1997.
[29] N. J. Crammond, “The thaumasite form of sulfate attack in the UK,” vol. 25, pp. 809–818, 2003.
[30] F. Alapour and R. D. Hooton, “Sulfate Resistance of Portland and Slag Cement Concretes Exposed to Sodium Sulfate for 38 Years,” no. 114, 2017.
[31] S. J. Barnett and A. R. W. Jackson, “Study of thaumasite and ettringite phases formed in sulfate / blast furnace slag slurries using XRD full pattern fitting,” vol. 24, pp. 339–346, 2002.
[32] ASTM C452-15, “Standard Test Method for Potential Expansion of Portland-Cement Mortars Exposed to Sulfate,” West Conshohocken, PA: ASTM International, 2015.
[33] ASTM C1012/ C1012M-15, “Standard Test Method for Length Change of Hydraulic-Cement Mortars Exposed to a Sulfate Solution,” West Conshohocken, PA: ASTM International, 2015.
[34] ASTM C109/ C109M-16a, “Standard Test Method for Compressive Strength of Hydraulic Cement Mortars (Using 2-in. or [50-mm] Cube Specimens),” West Conshohocken, PA: ASTM International, 2016.
[35] R. P. Khatri and V. Sirivivatnanon, “Role of Permeability in Sulphate Attack,” *Cem. Concr. Res.*, vol. 27, no. 8, pp. 1179–1189, 1997.

[36] E. Güneyisi and M. Gesoğlu, “A study on durability properties of high-performance concretes incorporating high replacement levels of slag,” *Mater. Struct.*, vol. 41, no. 3, pp. 479–493, 2008.
[37] A. S. Al-Gahtani, Rasheeduzzafar, and S. S. Al-Saadoun, “Rebar Corrosion and sulfate resistance of BFS cement,” *J. Mater. Civ. Eng.*, vol. 6, no. 2, pp. 223–239, 1994.
[38] Y. Kim, K. Lee, J. Bang, and S. Kwon, “Effect of W / C Ratio on Durability and Porosity in Cement Mortar with Constant Cement Amount,” vol. 2014, 2014.
[39] V. M. Reddy and M. V. S. Rao, “Effect of w/c ratio on workability and mechanical properties of high strength Self Compacting Concrete (M70 grade),” *J. Mech. Civ. Eng.*, vol. 11, no. 5, pp. 15–21, 2014.
[40] D. Stark, “Longtime Study of Concrete durability in Sulfate Soils.”
[41] G. J. Osborne, “The Sulphate Resistance of Portland and Blastfumace Slag Cement Concretes,” *ACI Spec. Publ.*, vol. 126, pp. 1047–1072, 1991.
[42] A. Zayed, “Cement Composition and Structural Durability in Florida,” 2003.
[43] ASTM C114-15, “Standard Test Methods for Chemical Analysis of Hydraulic Cement,” West Conshohocken, PA: ASTM International.
[44] ASTM C1365-06(2011), “Standard Test Method for Determination of the Proportion of Phases in Portland Cement and Portland-Cement Clinker Using X-Ray Powder Diffraction Analysis,” West Conshohocken, PA: ASTM International, 2011.
[45] P. E. Stutzman, “Guide for X-Ray Powder Diffraction Analysis of Portland Cement and Clinker,” Gaithersburg, 1996.
[46] D. L. Bish and R. C. Reynolds, “Sample Preparation for X-Ray Diffraction,” in *Modern Powder Diffraction*, D. L. Bish and J. E. Post, Eds. Washington, DC: The Mineralogical Society of America, 1989, pp. 73–99.
[47] H. F. . Taylor, *Cement chemistry*, 2nd ed. London, UK: Thomas Telford Publishing, 1997.
[48] P. Stutzman, “Powder Diffraction Analysis of Hydraulic Cements: ASTM Rietveld Round Robin Results on Precision,” *Int. Cent. Diffr. Data*, vol. 48, pp. 33–38, 2005.
[49] B. O. Connor, B. B. H. O. Connor, and M. D. Raven, “Application of the RIETVELD Refinement Procedure in Assaying Powdered Mixtures Application of the Rietveld Refinement Procedure in Assaying Powdered Mixtures,” no. July 2016, 1988.
[50] D. Jansen, C. Stabler, F. Goetz-Neunhoeffer, S. Dittrich, and J. Neubauer, “Does Ordinary Portland Cement Contain Amorphous Phase? A Quantitative Study Using an External Standard Method,” *Powder Diffr.*, vol. 26, no. 1, pp. 31–38, Mar. 2011.
[51] M. A. G. Aranda, Á. G. De Torre, and L. León-reina, “Rietveld Quantitative Phase Analysis of OPC Clinkers, Cements and Hydration Products,” vol. 74, no. Young 1993, pp. 169–209, 2012.
[52] I. C. Madsen, N. V. Y. Scarlett, and A. Kern, “Description and survey of methodologies for the determination of amorphous content via X-ray powder diffraction,” *Zeitschrift für Krist.*, vol. 226, no. 12, pp. 944–955, Dec. 2011.
[53] ASTM C188-15, “Standard Test Method for Desnity of Hydraulic Cement,” West Conshohocken, PA: ASTM International, 2015.
[54] ASTM C204-16, “Standard Test Methods for Fineness of Hydraulic Cement by Air-Permeability Apparatus,” West Conshohocken, PA: ASTM International, 2016.
[55] E. C. Arvaniti, M. C. G. Juenger, and S. A. Bernal, “Physical characterization methods for supplementary cementitious materials,” pp. 3675–3686, 2015.

[56] L. Courard, S. Leroy, J. L. Provis, and A. Klemm, “Determination of particle size , surface area , and shape of supplementary cementitious materials by different techniques,” pp. 3687–3701, 2015.
[57] A. Sedaghat, S. M. Asce, N. Shanahan, S. M. Asce, A. Zayed, and M. Asce, “Predicting One-Day , Three-Day , and Seven-Day Heat of Hydration of Portland Cement,” *J. Mater. Civ. Eng.*, vol. 27, no. 9, pp. 1–12, 2015.
[58] ASTM C778-13, “Standard Specification for Standard Sand,” West Conshohocken, PA: ASTM International, 2013.
[59] ASTM C305-14, “Standard Practice for Mechanical Mixing of Hydraulic Cement Pastes and Mortars of Plastic Consistency,” West Conshohocken, PA: ASTM International, 2014.
[60] ASTM C511-13, “Standard Specification for Mixing Rooms, Moist Cabinets, Moist Rooms, and Water Storage Tanks Used in the Testing of Hydraulic Cements and Concretes,” West Conshohocken, PA: ASTM International, 2013.
[61] N. Shanahan and A. Zayed, “Role of tricalcium silicate in sulfate resistance,” *Adv. Cem. Res.*, vol. 27, no. 7, pp. 409–416, 2015.
[62] L. Raado and T. Hain, “EFFECT OF PORTLAND CEMENT COMPOSITION ON SULPHATE RESISTANCE,” no. Table 1.
[63] M. M. López, Y. Pineda, and O. Gutiérrez, “Evaluation of Durability and Mechanical Properties of the Cement Mortar Added with Slag Blast Furnace,” *Procedia Mater. Sci.*, vol. 9, pp. 367–376, 2015.
[64] J. P. H. Fearson, ““Sulfate Resistance of Combinations of Portland Cement and Ground Granulated,” p. 1986, 1986.
[65] S. Ogawa, H. Hyodo, H. Hirao, K. Yamada, A. Matsui, and D. Hooton, “Sulfate Resistance Improvement of Blended Cement Based on Ground Granulated Blast Furnace Slag,” no. August, 2008.
[66] C. Yu, K. Scrivener, and W. Sun, “COMPARSION BETWEEN EXPANSION AND MICROSTRUCTURAL CHANGES OF MORTARS UNDER SULFATE ATTACK,” in *Second International Conference on Microstructural-related Durability of Cementitious Composites*, 2012, no. April.
[67] ACI Committee 201, “201.2R-16 Guide to Durable Concrete,” 2016.

APPENDIX A: ERROR BARS ASSOCIATED WITH MEASUREMENTS

This section is included to portray the error bars associated with the collected data.

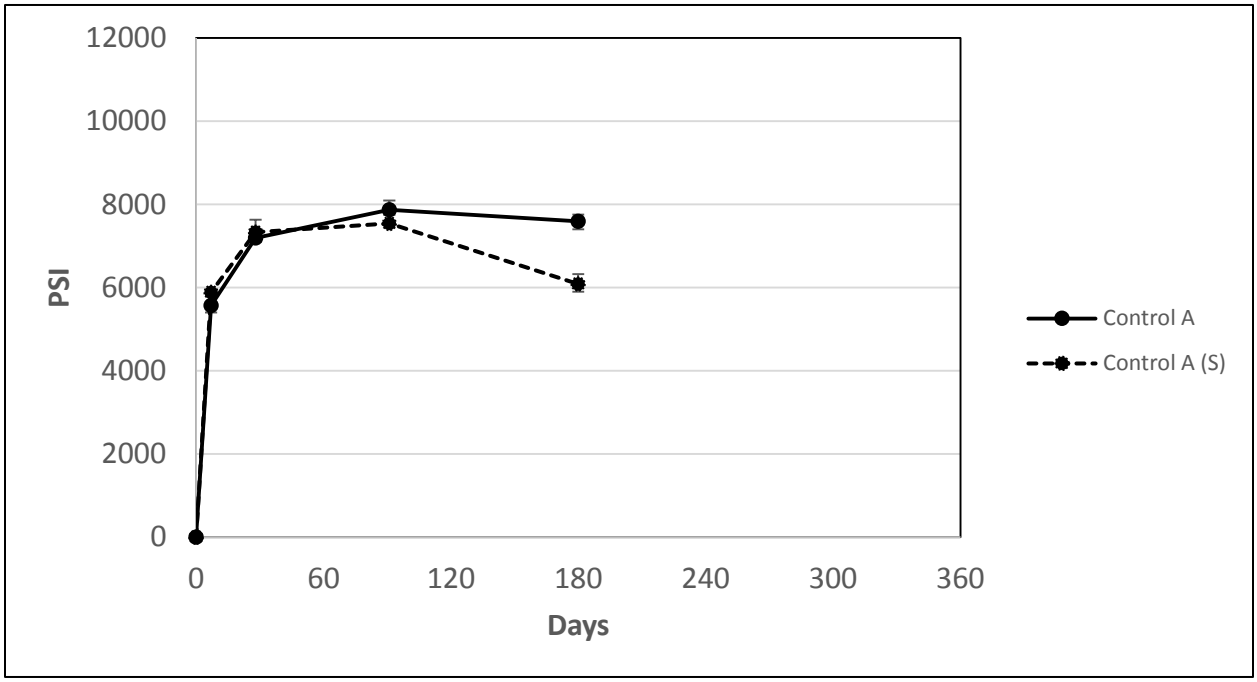

Figure A.1: Error Bars Associated with Control A

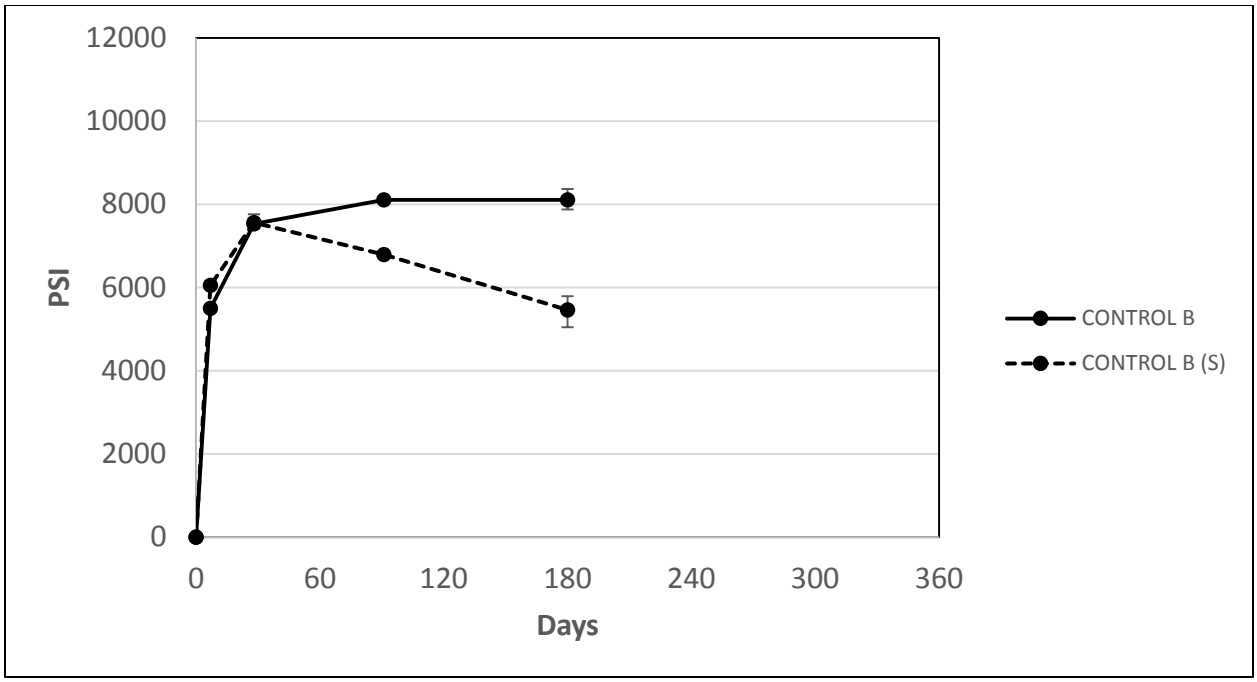

Figure A.2: Error Bars Associated with Control B

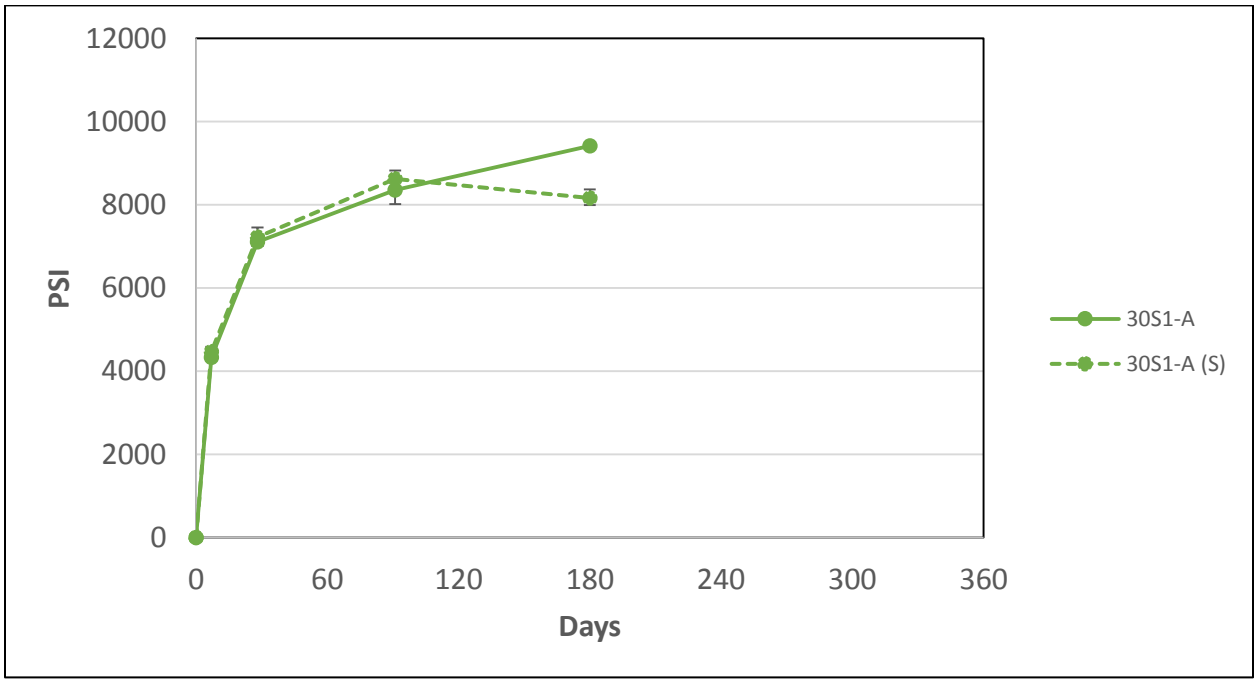

Figure A.3: Error Bars Associated with 30S1-A

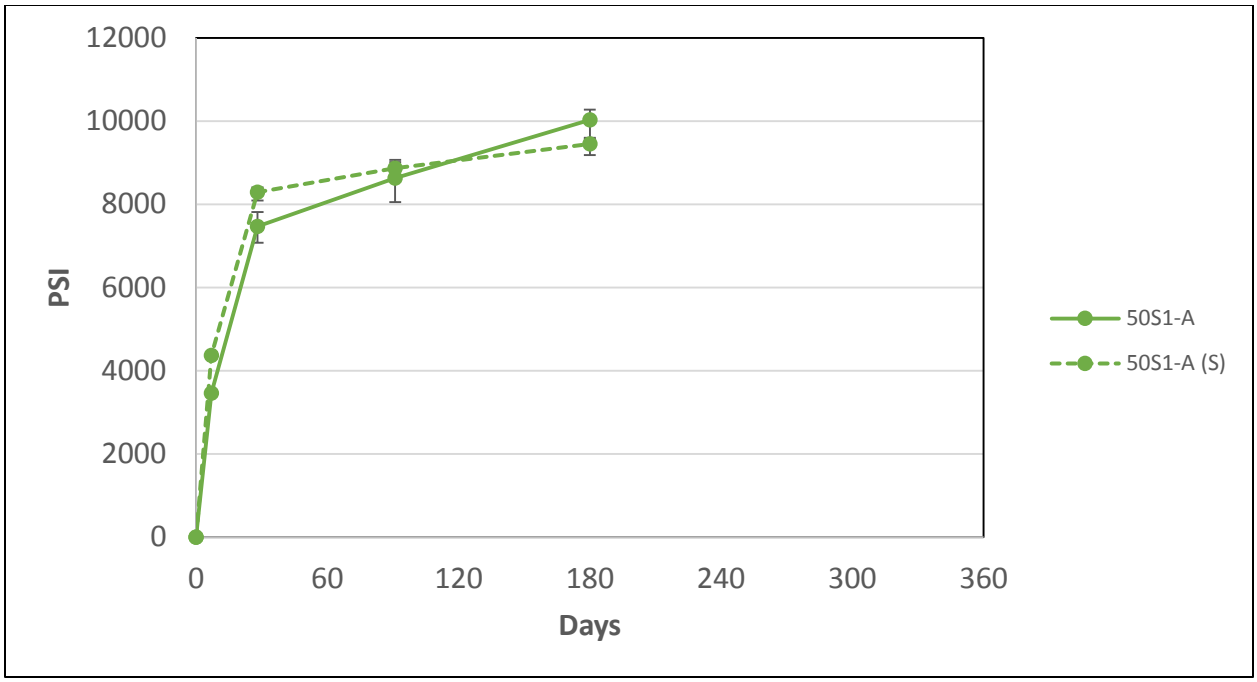

Figure A.4: Error Bars Associated with 50S1-A

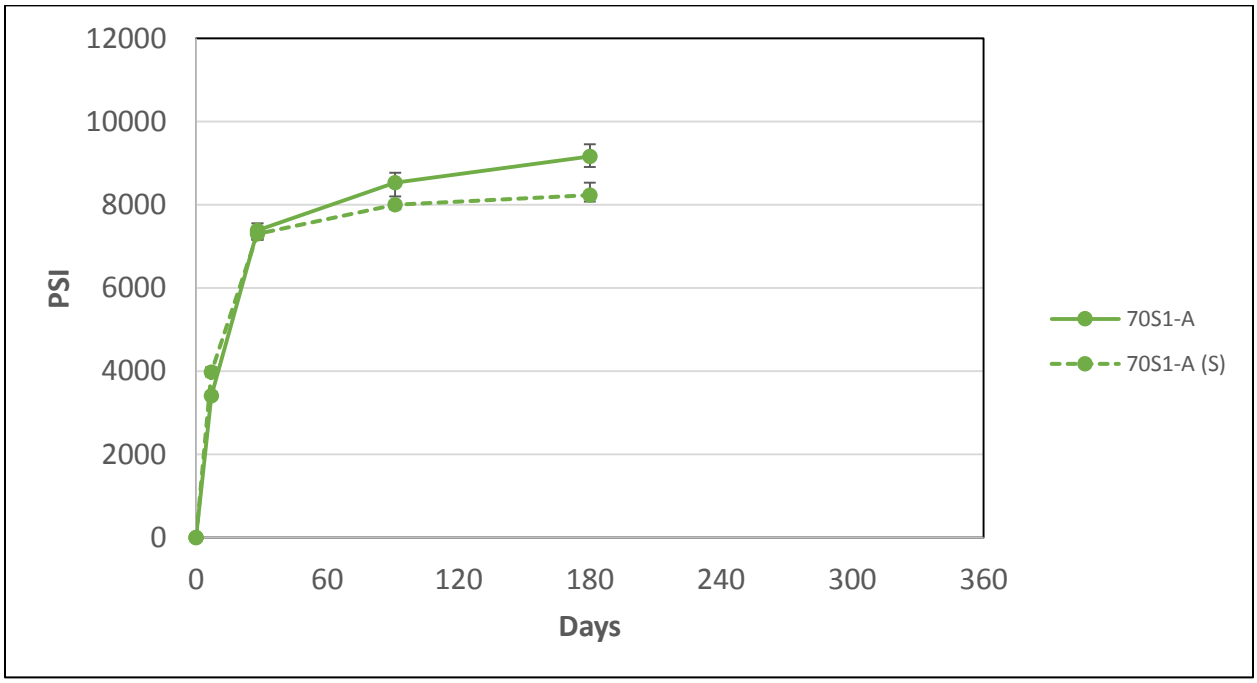

Figure A.5: Error Bars Associated with 70S1-A

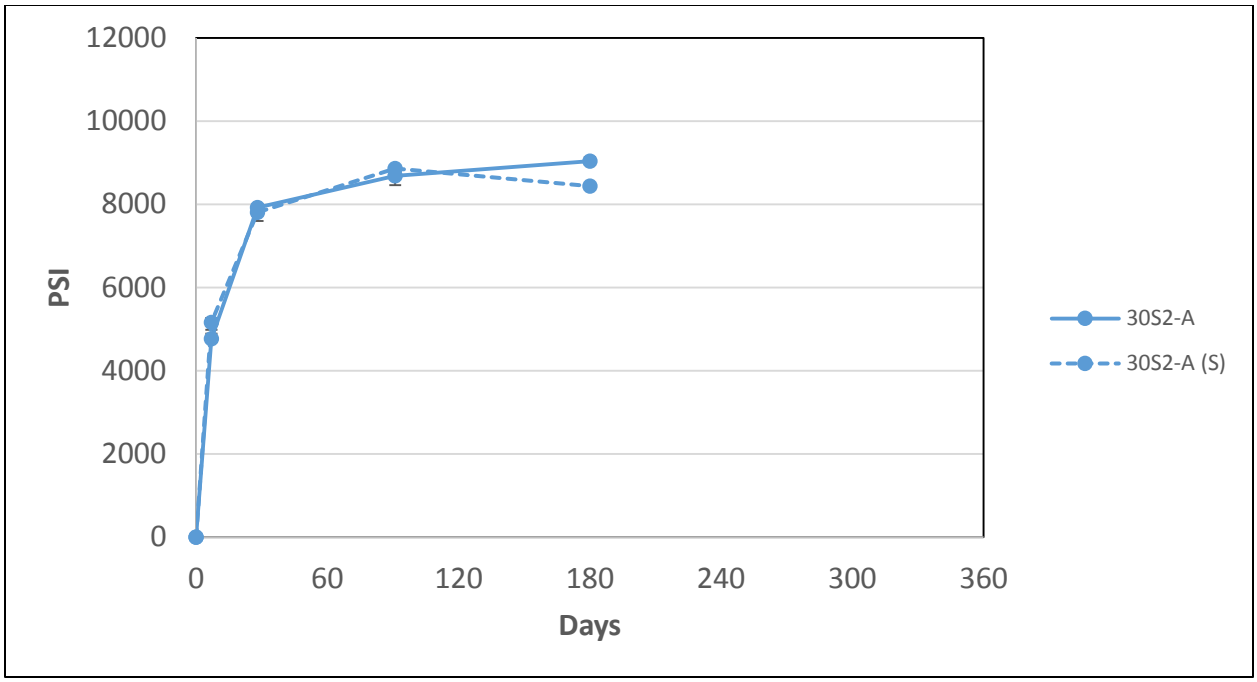

Figure A.6: Error Bars Associated with 30S2-A

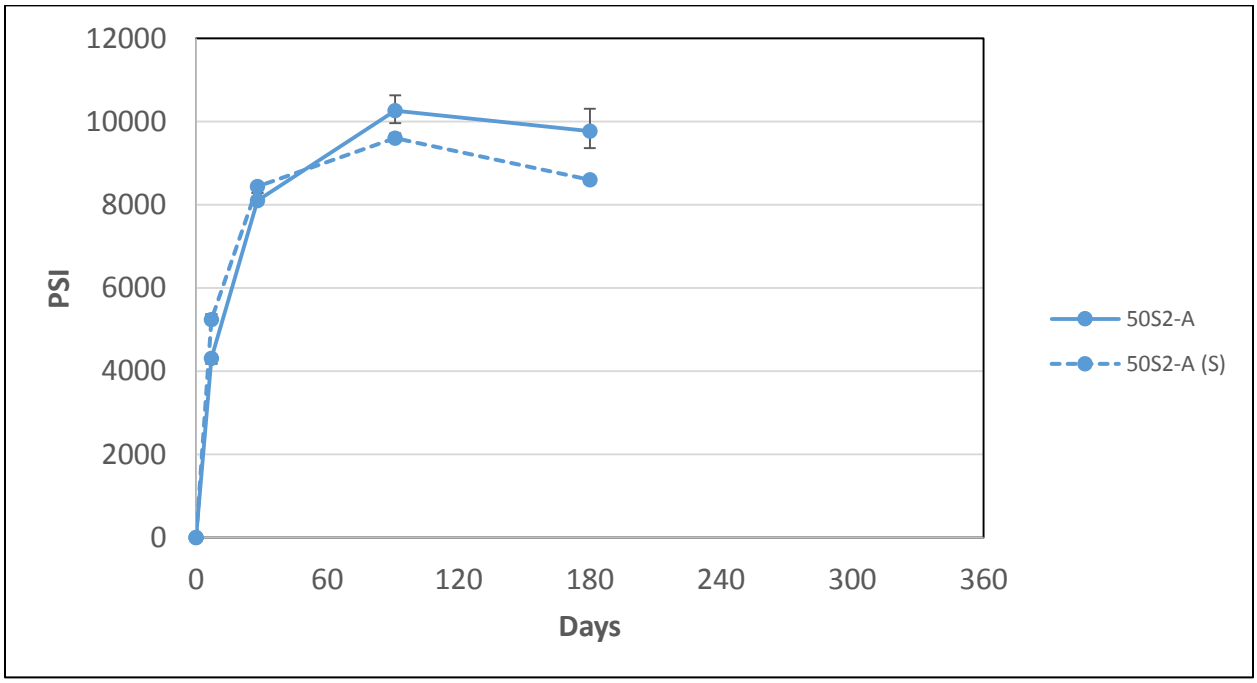

Figure A.7: Error Bars Associated with 50S2-A

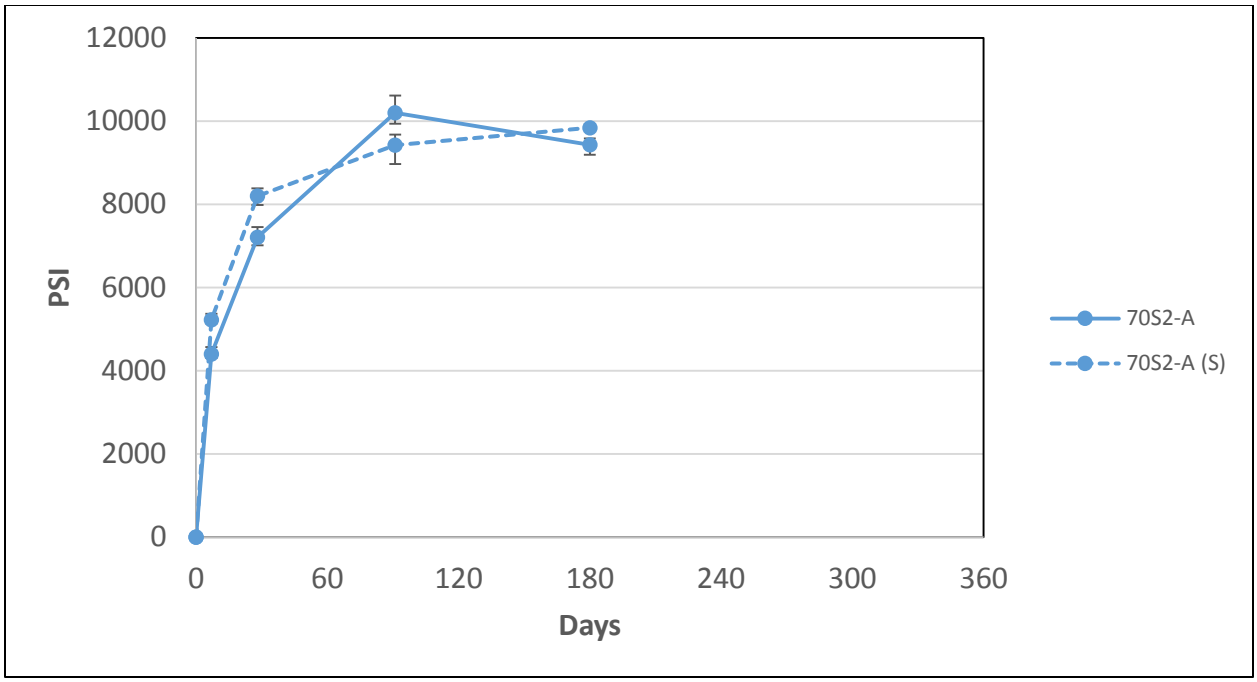

Figure A.8: Error Bars Associated with 70S2-A

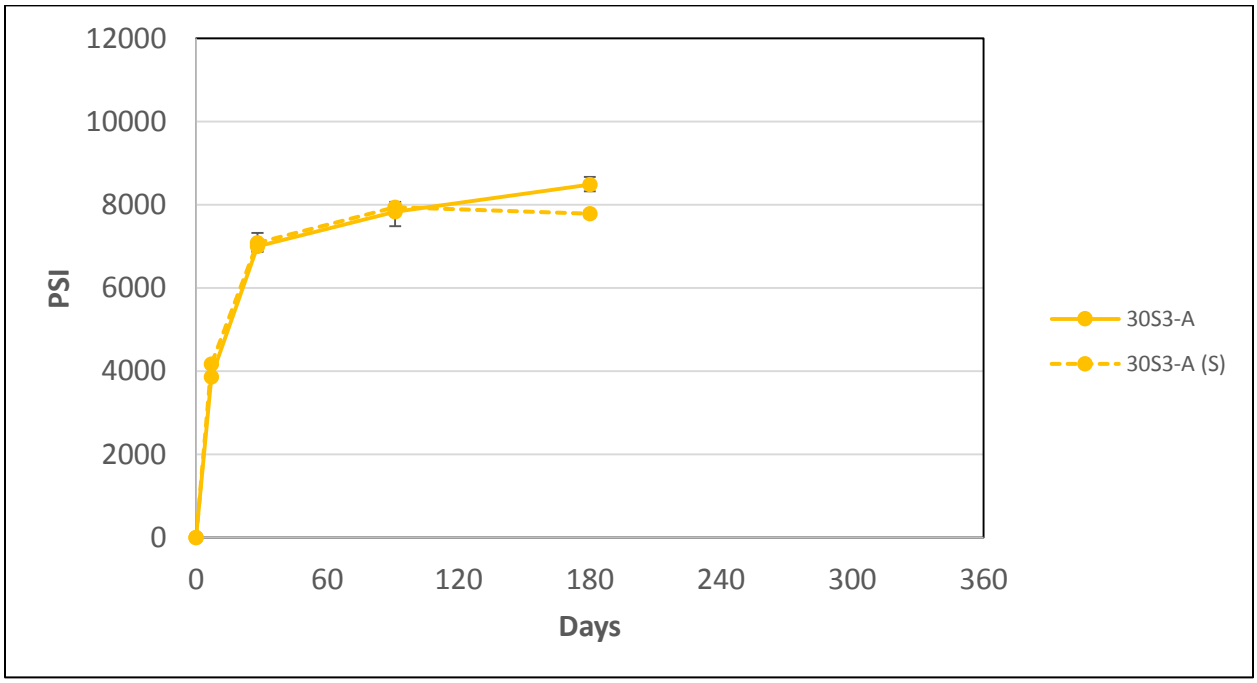

Figure A.9: Error Bars Associated with 30S3-A

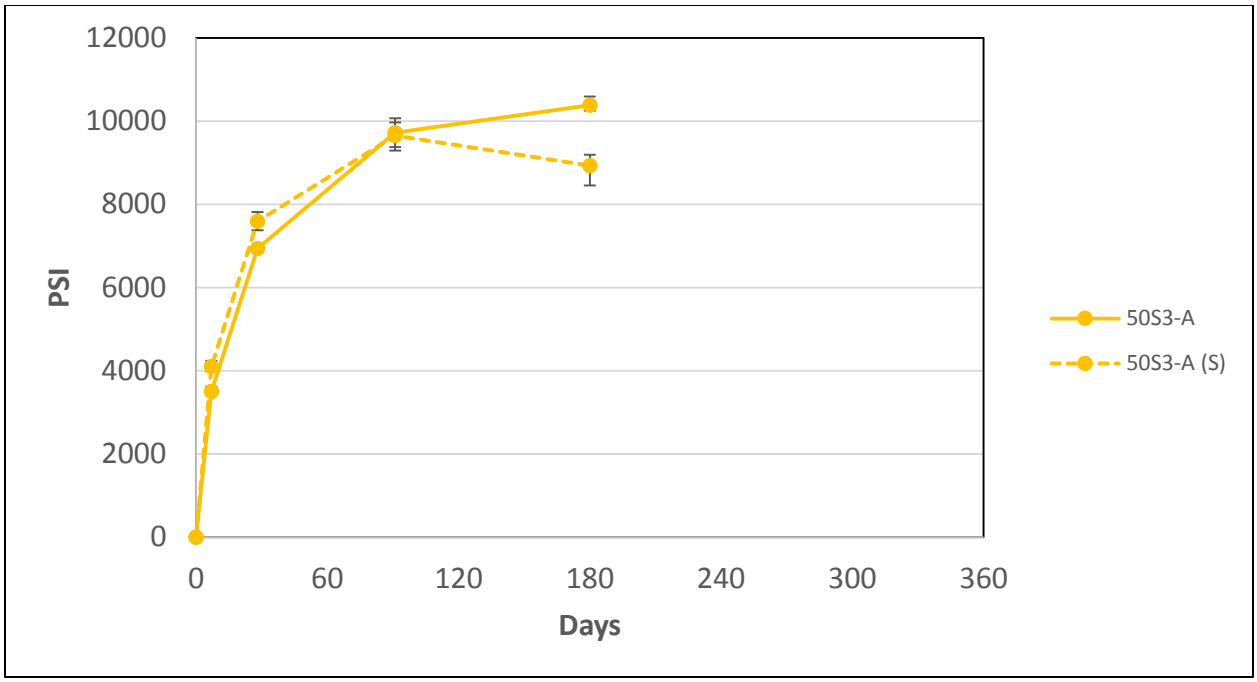

Figure A.10: Error Bars Associated with 50S3-A

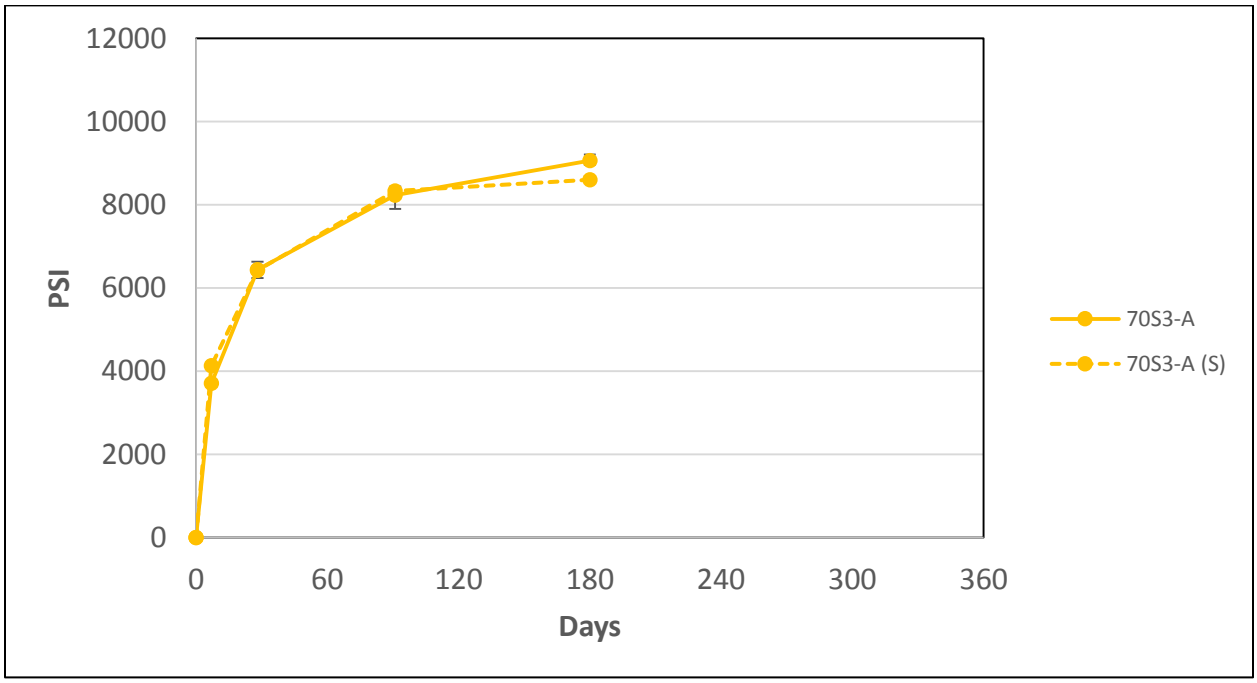

Figure A.11: Error Bars Associated with 70S3-A

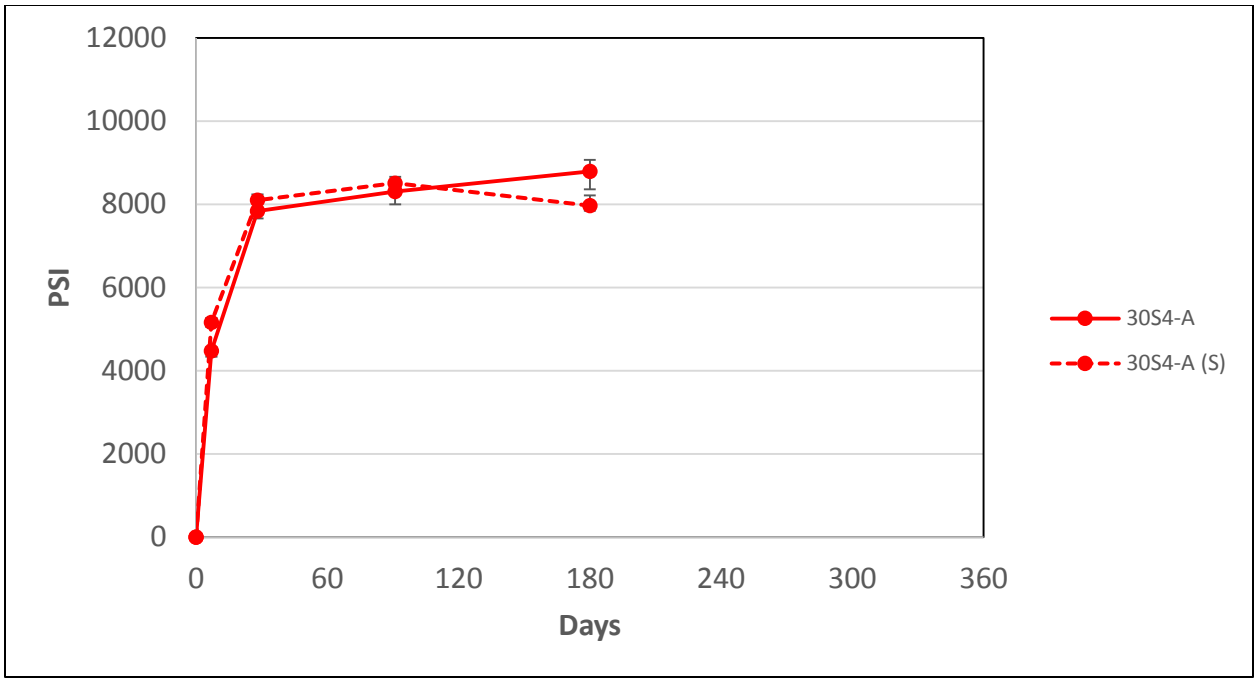

Figure A.12: Error Bars Associated with 30S4-A

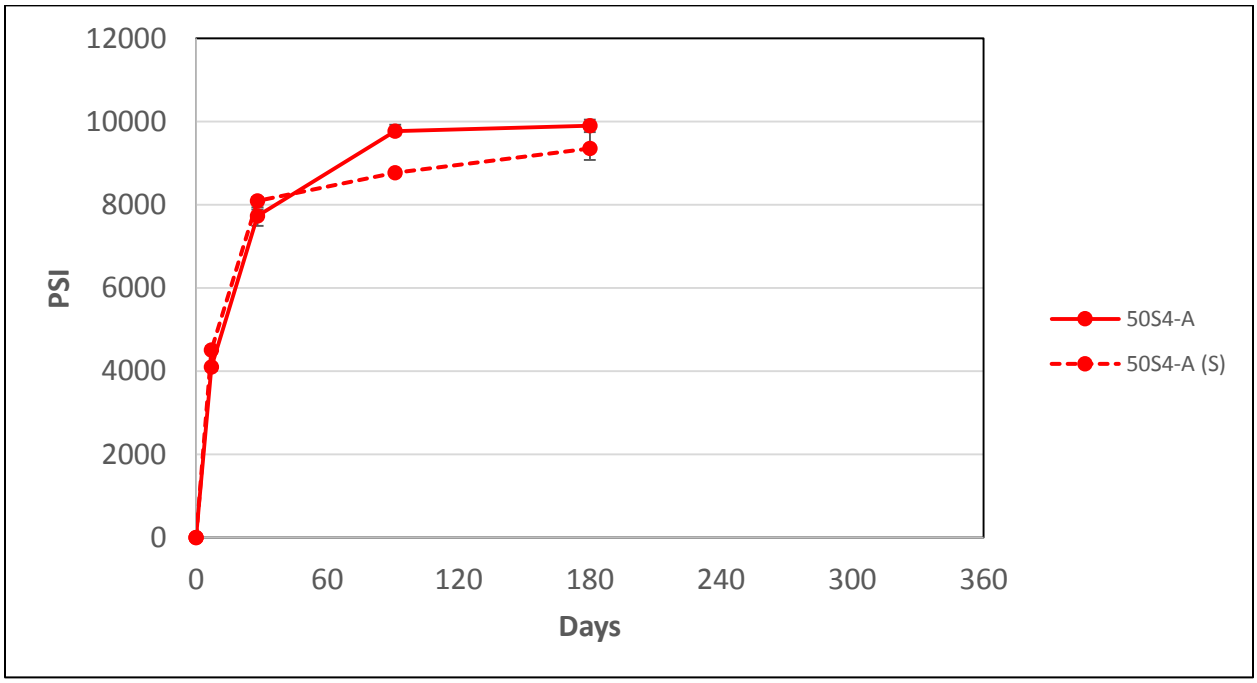

Figure A.13: Error Bars Associated with 50S4-A

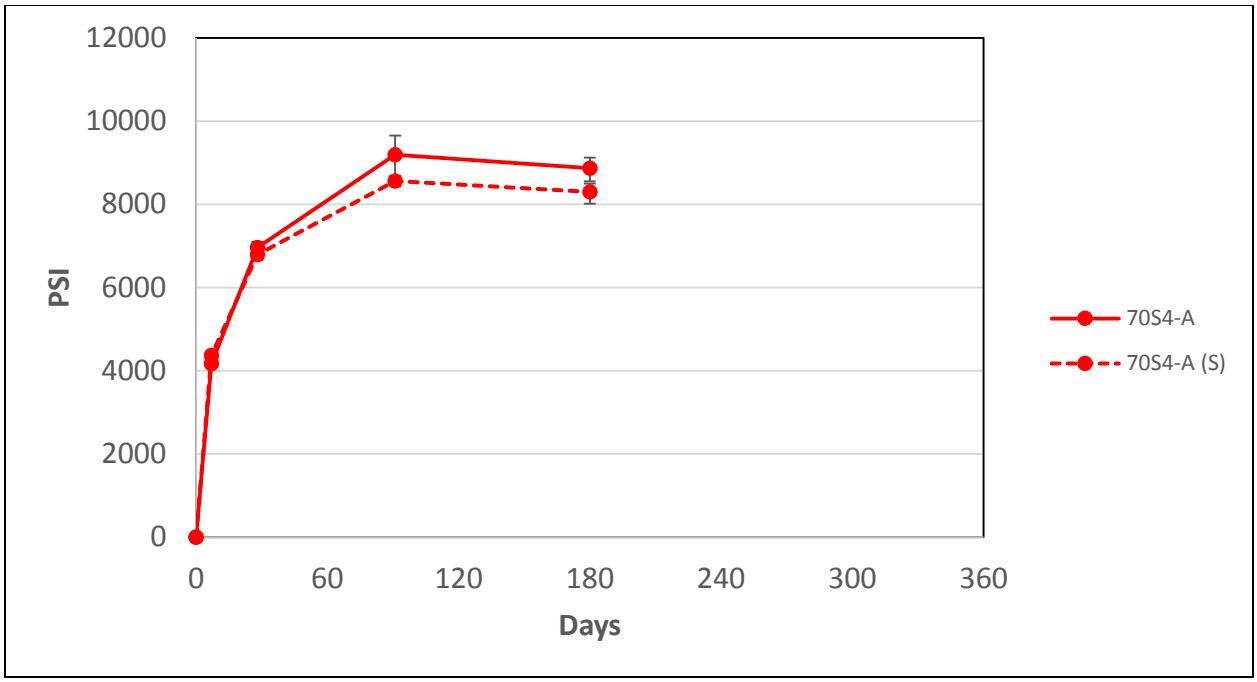

Figure A.14: Error Bars Associated with 70S4-A

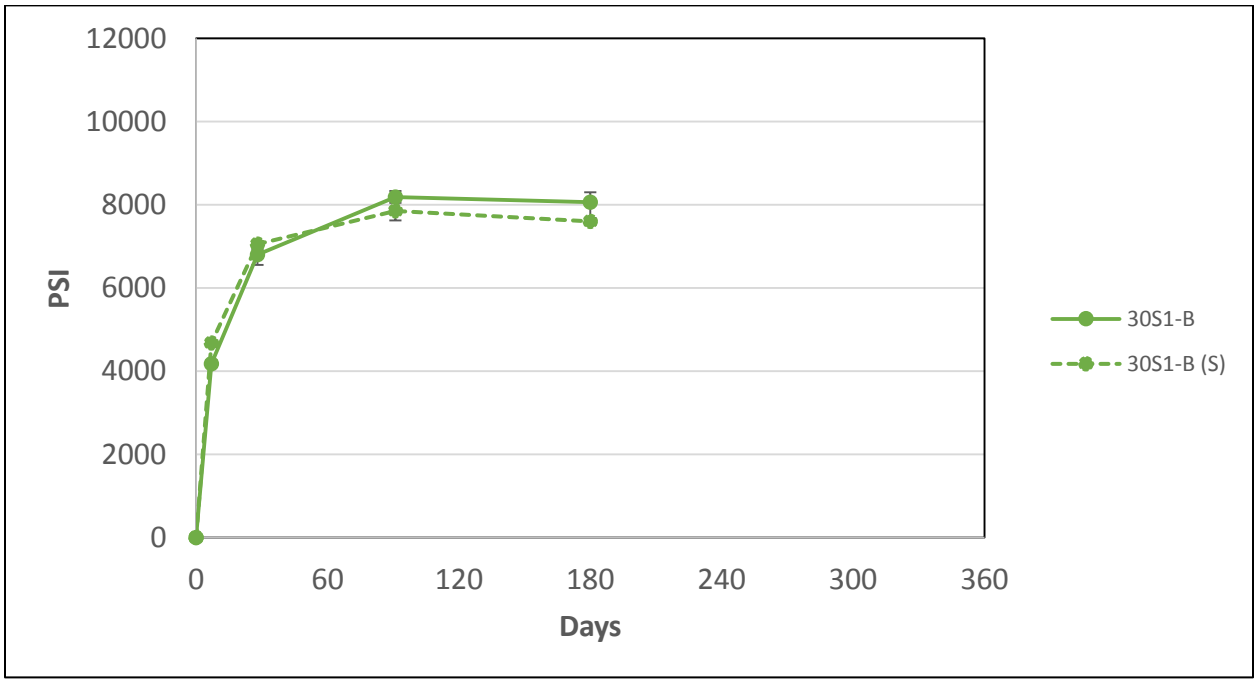

Figure A.15: Error Bars Associated with 30S1-B

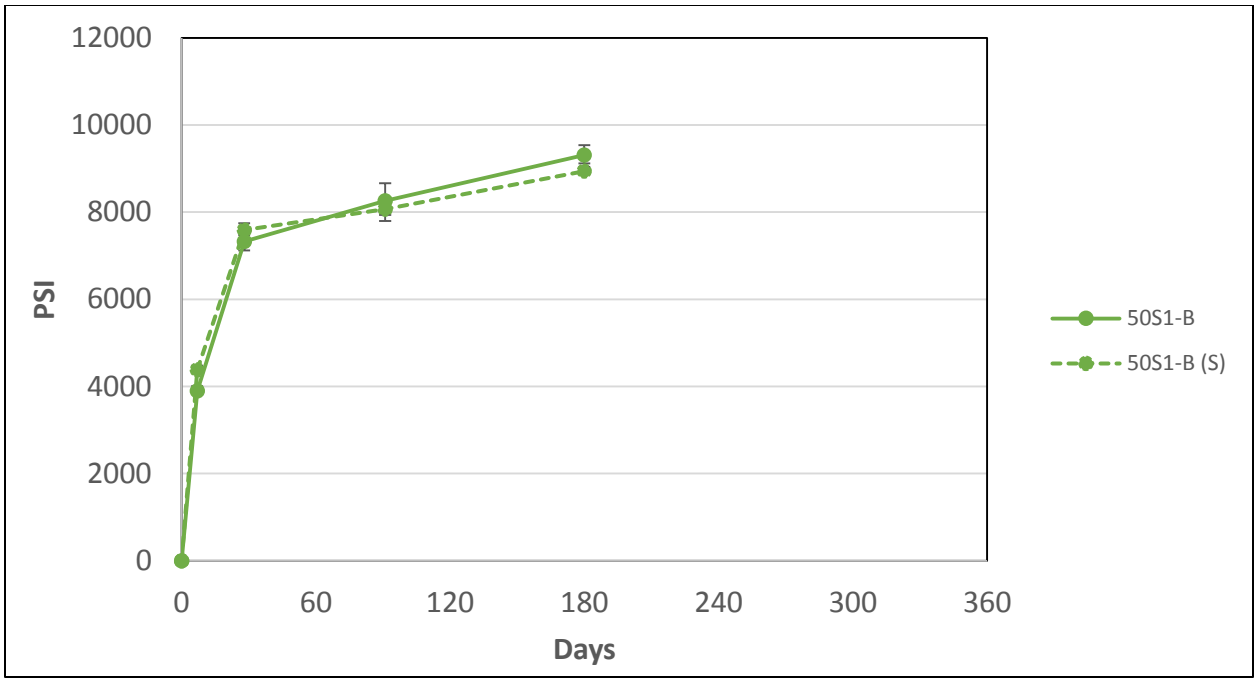

Figure A.16: Error Bars Associated with 50S1-B

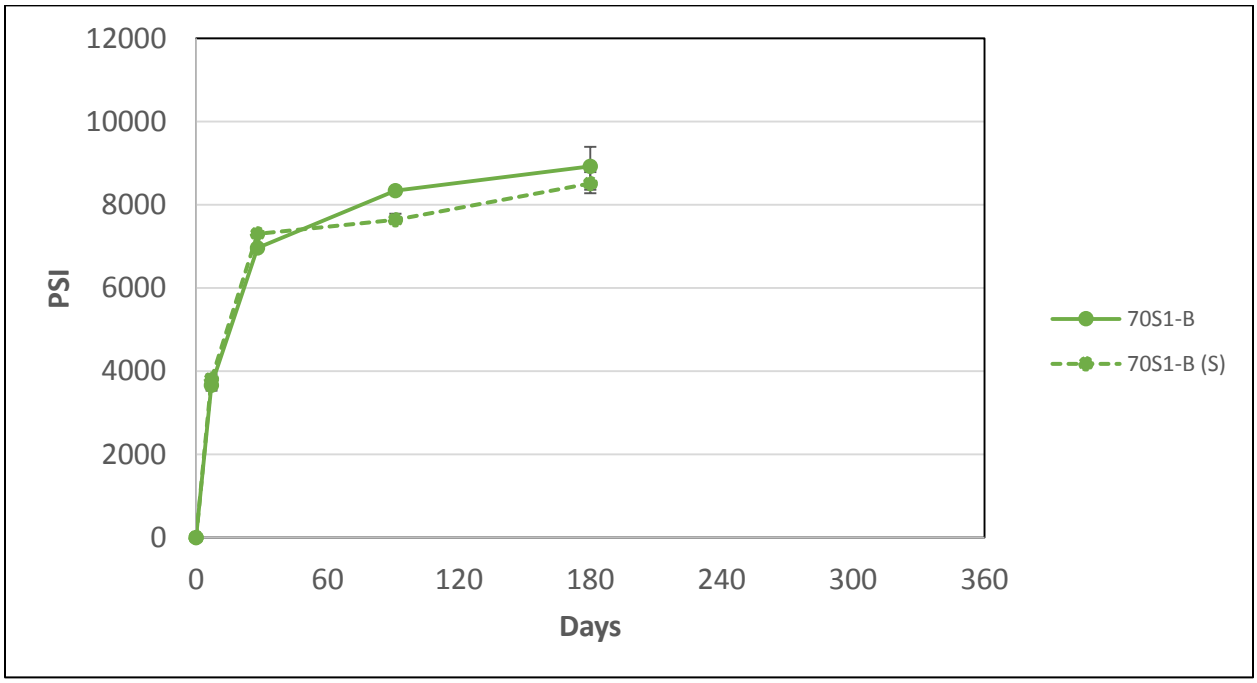

Figure A.17: Error Bars Associated with 70S1-B

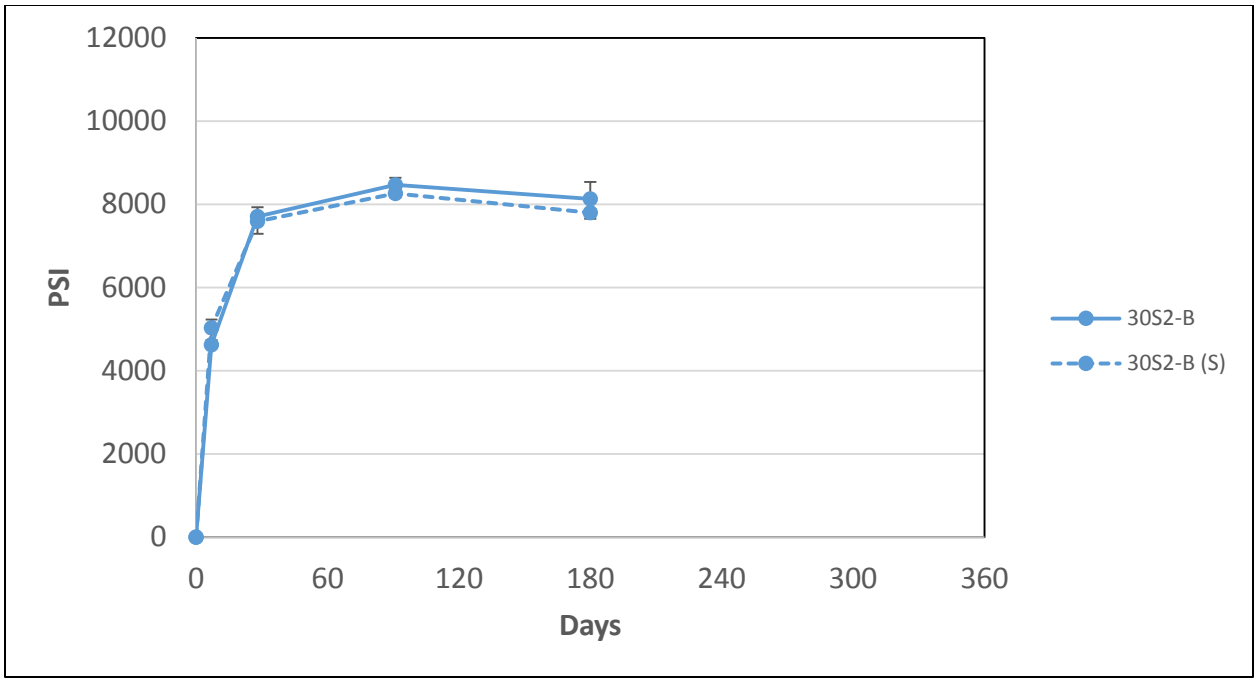

Figure A.18: Error Bars Associated with 30S2-B

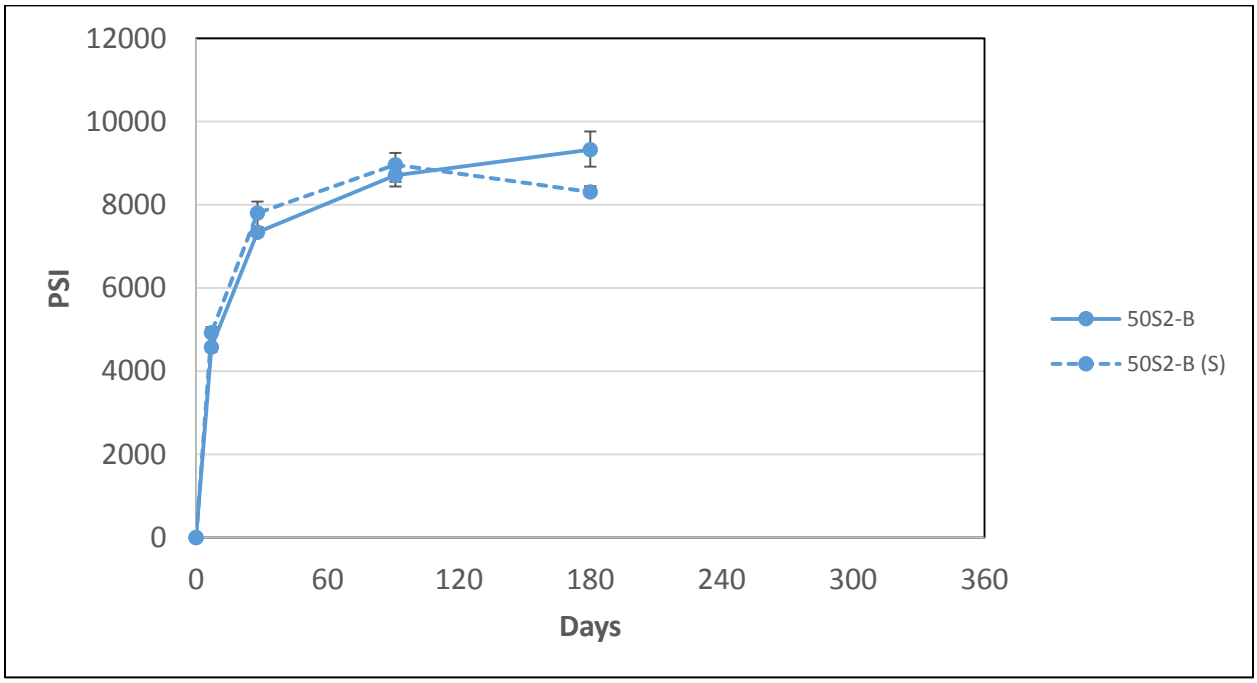

Figure A.19: Error Bars Associated with 50S2-B

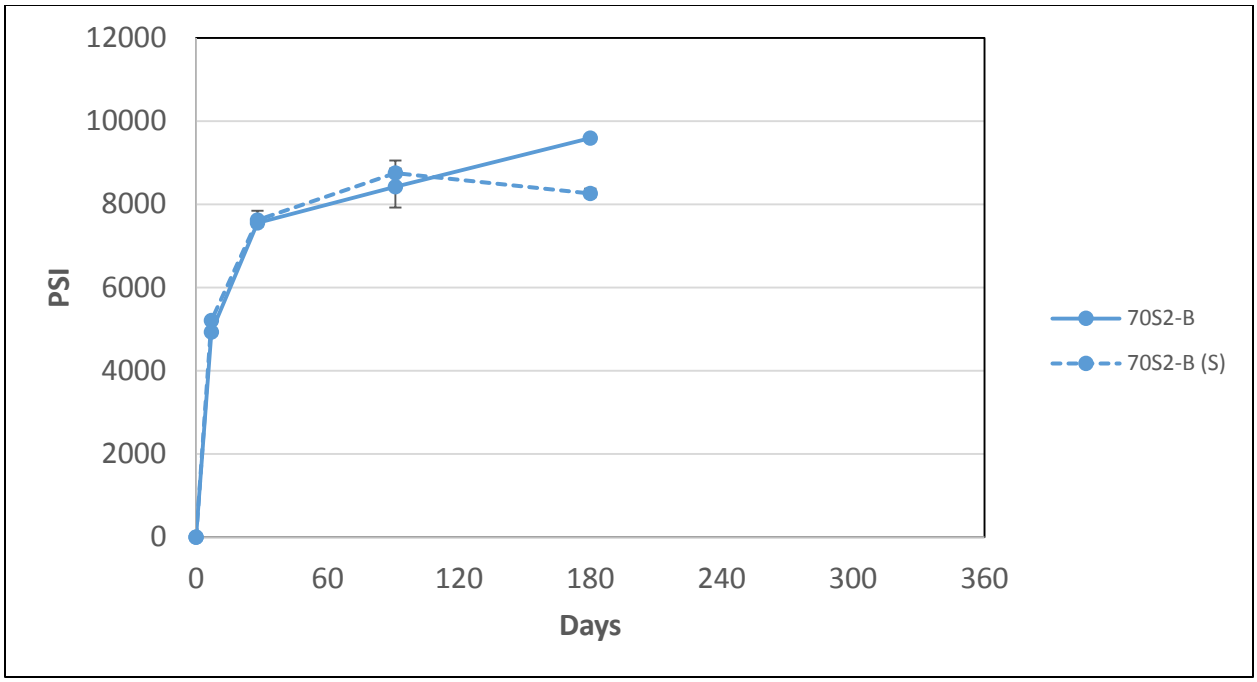

Figure A.20: Error Bars Associated with 70S2-B

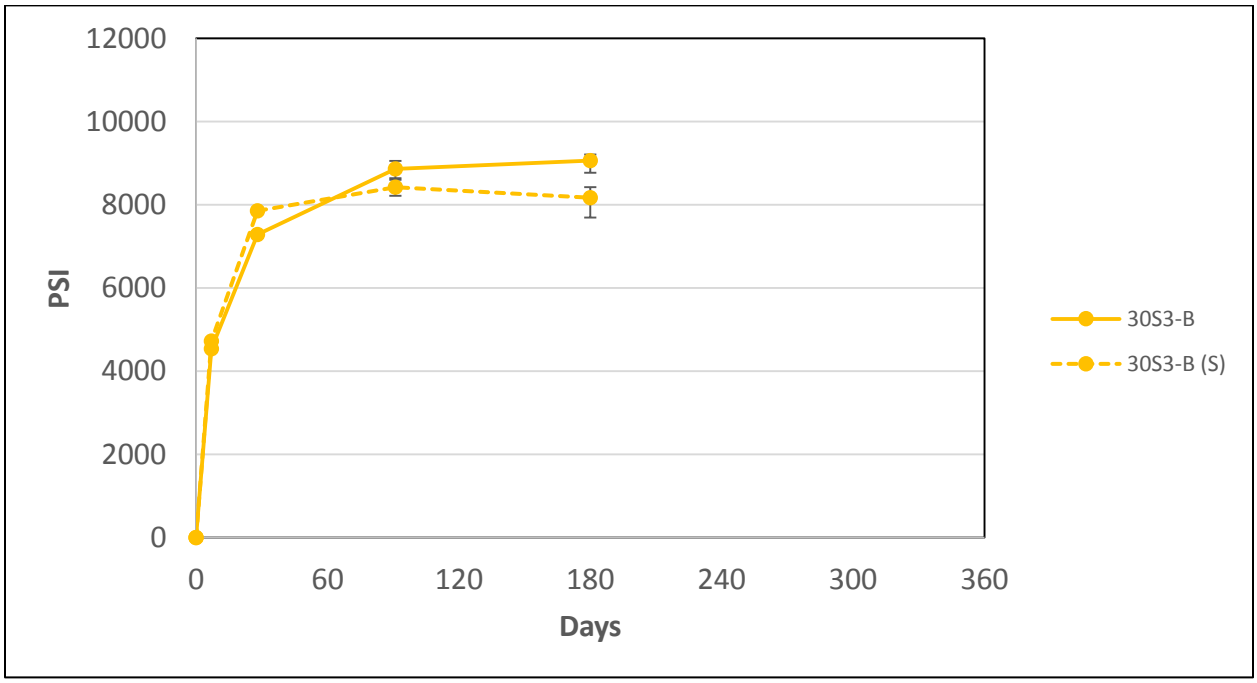

Figure A.21: Error Bars Associated with 30S3-B

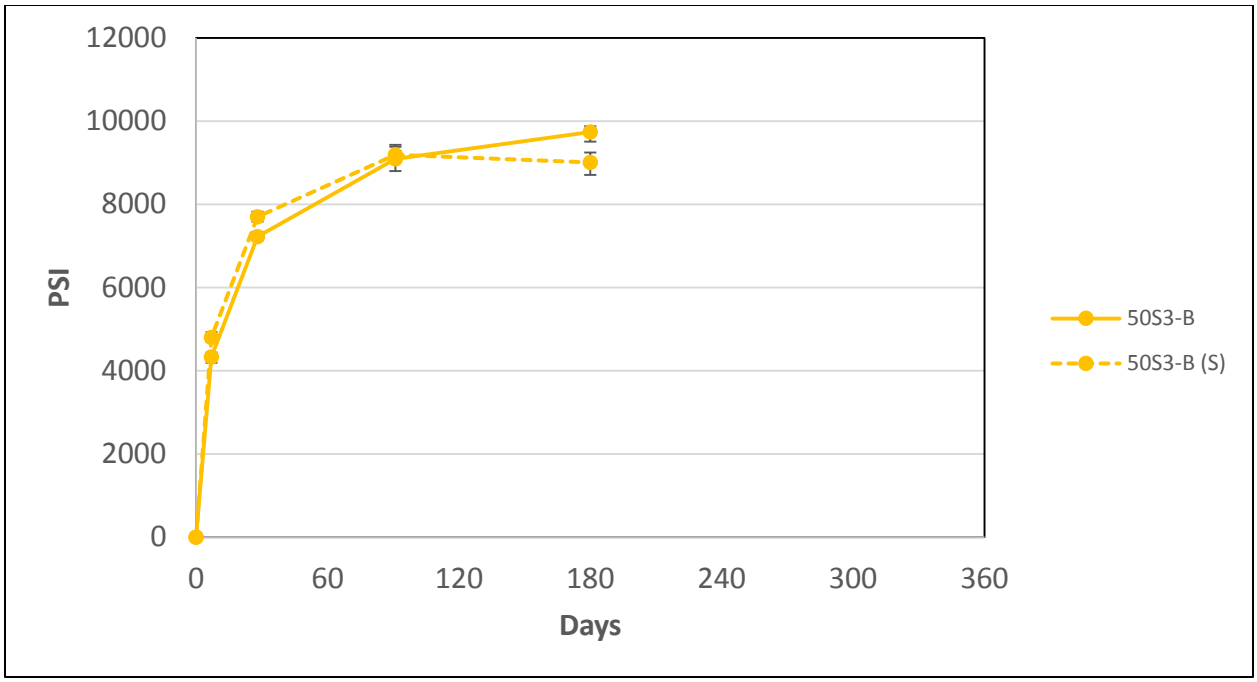

Figure A.22: Error Bars Associated with 50S3-B

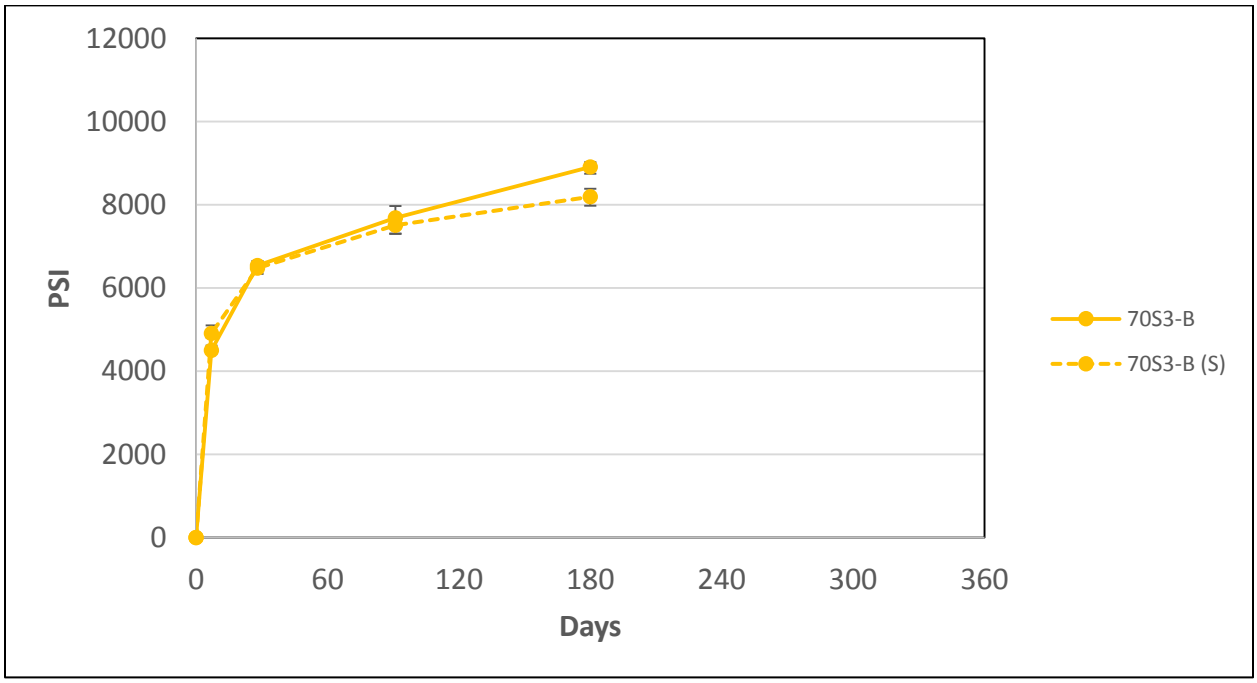

Figure A.23: Error Bars Associated with 70S3-B

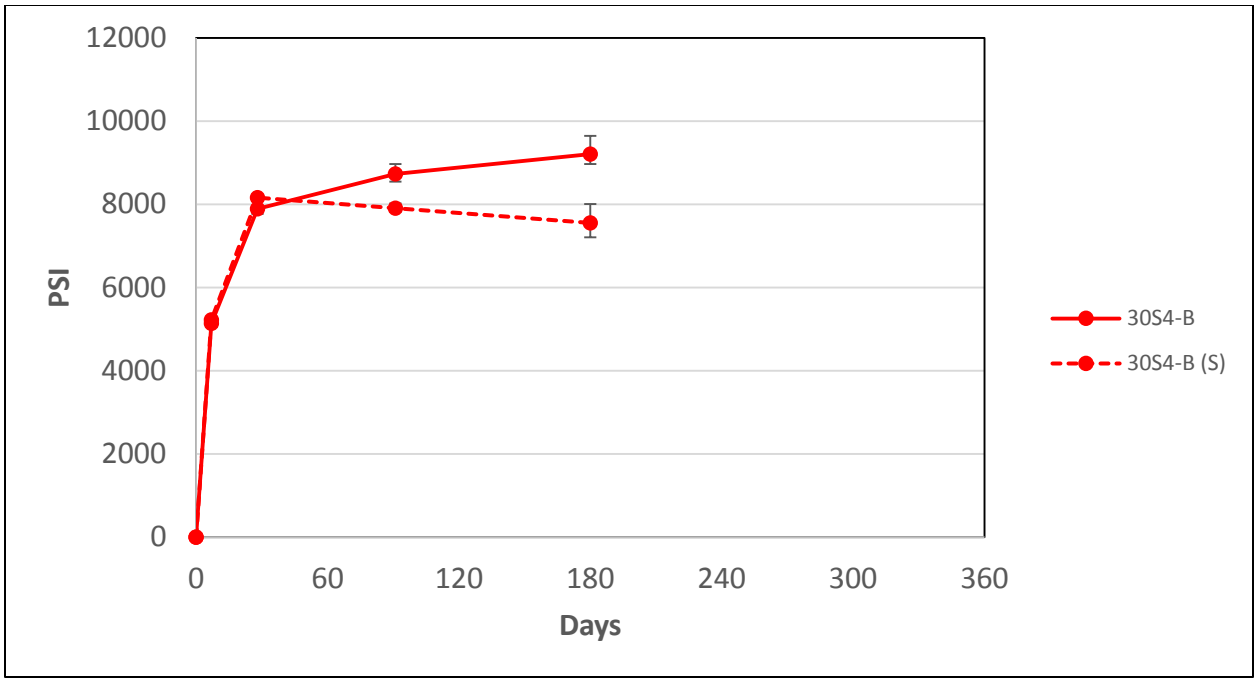

Figure A.24: Error Bars Associated with 30S4-B

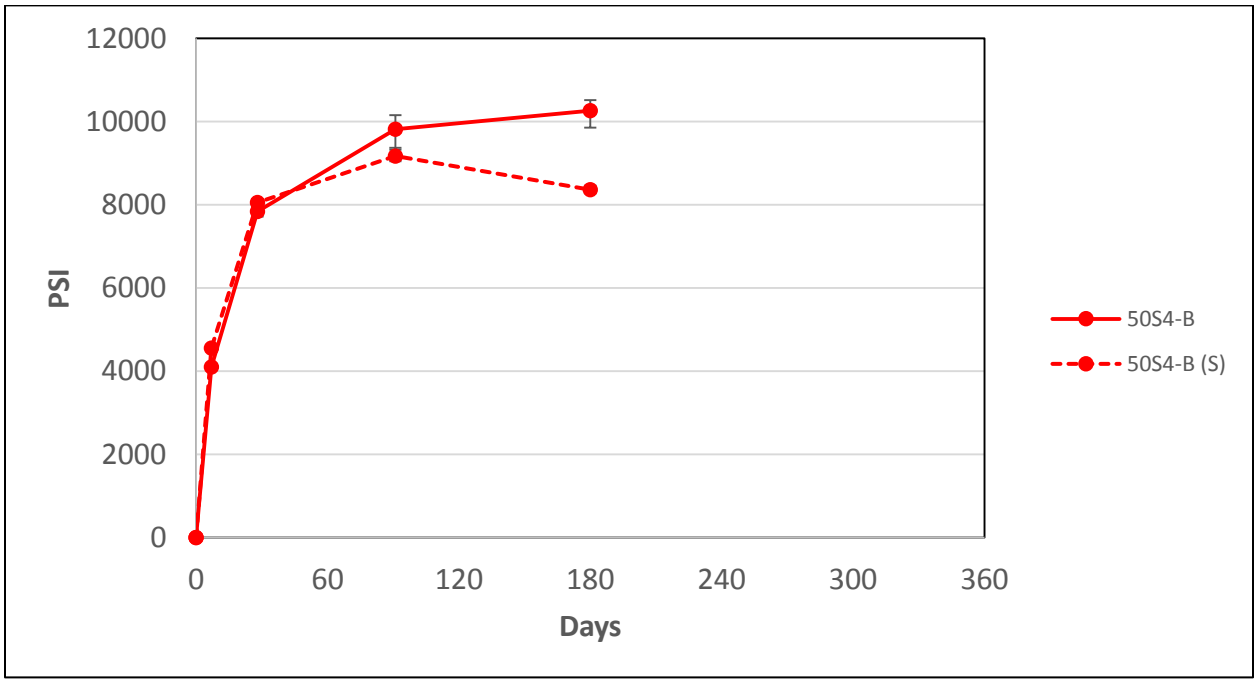

Figure A.25: Error Bars Associated with 50S4-B

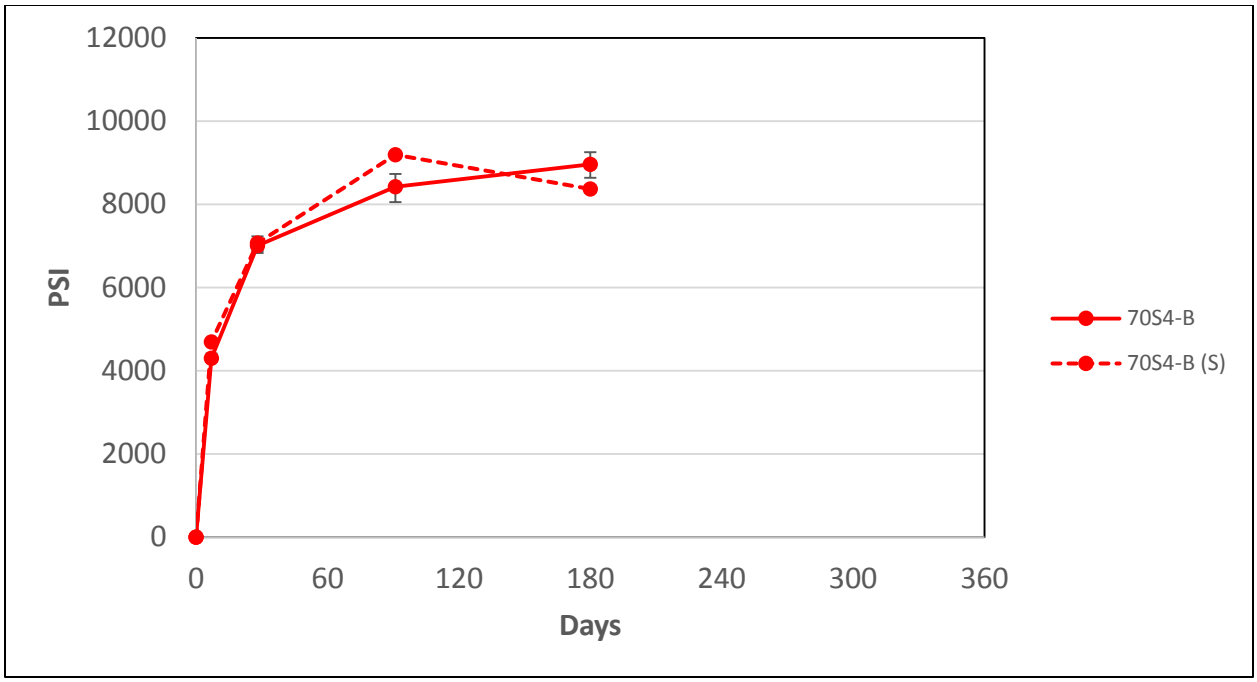

Figure A.26: Error Bars Associated with 70S4-B